# Synapses Never Sleep: Uncovering Daily Rhythms in Mouse Forebrain Synapses Using Integrative Omics

---

**Dissertation**

**zur**

**Erlangung der naturwissenschaftlichen Doktorwürde**
**(Dr. sc. nat.)**

**vorgelegt der**

**Mathematisch-naturwissenschaftlichen Fakultät**

**der**

**Universität Zürich**

**von**

Sara Bernardez Noya

**aus**

Spanien

**Promotionskommission**

Prof. Dr.Steven A. Brown (Vorsitz)
Prof. Dr. Maria Robles
Prof. Dr. Michael Kiebler
Prof. Dr. Shiva Tyagarajan

**Zürich,** 2020

Eles saben para quén.

*They know for whom.*

(Tamén para min)

*(Also for me)*

## Summary

It requires only a bit of self-attention or societal observation to realize that altering natural rhythmic behaviors such as sleep and wake cycles has dramatic effects on health. In reverse, many neuropsychiatric disorders share as a common symptom altered circadian behaviors or altered sleep patterns; and sleep deprivation in healthy individuals is detrimental for memory. However, the molecular mechanisms underlying connections between the circadian cycle, sleep, and brain physiology remain mostly unknown.

This thesis attempts to address these questions by focusing on neuronal synapses, small specialized compartments whose correct composition determines neuronal communication and ultimately brain function. We comprehensively examined these synapses systematically at different times of day characterizing mRNA, protein and phosphorylation rhythms within them. In addition, we challenged normal homeostasis in this scenario by the disruption of sleep wake cycles, to delineate separate functions for sleep and the circadian clock.

The results are presented in two parts, each corresponding to a published manuscript.

In the first manuscript, it is revealed that two-thirds of synaptic transcripts display circadian accumulation independent of the levels in the soma. These mRNAs form two temporal and functional clusters, preceding dawn or dusk. Alongside, the synaptic proteome demonstrates the functional relevance of temporal gating: RNAs and proteins involving synaptic transmission anticipate the active phase, while those involving translation and energy metabolism anticipate sleep.

Unexpectedly, sleep deprivation completely abolishes proteome but not transcript oscillations.

In the second manuscript it is shown that in the synapses half of the phosphoproteins have large-amplitude rhythms peaking as well around dawn and dusk. Kinases follow the same fluctuations and their dynamic phospho-regulation is likely an underlying process. Functionally the phosphoproteome as a whole sustains temporal compartmentalization, favoring synaptic inhibition prior to sleep and excitation before wake. Sleep deprivation abolishes most phosphorylation cycles.

In conclusion, circadian- and sleep-driven mechanisms appear to work hand-in-hand to ensure proper physiology by coordinating molecules in space and time. The overall emerging picture is one where in synapses a circadian anticipation of physiological need is achieved by rhythmic messenger RNA accumulation, and this is followed by protein translation and phosphorylation responding directly to sleep-wake cycles.

# Ackowledgements

Every morning I smile when I say thank you. And paradoxically, I it took me a while to decide how to write the Ackowledgements.

As for many situations where I had to make a decission about science I repeated to myself a sentence that Steve repeated everytime we spoke about this document in the last weeks: “I can give you advice about language but otherwise, this is your Thesis”. Understood.

Complication again to start a list of names and what I ackowledge for each specific case. I would most probably forget someone and that I don’t want. But I don’t want to generalize and leave it as “thanks to all the people that helped me to achive this challenge”. This Thesis is achieved thanks to many people and experiences that spread frther than October 2015 when I came to Zürich.

So let’s be practical and mention those names I met while being here and had a more direct connection to the science written in these pages. Names of the blocks of the pyramid (see picture below = lab members present and past), collaborators, advisors, instructors, brainstorming peers, technical support, administrative help, cleaning service and people saying “Good morning” and speakers from inspirational talks ( I will not list the names of the last groups, for some I don’t know it).

Arianna, Danielle, Tanja, Shiva, Chantal, Yuan-Chen, Ermanno, Lennart, Sara, Ruth, Michael, Andrea, Christine, Ben, Hien, Dennis, Martee, Kyra, David, Teresa, Edward, Mari, Jacqueline, Charo, Dennis, Alex, Yulia, Cody, Sophia, Camilla, Melissa, Rona, Jean-Marc, Patrizzia, Norbert, Jessica, Kostas, Koen, Waleed, Yuri, Ludmila, Audrey, Sara, Steve, Saujanya, Ben, Jelena, Miho, Franzi, Julie, Irmak.

Lab retreat, Cascais, 2019.

# Abbreviations

| | |
|---|---|
| AMPA | A-Amino-3-Hydroxy-5-Methyl-4-Isoxazolepropionic Acid Receptor |
| BMAL1 | Bmal Circadian Regulator Protein |
| *Bmal1* | Bmal Circadian Regulator Gene |
| *CamK2a* | Casein Kinase 2 A Gene |
| CBP | CREB-Binding Protein |
| *Cke* | Casei Kinase Epsilon Gene |
| CLOCK | Clock Circadian Regulator Protein |
| *Clock* | Clock Circadian Regulator Gene |
| CPEB1 | Cytoplasmic Polyadenylation Element Binding Protein 1 |
| CRY | Cryptochrome Circadian Regulator Protein |
| *Cry* | Cryptochrome Circadian Regulator Gene |
| CT | Circadian Time |
| DD | Constant Darkness |
| DEC2 | Class E Basic Helix-Loop-Helix Protein |
| EEG | Electroencephalogram |
| FMRP | Fragile Mental Retardation Protein |
| GO | Gene Ontology |
| GRP | Gastrin-Releasing Peptide |
| *Homer1a* | Immediate Early Gene Homer1 |
| KO | Knockout |
| LC | Liquid Chromatography |
| MS | Mass Spectrometry |
| LD | Normal Light-Dark Cycle |
| LTP | Long Term Potentiation |
| mRNA | Messenger RNA |
| NMDA | N-Methyl-D-Aspartate Receptor |
| *Npas* | Neuronal PAS Domain Gene |
| NREM | Non-Ren Sleep |
| PER | Period Circadian Regulator Protein |
| *Per* | Period Circadian Regulator Gene |
| PKA | Protein Kinase A |
| RBP | Rna Binding Protein |
| RNA | Ribonucleic Acid |
| SCN | Suprachiasmatic Nucleus |
| SD | Sleep Deprivation |
| SHY | Synaptic Homeostatic Hypothesis |
| SIK3 | Serin/Threonine Protein Kinase 3 |
| SILAC | Stable Isotope Labeling By/With Amino Acids in Cell Culture |
| siRNA | Small Interference Ribonucleic Acid |
| SNIPPs | Sleep Need Index Phosphoproteins |
| SSIPPs | Sleep Surplus Index Phosphopeptides |
| SWA | Slow Wave Activity |
| TTFL | Transcriptional Translational Feedback Loop |
| VIP | Vasoactive Intestinal Peptide |

| | |
|---|---|
| WT | Wild Type |
| ZBP1 | Z-Dna Binding Protein 1 |
| ZT | Zeitgeber Time |

# Table of Contents

# 1. Introduction

## 1.1. Daily Rhythms in Neurobiology

Being tuned with the rhythm of life is a major indicator of well-being. When we break the rules of those rhythms we are prone to undergo a variety of symptoms such as metabolic issues, immune dysfunction or cognitive deficits. For example, when sleep patterns are altered, our alertness and attention decreases, highlighting the significance of daily rhythms on brain function. Indeed, the pioneer studies on experimental memory suggested that brain performance is intrinsically related to time-of-day (Ebbinghaus, 2013). Since then, circadian clocks and sleep pressure were identified as the main modulators of memory rhythms (reviewed in Schmidt et al., 2007 and Snider et al., 2018). Similarly, more recent findings indicate that diverse aspects of brain physiology such as cerebrospinal fluid flow and metabolite clearance are also under the control of sleep state and circadian time (Fultz et al., 2019, Xie et al., 2013, Myung et al., 2018). The progress made in the last decades to understand the molecular and cellular underpinnings of both circadian and sleep rhythms highlights that under normal conditions; they are synchronized with each other. As a result, daily rhythms of brain physiology emerge as a consequence of the interaction between circadian and sleep mechanisms.

This section is divided into three parts. The first and second describe the fundamental concepts of circadian and sleep cycles, their molecular mechanisms, and their physiological manifestations. The third unmasks the controversy between the role of circadian clocks and sleep in neurobiological functions and presents promising new methodologies that could help resolve this conflict.

### 1.1.1. Circadian Rhythms

From behavior to cellular biology, if we study bacteria, plants or animals across days, one can find numerous examples of processes with a period of approximately (circa-) one day (-diem). Circadian rhythms are singular when compared to other daily cycles because they persist even under constant conditions. For example absence of light and dark barely modifies the period of oscillations between wakefulness and sleep, catabolism and anabolism or growth and repair. The reason is that their timing is dictated by endogenous mechanisms: “Clocks”.

#### 1.1.1.1. Cellular oscillators

##### History of cellular oscilators

In the early 70’s a mutation in a gene called per caused alteration of circadian rhythms in the fruit fly Drosophila melanogaster (Konopka and Benzer, 1971). It took decades to discover another four genes: Timeless, Clock, Cycle and Cryptochrome (Sehgal et al., 1994, Allada et al., 1998, Rutila et al., 1998). The protein products of these genes are organized in a negative feedback loop of transcription and translation that is autoregulated and restarts every 24 hours. Based on the same mechanism but using different components, clocks were described in a variety of organisms from Neurospora (Dunlap, 1999) to mammals (Wilsbacher and Takahashi, 1998). More recently, circadian rhythms were also observed in cells lacking the transcriptional apparatus such a red blood cells (O’Neil and Reddy, 2011).

##### The TTFL; the transcriptional-translational clockwork in mammals

The protein products of four gene classes: CLOCK, BMAL1, PER1-3 and CRY1-2 are the core components of the transcriptional clock in mammals and their discovery was

like making a puzzle. Homology cloning and sequence alignment with the Drosophila PER served to identify three PER genes in mammals (Tei et al., 1997, Reppert and Weaver, 2002). By contrast, CRY was discovered after identifying abnormal circadian behaviors in *Cry*-deficient mice (van der Horst et a., 1999). The discovery of the mammalian CLOCK was an achievement preceding its discovery in the fly (King et al., 1997) and shortly after, co-expression screens brought up BMAL1, an homolog of the fly protein CYCLE (Hogenesh et al., 1998).

Further studies on the clockwork added new components including REV-ERBα, REV-ERBβ or RORα among others (reviewed in Brown et al., 2012). These elements participate as satellite loops that repress or activate the expression of the core genes providing robustness, boosting amplitude and driving precise temporal resolution (Ueda et al 2005).

The critical property of the network is that the dynamics of all the stages -- gene activation, protein synthesis, complex assembly, intracellular transport, protein inhibition and protein degradation -- extend to approximately 24 hours. In the cycle, *Bmal1* mRNA reaches a peak and 4 hours later the protein complex BMAL1/CLOCK enters the nucleus to activate the transcription of genes that harbor E-boxes. Between them we find *Per*, *Cry* and *RevErb*. 6 hours later PER/CRY complexes enter the nucleus to repress BMAL1/CLOCK complexes. The continued production of E-box containing genes, including C*r*y and *Per*, is prevented closing the autorregulatory feedback loop. With PER/CRY progressive degradation (about 6 hours) the blockade of BMAL/CLOCK decreases but BMAL1/CLOCK do not form right away because an auxiliary loop led by the transcription factors REVERB and ROR, controls *Bmal1* transcription in a way that are needed 8 more hours for Bmal1 to reach the peak again. 0 + 4 + 6 + 6 + 8 = 24 hours (Figure 1).

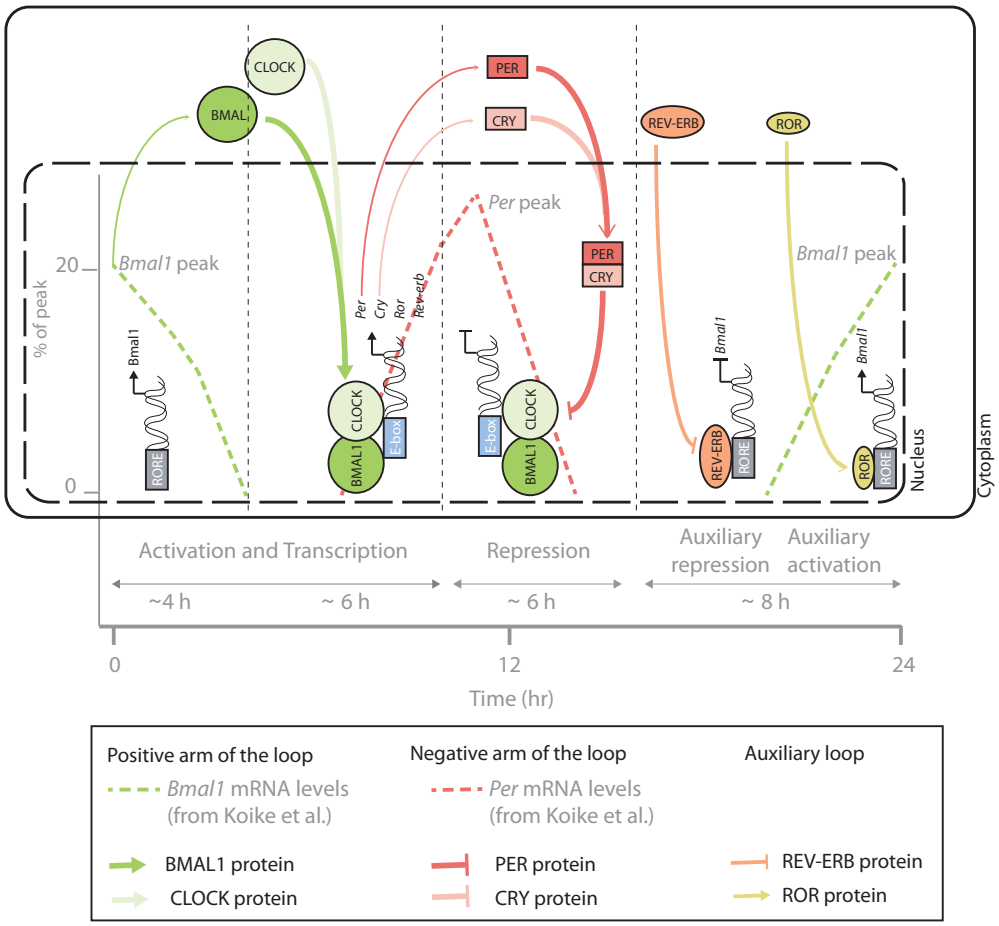


Figure1. The mammalian Clockwork. In mammals, the clockwork is composed of a main autorregulatory feedback loop whose positive arm is composed of the proteins BMAL and CLOCK. The complex of both proteins activates transcription of genes harboring E-boxes. Per and Cry are between those genes. PER and CRY proteins form the negative arm of the loop because its complex blocks BMAL and CLOCK preventing a continuous increase of their own levels. The 24 h time keeping is easily visualized with the timing of Bmal and Per mRNAs peak levels, resulting from the intrinsic dynamics of the main loop and the support of auxiliary loops such as the one formed by REV-ERB and ROR. Adapted from Koike et al., 2012 and Patke et al., 2020.

## An integrated view of cellular mammalian timekeeping

A part from the TTFL other clocks exist in nature. Cyanobacteria, organisms that lack nuclei, exhibit circadian rhythms and they depend on the protein products of three genes: *KaiA*, *KaiB* and *KaiC* (Kondo et al., 1993, Garces et al., 2004). A network of interactions between the three elements generates dynamics of phosphorylation in KAIC that are the basis for the generation of circadian rhythms (Williams et al., 2002).

In addition, erythrocytes that lack nuclei also exhibit 24-hour rhythms. In this case oscilations in the oxidation of peroxiredoxins were measured in vitro using blood (O'Neil and Reddy, 2011) and while this oscillator fails to explain the timekeeping in mammals, it persists even when there is a deficient TTFL for example when nascent transcription and translation are inhibited (Tomita et al., 2005).

To integrate the signals form the transcriptional dependent and independent clocks, the most updated models position the TTFL as coordinator of different timekeeping signaling and metabolic networks conferring robustness to external perturbations. This new stream pairs well with the idea of how important it is to be programmed and tuned to the 24h day.

#### 1.1.1.2. Coordination of oscillators through the whole organism

##### Cell autonomous clocks

In multicellular organisms almost every cell has its own clock. When these cells are isolated circadian rhythms are still measurable. For example, dissociated neurons from the SCN still have circadian rhythms in their firing rate and clock gene expression (Welsh et al, 1995, Liu et al. 2007). This extends to individual fibroblast maintained in culture (Welsh et al., 2004) whose rhythms persist even if cells divide (Nagoshi et al., 2004). Despite the autonomy of clocks, the synchronization of their phases and the robustness of their rhythms depend on cell communication (Welsh et al, 1995, Liu et al. 2007).

##### SCN: central integrator

In mammals, to achieve coordination of clocks from all cells, the suprachiasmatic nuclei of the hypothalamus acts as a "pacemaker", an "orchestra conductor". The

suprachiasmatic nucleus receives light from the environment, integrates it and transmits this information throughout the whole body. Light information from the eyes is transmitted via the retinal-hypothalamic tract that is formed by the axons of ganglion cells. The axon terminals release glutamate in the ventrolateral region of the SCN activating NMDA and AMPA receptors. This increases firing rates in the recipient cells that will release the VIP and GRP neuropeptides to neighboring cells creating waves of firing. These waves give robustness and make the SCN a robust signal integrator.

The SCN deserves the title of master circadian pacemaker because it uses a variety of outputs that provide temporal information throughout the body. For example, the hypothalamic preoptic nucleus, responsible for body temperature homeostasis has neural connections with the SCN that imposes daily variations of temperature encoding. Temperature changes are able to entrain cultured fibroblasts and other peripheral tissues (Brown et al., 2012, Buhr et al., 2010) therefore; body temperature could be seen as a systemic timing cue from the SCN. Other systemic cues are autonomic nervous system innervation regulating glucocorticoid signaling responsible for the stress response, melatonin secretion and arousal signals dictating sleep and wake times, activity or feeding between others Astiz et al., 2019).

### Peripheral oscillators and its entraining signals

Although the SCN is considered as a central integrator, the independence and influence of peripheral clocks and other signals apart from light are not fully understood. Studies showed that absence of a functional clock in the liver blunts 90% of the circadian transcription (Kornmann et al., 2007) and reconstitution of the clock just in the liver restores a fraction of circadian transcription and metabolism (Koronowski et al., 2019). This indicates that the liver clock is sufficient to generate circadian rhythms in that

tissue. What is the external signal that coordinates the liver clock? Food intake could be one possibility. The evidence for that comes from experiments that changed the food schedule in mice and alter the clockwork phase in liver cells up to 12 hours. After one week, the phase resetting extended to other tissues besides the SCN (Damiola et al., 2000). In addition, manipulation of daily rhythms of food intake disrupts 70% of rhythmic gene expression in the mouse liver (Greenwell et al., 2019).

Apart from the liver clock, new studies in epidermal tissue also show that light can maintain synchronization of epidermal tissue in the absence of a functional clock in the SCN and respond autonomously to environmental changes (Weltz et al., 2019). Besides light and food, a plethora of influences are known to interfere with circadian variables in many species. Of special interest for this thesis are the effects of sleep. In humans, sleep deprivation alters the rhythmic profiles of transcripts and metabolites in the blood, abolishing or changing their phases (Archer et al., 2014, Davies et al., 2014, Honma et al., 2020). In mice, disrupting the sleep wake cycle has also effects on the oscillation of the liver and cerebral cortex transcriptome (Barclay et al., 2012, Maret et al., 2007, Hor et al., 2019). All these pieces of data suggest that the sleep-wake cycle modulates peripheral rhythms in the blood, the liver and the cortex but there is still much to learn.

#### 1.1.1.3. Molecular outputs of clocks

##### mRNA oscillations

The clockwork directly imposes periodicity through the expression of clock-controlled genes. These genes tend to come in two phases, in phase with Per or in phase with Bmal (Ueda et al., 2002). The two sets can change in terms of proportion and entity. In multicellular organisms, looking at the specific circadian mRNAs helps to understand the circadian physiology of any tissue. For example in six areas of the human brain

involved in different brain functions, hundreds of genes display daily rhythms and most of them were specific to each region (Li et al., 2013). In baboons, a close specie to humans, the transcriptional profiles of several tissues across the body were analyzed over 24-h and more than 80% protein coding genes displayed diurnal variation (Mure et al, 2018). Despite the fact that all tissues analyzed had cycling genes, they displayed unique phase distributions, indicating that they have different needs at different times of day. Another comprehensive study from mice, detected as well circadian genes in 12 organs. Thesis phases were as well particular to each but there was a general trend for transcripts to peak anticipating dawn and dusk highlighting a whole organism coordination to enter the rest and activity phases (Zhang et al., 2014).

### Protein oscillations

In the 1990's using pioneering proteomics techniques, the first circadian proteomes were detected in dinoflagellates (Milos et al., 1990). One decade later, liquid chromatography (LC), high performance liquid chromatography (HPLC) and in vivo stable-isotope labeling by amino acids in cell culture (SILAC), allowed large-scale and accurate protein identification and quantification. With these techninques, the rhythmic proteome of mouse liver and SCN were characterized (Chiang et al., 2014, Mauvoisin et al., 2014, Robles et al., 2014). The exponential increase in proteomic approaches continues until today reaching the same accuracy even with label-free methods and detecting not just proteins but their post-translational modifications (Robles et al., 2016).

### Post-translational oscillations

Despite the pervasiveness of circadian transcription and protein rhythms, up to 50% of rhythmic proteins do not have a rhythmic mRNA (Mauvoisin et al., 2014, Reddy et al.,

2006). To explain this discrepancy one must invoke circadian post-transcriptional regulation of RNA, translational control or post-translational modifications on proteins. For example, deadenylation and antisense RNAs can uncouple rhythms of transcription and translation (Kojima et al., 2010, Vollmers et al., 2012). In a separate circadian mechanism, some clock-controlled genes encode ribosomal protein mRNAs and ribosomal RNAs, which in turn influence ribosome biogenesis and thereby generate rhythms in translation rates (Jouffe et al., 2013). At later states, phosphorylation of proteins can be rhythmic and control the time of activity beyond the protein level (Robles et el., 2017).

## 1.1.2. Sleep-wake cycles

### 1.1.2.1. What is sleep?

Sleep is a behavioral state of quiescence. It is different from other quiet states because of the threshold of arousal that is needed to switch to active wake. This level is lower for sleep than for torpor, hibernation or anesthesia (death could finish the list) but is higher than for awake resting.

In nocturnal animals, sleep onset happens at dawn and is regulated by sleep-promoting neurons. Wake onset happens at dusk and it is promoted by wake-promoting neurons (the opposite in diurnal species). These cells are located in diverse but specific brain regions and the SCN is connected directly or indirectly to them (reviewed in Adamantidis et al., 2019). Ablating the SCN in a way that that cuts all its projections eliminates the sleep and wake cycles in nocturnal rodents (Tobler et al., 1983) or diurnal primates (Edgar et al., 1993) indicating circadian clocks are involved in their regulation.

However, sleep patterns are altered depending on their previous history. In fact, sleep is singular from all the other quiet states in that dependency. If sleep is restricted

chronically or prevented acutely, efforts to drive sleep increase concomitantly, meaning sleep is homeostatically regulated (Huber et al., 2011). The idea is that there is a "homeostat" that promotes the compensatory response to sleep loss and regulates, together with circadian clocks, the sleep-wake cycles. Unlike circadian clocks, the molecular nature of the "homeostat" remains unknown.

#### 1.1.2.2. The "homeostat": molecular correlates

The idea of a sleep "homeostat" presumes that homeostatic factors disappear with time spent asleep and accumulate with increased duration of wakefulness, also if wakefulness exceeds the time of a normal cycle. The first attempts to identify gene expression changes following the previous conditions found that in the rat cortex there are sets of genes associated with wakefulness and others with sleep (Tononi and Cirelli., 2001). Rather than correlating genes expression to wake or sleep state, other studies used slow wave activity as readout of the "homeostat". Doing this, microarray analysis of the cortex from different mouse strains identified Homer1 expression as the best correlate to sleep loss after both spontaneous or forced wake (Maret et al. 2007). In addition to transcriptomics, the use of proteomics and phosphoproteomics to detect homeostatic factors is starting to develop. For example, 20% of synaptic proteins and their phosphorylation sites showed regulation between wake and sleep (Diering et al., 2017). Proteinase kinase A and C, calcium- and calmodulin-dependent kinase II or type-1 inositol triphosphate receptor belong to this 20% and their role as signaling molecules could help to understand the molecular components of the sleep homeostat. Similarly, forced wake induced by sleep deprivation also increased phosphorylation levels and up to 80 proteins were identified as sleep-need-index phosphoproteins since their phosphorylation state paralleled EEG changes due to sleep loss (Wang et al.,

2018).

In addition to -omics, forward genetics have also being successful in finding candidates contributing to the molecular basis of the sleep homeostat. A single amino acid mutation of the protein kinase Sik3 increases NREM and sleep need. This mutation impairs the recognition of Protein Kinase A mediated by the adaptor protein 14-3-3 (Funato et al., 2016, Honda et al., 2018).

#### 1.1.2.3. The circadian and homeostatic regulation of sleep

The two-process model of sleep regulation unifies the dual contribution of circadian and homeostatic signals (Borbely, 1982, Daan et al., 1984, Borbely et al., 2016). In this model circadian regulation is represented by process C and sleep homeostasis by process S. Process C follows a cosine oscillation as all circadian rhythms and can be measured through core body temperatures or blood levels of different hormones. Process S increases and decreases exponentially during wake and sleep respectively, and this is reflected in the time course of slow wave activity of electroencephalogram.

The model was postulated to explain 24-h sleep-wake distribution in human but also applies for rodents that are nocturnal and have a polyphasic sleep (Franken et al., 1991, Huber et al., 2000). In rodents, Process S and therefore Slow Wave Activity are low at the beginning of the dark phase. In the first 4 hours, that contain the majority of rodent activity, slow waves increase and reach a maximum with light onset. From there, mice have their larger sleep episodes and slow waves decrease exponentially to reach minimums. Forced wake using sleep deprivation starting at light onset prolongs the exponential increase until the end of the disturbance, and then start decreasing and reach the same minimums as if no deprivation occurred (Huber et al., 2000).

#### 1.1.2.4. Circadian and sleep interaction

Circadian and homeostatic processes can work independently, and a proof for that is that homeostatic sleep regulation happens even in arrhythmic animals where the circadian pacemaker has been lesioned (Tobler et al., 1983).

In addition, homeostatic and circadian mechanisms influence each other. The first observations of how sleep-wake state feedback onto the clock appeared almost by serendipity. Back in the 80's it was proven that social interactions could interfere with the phase of the pacemaker (Mrosovsky, 1988). More dedicated experiments came later to show that some arousal signals such as running (stimulated by the access to a wheel) were able to entrain free-running rhythms (Yamanaka et al., 2013). Changing the experimental strategy, using sleep deprivation as a way to interfere with the normal dynamics of the homeostat has been shown to attenuate phase shifts that are normally induced by light (Challet et al., 2001, Burgess, 2010). In the other direction, studies with clock mutant mice showed that the homeostatic response depends on internal circadian time. For example, Cry1/2 double mutants and Bmal1 knockouts, which are arrhythmic, have an overall intense NREMS in base line and they lack a rebound after sleep deprivation (Wisor et al., 2002, Laposky et al., 2005). Per3 knockout mice show also increased NREMS in the light phase or after sleep deprivation (Hasan et al., 2011) and Per1,2 double knock out mice, despite expressing a normal sleep wake cycle, had also higher sleep drive after sleep deprivation (Shiromani et al., 2004). And the description of phenotypes can be extended to other clock genes such as Clock, Npas, CKe, Cbp or Dec2 (reviewed in Franken and Dijk, 2009).

## 1.1.3. Circadian versus sleep regulation of daily rhythms in neurobiology

### 1.1.3.1. Electrophysiological observations

Electrical activity of living neurons follows daily cycles. In both rats and monkeys, the amplitude of excitatory postsynaptic potentials of the granule cells of the hippocampus oscillates and is larger during the active phase of the animals; the dark phase in rats and the light phase in monkeys (Barnes et al., 1977). Also from hippocampal slices, where synaptic inputs from other brain areas are removed, the incidence and magnitude of long-term potentiation changes between the light and dark phases (Harris and Teyler, 1983, Nakatsuka and Natsume, 2013). At the brain scale, slow waves also change between day and night (Borbely, 1982). Concomitant with their increase, toxin clearance and cerebrospinal fluid flow are boosted (Xie et al., 2013, Hablitz et al., 2019, Fultz et al., 2019).

In the previous examples, the transition between wake and sleep happens simultaneously with critical transition times for the circadian cycle. It would be wrong to attribute cycles of synaptic potentials, LTP, slow waves and brain flow solely to circadian clocks or the sleep homeostat.

### 1.1.3.2. Morphological changes

Synaptic spines appear or disappear and enlarge or shrink in a very dynamic way. Some of these changes are coupled to the time of day. In rat hippocampus, spine density is higher at the beginning of the night, the time when peak performance on working memory tasks is observed (Ikeda et al., 2015). In mice somatosensory cortex, inhibitory synapses increase in density during the dark phase coinciding with maximum locomotor activity. By contrast the number of excitatory synapses is highest during the

light phase (Janinska et al., 2014). The formation of spines and filopodia (precursors of mature spines) is higher during the dark period while the elimination, during the light period (Yang and Gan, 2012) and two-photon microscopy on young mice revealed that spine gain prevails during wake, resulting in a net increase in spine density, while spine loss is larger during sleep, resulting in a net spine decrease (Maret et al., 2011). Those daily morphological fluctuations of synapses were linked to sleep cycles in "The synaptic homeostasis hypothesis" dictating that during the wake phase, synaptic potentiation predominates, and during the sleep phase, downscaling (Cirelli and Tononi, 2003 and reviewed in Tononi and Cirelli, 2014).

Due to the concomitance of sleep with the dark and wake with light in the previous experimental set-ups, if synaptic remodeling depends on sleep state or on circadian time might be debated.

#### 1.1.3.3. Sleep deprivation around the clock to differentiate between circadian and sleep regulation

At light onset in normal conditions (ZT0), slow wave activity in mice is the highest. However, 4h or 6h of sleep deprivation starting from that point, increase slow waves until a new maximum. Similarly, if sleep deprivation starts at other times of day when slow wave activity is lower, the increase reaches always the previous asymptotic value (Huber et al., 2000, Maret et al., 2007, Noya et al., 2019). Measuring slow waves in sleep deprived animals were the sleep deprivation starts at different times of day; a model can be derived where Process S is constantly high rather than oscillatory (Figure. 2)

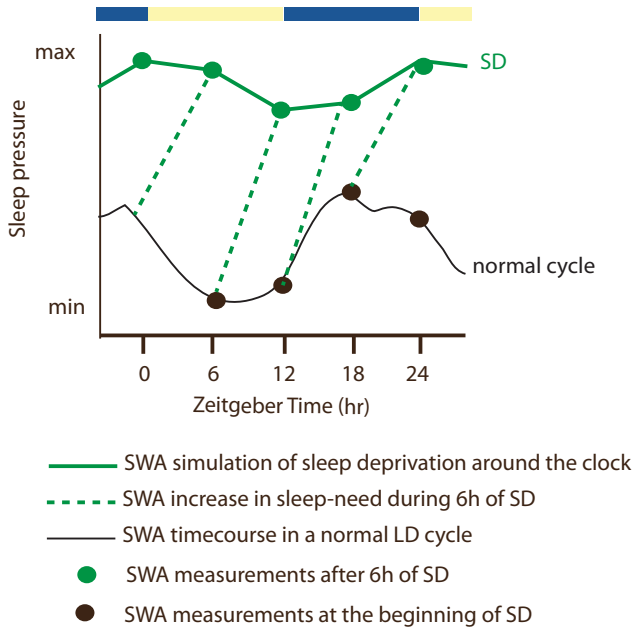


Figure 2. Simulation of sleep need in the around-the-clock sleep-deprivation experiment. (Adapted from Maret et al., 2007).

Using the sleep deprivation around the clock, it was shown that the expression of some genes paralleled the slow wave model indicating that daily dynamics of gene expression depend on circadian and homeostatic or solely homeostatic regulation (Maret et al., 2007). However there were some genes whose expression did not change with the sleep deprivation and the dynamics were still circadian.

The application of this experimental design in the morphological and electrophysiological studies described previously would have helped to shed light onto the extent to which circadian and sleep contribute to daily rhythms of neurobiological processes.

## 1.2. The role of synapses in neurobiology

Neurophysiology and neuromorphology have focused around synapses. This is not surprising, because if neurons are cells specialized to transmit signals, synapses are the

structures where this happens.

Dendrites and axons are filaments that extrude from the cell body of neurons like branches of a tree. The majority of synapses of a cell are located along them. Although single synapses have a low effect on the propensity to generate an action potential, collectively they are essential in the context of neuronal networks or brain physiology. And there are a few reasons for that; their volume represents about 30 to 60 times more of the soma, they are capable of specialized information processing and synapses from a single neuron can be connected throughout extensive regions of the brain.

### 1.1.4. The autonomy of synapses

#### 1.1.4.1. RNA transport

The specialization of dendritic function is in part due to the differential localization of mRNAs at synapses. The most updated numbers estimate that more than half of a neuron's transcriptome can be found at synapses (Cajigas et al., 2012). A simple diffusion of RNAs through the cytoplasm fails to explain that only specific RNAs can reach the synapses. Indeed, different models for a directed transport have being formulated (Palacios and Johston, 2001, Doyle and Kiebler, 2011) and all of them include three common features; synaptic RNAs have specific signals, these signals are recognized by RNA binding proteins (RBPs) to form complexes, and the complexes use motor proteins to travel along the cytoskeleton.

The signal on mRNAs that targets them to specific locations are called cis-acting elements. The best characterized cis-acting elements locate at the 3'UTR end and have the following features: they can repeat and be redundant, the steps of the transport process are mediated by different elements, and both the sequence and the secondary structure can be recognized by RNA-binding proteins (RBPs) (reviewed in Martin and

Ephrusi, 2009).

The studies to identify RBPs in the nervous system have found a plethora of proteins that recognize synaptic mRNAs. Between them ZBP1, cytoplasmic polyadenylation element binding protein 1 (CPEB1), fragile X mental retardation protein (FMRP), Staufen1, Staufen2, Pumilio and Pur alpha (Pur α) are the best characterized (reviewed in Tolino et al., 2012). The role of RBPs goes beyond the recognition of synaptic mRNAs. They participate in the export through the nuclear pores, facilitate the assembly of the transport granules or recruit adaptor and motor proteins between others (reviewed in Marchand et al., 2012) and with technical improvements (Schieweck et al., 2018), more and more RBPs have been discovered.

To help molecules to arrive to synapses, neurons have a dynamic and organized cytoskeleton that serves as a road network for motor proteins. In axons and dendrites, microtubules and neurofilaments form longitudinal filaments and in spines, actin assembles tridimensional scaffolding. Depending on the nature of the cytoskeleton and the direction of movement, the molecular motors responsible to move cargoes are different. Of specific interest for us are the motor proteins that move RNA granules from the neuron soma along axons to reach postsynaptic sites, the kinesins, and along dendrites to reach presynaptic sites, the kinesins and dyneins (reviewed in Hirokawa et al, 2006).

#### 1.1.4.2. Local translation

Synapses can autonomously conduct translation. The first evidence of this came with electron micrographs showing a few sparse polysomes near or inside dendritic spines (Steward and Levy, 1982). From this observation developed the idea that in basal conditions local translation is a minor source of synaptic proteins (Kosik et al., 2016).

Translation rates change when for example long-term potentiation is induced, under glutamate uncaging or neuronal silencing (Buxbaum et al., 2014, Yoon et al., 2016, Bauer et al., 2019). This is, synaptic activity allows synapses to remodel individually by enhancing local translation (Hanus and Schuman, 2013). In addition, the effects of synaptic activity goes beyond just translation, and regulates as well the mRNA sorting to synapses before translation (Sharangdhar et al., 2017, Bauer et al., 2019), the localization to active sites (Johnson et al., 2006), or the modulation of post-translational modifications such as phosphorylation, methylation, or sumoylation (reviewed in Martin and Ephrusi, 2009).

Local translation may have a much larger effect than originally thought. For example the Camk2a protein levels decreased an 85% when the mRNA was deleted only in dendrites (Miller et al., 2002). And this might not be an isolated case because synaptic mRNAs are preferentially translated by monosomes, a ribosome population that is predominantly active in neuronal processes (Hafner et al., 2019, Biever et al., 2020) that until now was not considered in most of the studies about active translation.

Probably both basal and activity-dependent synaptic translation is important: individual synaptic fine-tunings will sum up and reflect the adaptation of brain function to external inputs. Multi-omics approaches can serve as the integrative strategy to compare basal conditions and activity changes at the level of mRNA, protein and its modifications in a way that has been beyond our reach until now.

### 1.1.5. Molecular complexity of synapses

Visualizing polysomes with electron microscopy in synapses across the brain exposed the possibility of local translation (Steward and Levy, 1982) and the homeostatic synaptic hypothesis was supported by the broad and dynamic visualization of plasticity

using two-photon microscopy (Tononi and Cirelli, 2015). These are examples of how unbiased and system-wide approaches can integrate thousands of single synaptic signals into a comprehensive view of brain function. From the biochemical palette, -omics can help on characterizing this view but there are some challenges to overcome. First, the preparation of the sample should separate synapses from the rest of the cell and second the technique should be sensitive enough to identify and quantify molecules that might have low copy numbers.

During the last decade, the technical developments in genomics led into the first synaptic transcriptome of the brain by microdissecting individual synaptic neuropils from the rat hippocampus (Cajigas et al., 2013). This synaptic neuropil comprises dendrites, axons, glia, and a sparse population of interneurons, but lacks principal neuron cell bodies. Other synaptic transcriptomes were obtained after biochemical purification of synaptoneurosomes (Kimberly et al., 2006). Doing this, synaptic mRNAs are concentrated, thereby increasing the ratio of synaptic to somatic mRNA and allowing discrimination of expression changes in synaptically localized genes.

This sample preparation strategy served to show for the first time a large-scale remodeling of the synaptic proteome and phosphoproteome comparing wake and sleep (Diering et al., 2017) reflecting the potential of mass spectrometry-based proteomics to investigate synaptic proteins and their functions in an unbiased way (Hosp and Mann, 2017).

With the material and the techniques available now, the molecular system-wide analysis of synapses might be the way to go to meet the players of the sleep “homeostat” or to identify what is exclusively regulated by circadian or sleep cycles.

# 2. Aims

Transcriptional control is the most studied direct output of circadian clocks. Unbiased high-throughput transcriptomics has already served to identify aspects of physiology with circadian rhythmicity, explaining the partitioning in time of different cellular processes and behaviors. Technical advances allowed the expansion of circadian -omics to proteins and their modifications, and to resolve even small cellular compartments. Yet, the circadian transcriptomics, proteomics and phosphoproteomics of brain synapses were never studied. **The first aim of this thesis was to create for the first time a comprehensive catalog of the mRNA, protein and phosphorylations occurring in mouse brain synapses over time.** In this way, the temporal compartmentalization of synaptic function could be examined. To achieve that, synapses of the mouse forebrain were isolated using a biochemical procedure, the synaptoneurosomal fractionation. This technique compares the initial tissue, in this case the forebrain, with an enriched version containing pre- and postsynaptic elements. The samples were obtained from a time course across 24 hours and mRNAs, ,proteins purified . Then, transcripts, proteins and phosphopeptides were quantified and temporal dynamics evaluated using algorithms that detect cycling elements with a period of 24 h.

The oscillations in synaptic mRNAs, proteins and phosphorylations across the day could result from endogenous clock regulation. However, slow waves that characterize the homeostatic sleep process undergo daily cycles and rely on synaptic communication. Therefore the molecular oscillations could also be the cause or consequence of sleep homeostasis. While research has focused on identifying behavioral, physiological and cellular processes regulated by circadian or sleep homeostasis mechanisms, our unbiased molecular screening emerges as an ideal way to

shed light on the relative contribution of each at the molecular level. Therefore, **the second aim of the thesis was to identify the contribution of circadian clocks and homeostatic sleep on oscillations of mRNAs, protein and phosphorylation.** To do that we disentangled circadian and sleep cycles and searched for mRNAs, proteins and phosphorylations whose cycles in the 24 h time course no longer fit circadian criteria under conditions of sleep deprivation. The intervention consisted of elevating the sleep pressure at different times in the circadian day roughly until the maximum reached in a normal day.

# 3. Declaration of Contributions

I declare that this thesis was composed by myself, that the work contained herein is my own except the contributions stated in the following paragraph and the Acknowledgement sections of the manuscripts cited below. I also declare that this work has not been submitted for any other degree or processional qualification except the two manuscripts cited below.

- Specific mention to Jessica Willi, Yulia Gonskikh and Norbet Polaceck for their collaboration in a pilot study mentioned in the Discussion and Outlook.
- Parts of this work have been published in;
    - Brüning, F., Noya, S.B., Bange, T., Koutsouli, S., Rudolph, J.D., Tyagarajan, S.K., Cox, J., Mann, M., Brown, S.A., and Robles, M.S. (2019). Sleep-wake cycles drive daily dynamics of synaptic phosphorylation. Science *366*.
    - Noya, S.B., Colameo, D., Brüning, F., Spinnler, A., Mircsof, D., Opitz, L., Mann, M., Tyagarajan, S.K., Robles, M.S., and Brown, S.A. (2019). The forebrain synaptic transcriptome is organized by clocks but its proteome is driven by sleep. Science *366*.

# 4. Results

## 1.3. Results Preamble

This thesis follows a cumulative format. Therefore the results to answer the aims stated in the previous sections are shown and compiled in two published manuscripts.

Each manuscript is included as the full published version preceeded by the structured abstract and figure captions. Materials and Methods and Supplementary Figures are included in the Appendix. Tables can be accessed in the indicated links in the Appendix. Databases can be accessed online using the guidelines described in Data and materials availability also included in the Appendix.

## 1.4. Manuscript 1.The Forebrain Synaptic Transcriptome is Organized by Clocks, but its Proteome is Organized by Sleep

Sara B. Noya[1], David Colameo[1], Franziska Brüning[2,4], Andrea Spinnler[1], Dennis Mircsof[1], Lennart Opitz[3], Matthias Mann[4], Shiva Tyagarajan[1], Maria S. Robles[2], and Steven A. Brown[1]

**INTRODUCTION:** Temporally consolidated behaviors such as sleep normally occur in synchrony with endogenous circadian rhythms and both have been reported to contribute to global daily oscillations of transcription in brain. Neurons have further adapted specialized means to traffic mRNA into distant dendritic and axonal arbors, where it is locally translated. Together, these mechanisms allow coordination of physiology with environmental needs.

**RATIONALE:** About six percent of the forebrain transcriptome oscillates in a time-of-day dependent manner, and it has been proposed that this oscillation is mostly driven by sleep-wake state to enable daily changes in synaptic structure and function. In turn, such synaptic scaling is thought to form a critical feature of the sleep-wake process. Given the highly local capacity for synaptic remodeling, an essential missing link in this argument is the effects of circadian clocks and sleep pressure upon mRNA and related protein abundance at synapses themselves. To address this question, we examined daily rhythms in of transcript and protein abundance in transcriptome and proteome of synapses from the mouse forebrain, using biochemically purified synaptoneurosomes isolated across the 24-hour day both at normal sleep pressure and at constant high sleep pressure.

**RESULTS:** Remarkably, 67% of synaptic mRNAs show circadian oscillations, with a mean amplitude of more than twofold. 93% of these oscillating

transcripts were exclusively rhythmic in synaptoneurosomes, suggesting an entirely posttranscriptional origin for synaptic mRNA oscillations. This observation was supported by single-molecule fluorescence in situ hybridization. Rhythmic synaptic transcripts formed two distinct waves, anticipating either dawn or dusk, and both required a functional circadian clock. These two waves showed completely different functional signatures: synaptic signaling preceded the active phase, while metabolism and translation preceded the resting phase. Comprehensive circadian characterization of the synaptic proteome demonstrated the functional relevance of this temporal gating for synaptic function and energy homeostasis. Overall, the oscillations of 75% of synaptic proteins were concomitant with their rhythmic transcripts, indicating a key role for local synaptic translation. Under conditions of high sleep pressure, one fourth of mRNAs remained identically circadian, and most preserved some degree of circadian rhythmicity. In striking contrast, no significant circadian rhythm could be detected in any protein when sleep pressure was constantly high.

**CONCLUSION:** Examining the dynamics of mRNAs in the synaptic landscape revealed the largest proportion of circadian transcripts in any tissue, cell or organelle described to date. These synaptic oscillations are controlled posttranscriptionally and the daily dynamics of transcripts and their related proteins clearly delineate different cellular modes between sleep and wake. Our study provides novel insights into the connectivity between sleep and circadian rhythms, and suggests an elegant paradigm whereby a molecular clock provisions synapses with mRNAs prior to dawn and dusk, that are later translated in response to activity-rest cycles.

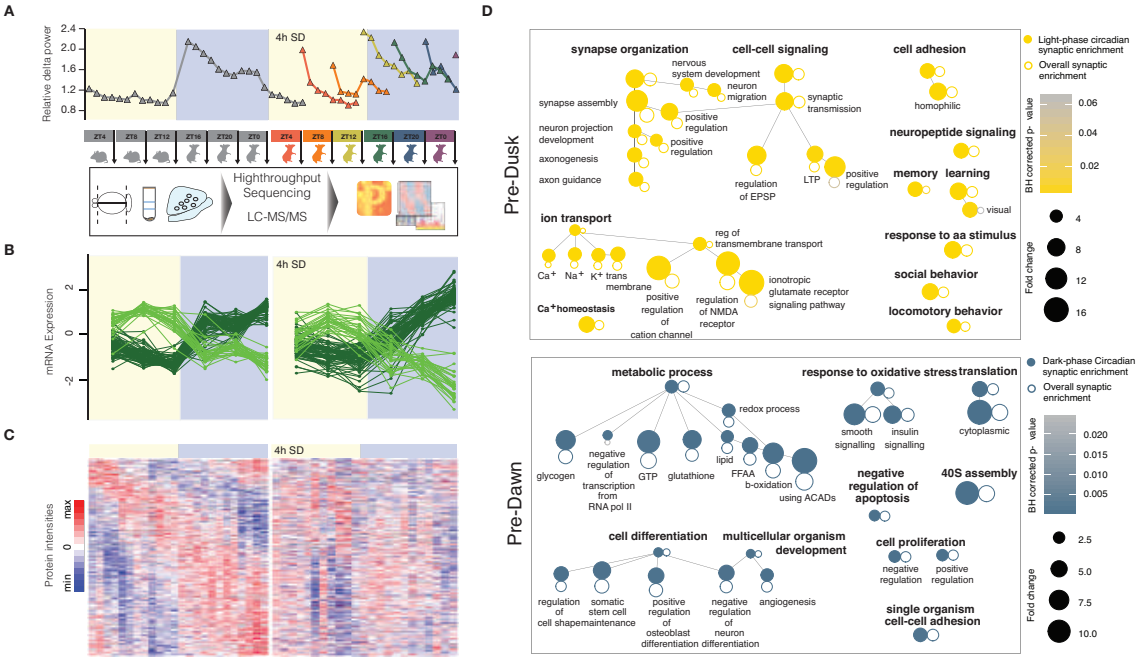


**Circadian clocks regulate synaptic mRNAs but sleep regulates their proteins. (A)** Workflow: Forebrain synaptic transcriptome and proteome across the day at high and low sleep pressure. **(B)** One forth of synaptic transcripts maintains identical circadian rhythmicity under high sleep pressure, but **(C)** all proteomic circadian rhythms are abolished. **(D)** Gene ontology highlights the complete temporal segregation of pre-dawn and pre-dusk synaptic function.

### 4.1.1. Entire manuscript 1

**Abstract**

Neurons have adapted mechanisms to traffic RNA and protein into distant dendritic and axonal arbors. Taking a biochemical approach, we uncover that forebrain synaptic transcript accumulation shows overwhelmingly daily rhythms, with two thirds of synaptic transcripts showing time-of-day-dependent abundance independent of oscillations in the soma. These transcripts formed two sharp temporal and functional clusters, with transcripts preceding dawn related to metabolism and translation, whereas those anticipating dusk to synaptic transmission. Characterization of the synaptic proteome around the clock demonstrates the functional relevance of temporal gating for synaptic processes and energy homeostasis. Surprisingly, sleep deprivation completely abolished proteome but not transcript oscillations. Altogether, the emerging picture is one of a circadian anticipation of mRNA needs in the synapse followed by translation as demanded by sleep-wake cycles.

**One Sentence Summary:** In forebrain, a circadian transcriptome but a sleep-driven proteome.

**Introduction**

A cell-autonomous circadian clock based upon feedback loops of transcription and translation functions in nearly every cell of the mammalian body, and influences most aspects of physiology. In the brain, the most obvious manifestation of circadian control is the consolidation of sleep into day or night. In synchrony with sleep and wake, daily rhythmic oscillations also occur in a significant fraction of the brain transcriptome, ranging from 3-4% in retina,

cerebellum, brainstem, and hypothalamus to 8-10% in cortex and suprachiasmatic nuclei (*1-4*). These oscillations are likely driven in part by rhythmic assembly and disassembly of transcription complexes and chromatin modifiers orchestrated by circadian clock-specific activators and repressors like BMAL1/NPAS1, PERIOD (PER1 and PER2) and CRYPTOCHROME (CRY1 and CRY2), as observed in other tissues (*5-8*). However, it has become increasingly apparent that post-transcriptional processes play an important role in circadian regulation. In liver and suprachiasmatic nuclei (SCN), the best-studied circadian tissues to date, evidence of circadian messenger RNA (mRNA) processing, polyadenylation, and translation have appeared (*9-11*). Complicating matters still further, circadian oscillations in mRNA levels can also be driven by temporally consolidated behaviors. In liver, timing of food intake contributes to rhythmic transcription (*12*); and in cortex, sleep-wake cycles play a major role (*3*).

Relative to all other cell types, neurons present a special case because mRNA is distributed to potentially distant compartments like axonal terminals and postsynaptic spines. Although the axodendritic arbor contains only around 10% of total transcripts (*13*), a large literature demonstrates that mRNAs are actively transported to neurites (*14-16*). Downstream, local synaptic translation of mRNA has been postulated to be an important mechanism in memory (*17, 18*), and both synaptic size and total protein abundance are dynamically scaled by wake and sleep (*19, 20*).

Despite this context, circadian and sleep-wake-dependent regulation of synaptic transcript pools in brain, as well as their functional importance, remain entirely unexplored questions. Multi-omic approaches have been increasingly employed to understand complex questions of cellular regulation, and therefore

might also be useful to explore the connectivity between the clockwork and sleep (*21*). In this paper, we employ a combination of biochemical fractionation, deep sequencing, single-transcript confocal microscopy, and mass spectrometry (MS)-based quantitative proteomics to analyze the origin and function of rhythmic daily oscillations in the transcripts and proteins of forebrain synapses. From these studies, we derive the simple paradigm that a clock-gene dependent mechanism is needed to provision synapses with mRNAs in circadian fashion, which are then translated in response to sleep-wake cycles.

## Results

### The forebrain synaptic transcriptome shows pervasive daily rhythmicity

To generate a time-resolved map of the synaptic transcriptome from the mouse forebrain, we purified synaptoneurosomes using biochemical fractionation with discontinuous Percoll gradients (*22*). Synaptoneurosomes represent axonal nerve terminals (cytoplasm, synaptic vesicles, mitochondria, and cytoskeleton) and attached postsynaptic structures. We collected forebrains every 4 hours (h) across the day in biological triplicates under natural conditions (light:dark; LD), and identified mRNAs by high-throughput sequencing in the forebrain homogenates and the purified synaptoneurosomes (Fig. 1A). After normalization and thresholding (see Materials and Methods) we detected 14073 unique transcripts. These transcripts overlapped almost completely with those identified in the hippocampal neuropil (*23*), a highly projection-enriched brain region (Fig. 1B), as well as with other similar transcriptomes of forebrain synapses (*24*)(fig. S1A). In addition, quantitative PCR (qPCR) demonstrated enrichment of known synaptic mRNAs and depletion of nuclear ones (fig. S1B). These measures confirm the validity of our biochemical approach. In total,

reasoning that a fold change ≥ 1.5 in synaptic vs. forebrain abundance should represent a reasonable criterion to identify a specific synaptic element, we found 3104 unique synaptically enriched mRNAs (Fig. 1B and Table S1). Gene ontology analysis corroborates the overwhelming predominance of synaptic annotations among these transcripts, as well as their stepwise enrichment across the analytical steps of the procedure (Fig. 1C).

Using the Perseus computational platform (*25*), we analyzed these synaptic enriched mRNAs for evidence of daily rhythmicity (period 24h, $q<0.05$), and found that 2085 (67%) were cycling, the highest proportion of rhythmic transcripts estimated in any tissue, cell or organelle described to date (Fig. 1D and Table S2; results with other q-value cutoffs shown in fig. S1C). The average fold change was 1.8 (Fig. 1E) and the majority showed a peak-trough amplitude of 1.5 or greater (fig. S1D). The 2085 cycling features overlapped substantially with those detected using other algorithms (91% with JTK; period=24 h, $q<0.05$) (*26*) (fig. S2A). In parallel we analyzed the forebrain transcriptome and found that only 6% of it was oscillating (Fig. 1F, fig. S2B and Table S3). Remarkably, 93% of synaptic circadian transcripts were cycling exclusively in the synapse, only 7% were cycling also in the whole forebrain and with reduced amplitudes (Fig. 1G and fig. S2C). This minimal overlap implies that daily oscillations in the synaptic transcriptome are entirely or nearly entirely driven by post-transcriptional processes.

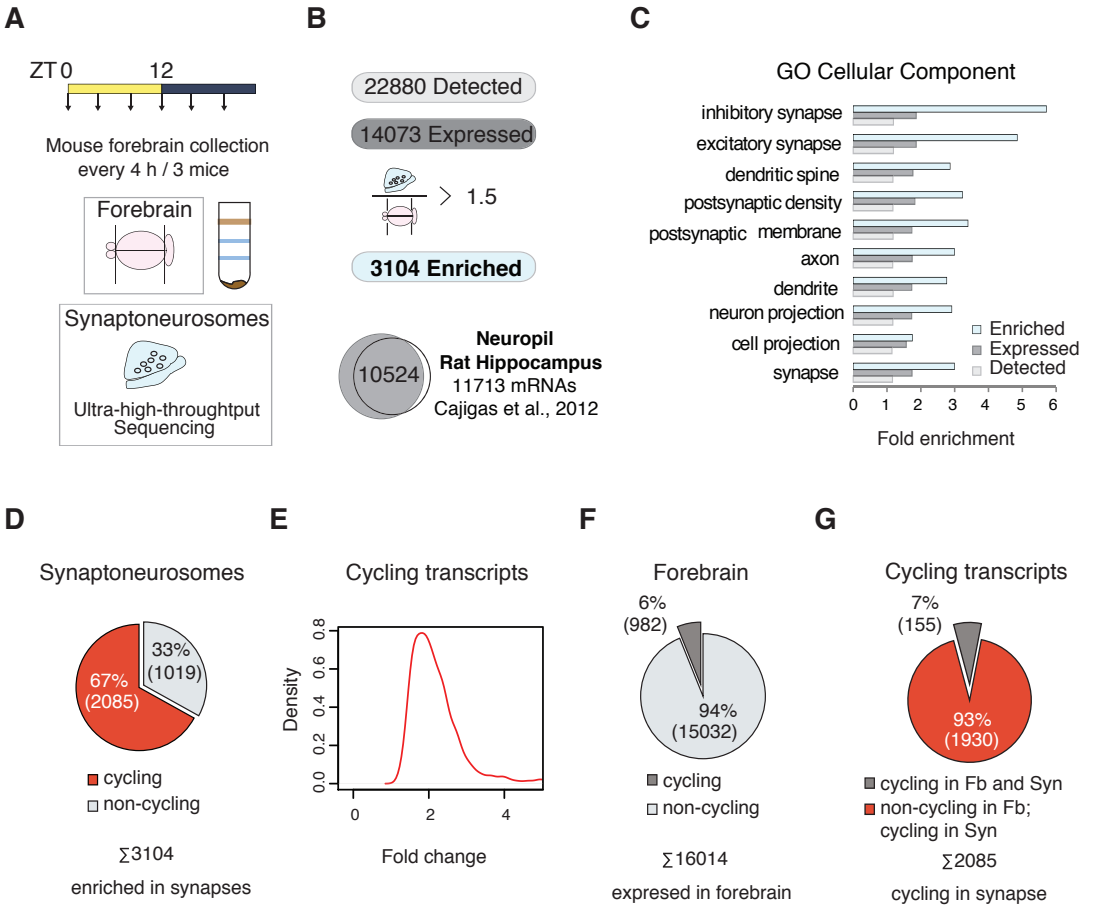


**Fig.1. Daily rhythms within the synaptic transcriptome. (A)** Workflow: Forebrains from mice were collected in biological triplicates at 6 times across the day. Synaptoneurosomes were prepared, RNA isolated and sequenced, followed by data analysis using the Perseus software. **(B)** Number of transcripts from successive steps of the synaptoneurosome workflow. Synaptic transcripts were those 1.5x fold enriched in synapses versus total forebrain. (Right) Detected transcripts correspond closely to those identified in synaptic neuropil. **(C)** Top ten GO Cellular Component annotations (http://www.funrich.org, BH adjusted p<0.001) in the synaptic transcriptome. Bars show the calculated fold enrichment versus the mouse genome for synaptic-enriched (blue), detected (light grey) and expressed (dark grey) GO-associated transcripts. **(D)** Pie chart depicting the fraction of cycling mRNAs (period=24h, q-value<0.05) among enriched synaptic mRNAs. **(E)** Density distribution of circadian amplitudes (peak/trough) of cycling synaptic transcripts from D. **(F)** Fraction of cycling mRNAs (period=24h, q-value<0.05) in the whole forebrain. **(G)** Comparison of synaptic-enriched circadian RNAs in synaptoneurosomes versus total forebrain. Note that of the synaptic cycling mRNAs (2085) only 7% (155) cycle in the forebrain and the synapse (grey) and 93% (1930) have cycle exclusively in synapses.

In principle, oscillations in the abundance of synaptic transcripts could arise either from transport of mRNAs, or from local control of their stability. Both to verify our transcriptional results and to distinguish between these possibilities, we employed single-mRNA *in situ* hybridization (FISH) using the mRNAscope® strategy (see Materials and Methods). As test cases, we selected the vesicular glutamate transporter *Slc17a7* (Vesicular Glutamate Transporter 1) and *Lingo1* (Leucine Rich Repeat And Ig Domain Containing 1), with previously reported synaptic function, high levels of expression in hippocampal *Cornu Ammonis* area 1 (CA1) and cortex (*27, 28*) and with high amplitude in our circadian analysis. As a control, the circadian clock mRNA *Cry1* was also imaged. Using custom automated imaging workflows (see Materials and Methods) we visualized and quantified axodendritic and somatic mRNAs separately in hundreds of images. Similar to previous reports (*29*), *Cry1* mRNA in the hippocampus increased towards the end of the dark period, and the same trend was observed in the cortex (fig. S3 A and B). For synaptic cycling mRNAs, robust oscillations were observed in the axodendritic compartment (Fig. 2A and fig. S4), with maximum levels at Zeitgeber Time (ZT) 4 and trough levels at ZT12 in both CA1 and cortex (Fig. 2B). We further quantified CA1 dendritic structures according to distance from the pyramidal cell layer. Equal daily rhythms of mRNA abundance were observed at all distances (Fig. 2C). Even though synaptic density dramatically increases with distance (*30*), we found identical circadian amplitude at all distances, suggesting that the synaptic oscillations of transcript abundance are likely generated through transport along the dendritic arbor. However, other explanations such as regulated RNA stability certainly also remain possible.

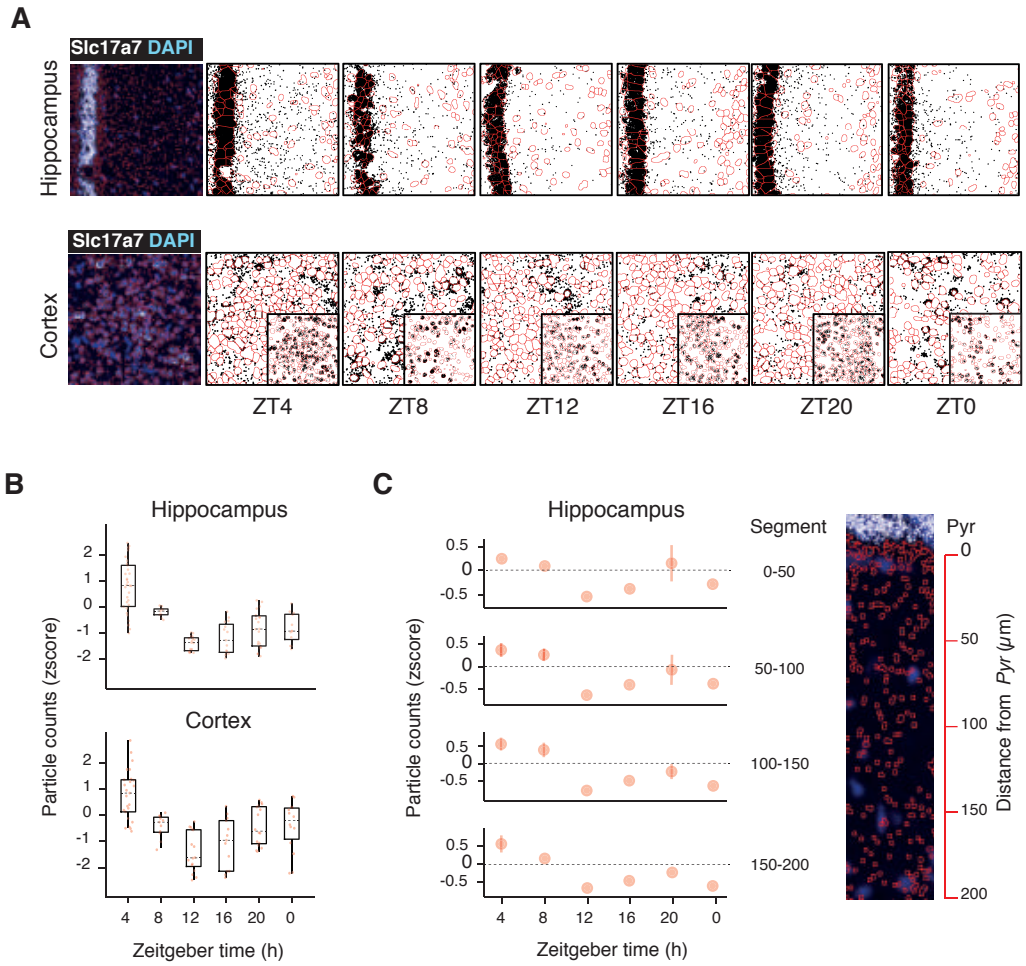


**Fig. 2. mRNA FISH visualization of *Slc17a7 (VGlut1)* diurnal abundance in hippocampus and cortex. (A)** Confirmation of rhythmicity by single-molecule fluorescence in situ hybridization (FISH) of *Slc17a7 (VGlut1)* in the *stratum radiatum* of the CA1 of the hippocampus (top panels) and in the axodendritic compartment of cortex (lower panels). For better visualization, red line traces nuclei, and single mRNA speckles are increased to 0.5 µm. Insets: mRNA in the somatic areas of the cortex. **(B)** Quantification of mRNA abundances in A (n=13-18, from 3 biological replicates). **(C)** Quantification of mRNA in *stratum radiatum* normalized and plotted as a function of distance from the *pyramidale (Pyr)* segments. Sample image shown at right.

## Synaptic oscillations anticipate dawn and dusk and depend on a functional clock

Cycling synaptic transcripts clustered entirely into two temporal categories, with maxima anticipating dawn or dusk (lights-on and lights-off in our laboratory scenario; Fig. 3A). Because these peaks of transcript accumulation

anticipated light-dark transitions, we hypothesized that they were driven by a circadian clock. To verify this presumption, we did synaptoneurosome transcriptome analysis at two time points (ZT0 and ZT12) from mice kept in normal light-dark conditions, kept in constant darkness, or from *Bmal1* knockout mice (*Bmal1*$^{-/-}$), which lack an essential clock gene and therefore lack a functional circadian oscillator (*31*). Transcripts showing significant differences in abundance (exact binomial test, BH corrected p<0.05) between the two times in wild type mice under LD (Fig. 3B; significant in red) also showed differences when kept in darkness (Fig. 3C; significant in dark grey). Conversely, no significant changes were observed for those transcripts in *Bmal1*$^{-/-}$ mice (Fig. 3C; significant in green).

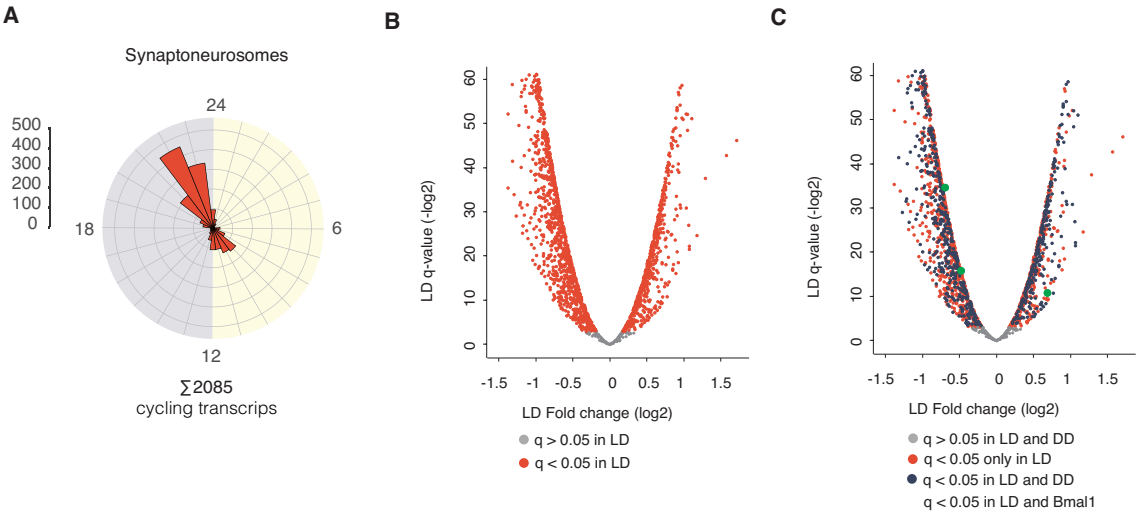


**Fig. 3. Synaptic RNA abundance anticipates dawn and dusk, and depends on a functional circadian clock. (A)** Phase distribution of the rhythmic synaptic transcriptome in LD. Angular axis, Zeitgeber Time; Magnitude, number of transcripts peaking at indicated time. **(B)** Volcano plot representing the fold change and q-value between ZT0 and ZT12 for the total synaptic rhythmic transcriptome from mice kept under light:dark conditions (12:12). Red dots, mRNAs with abundance significantly different between times (t-test, q<0.05, n=3); grey dots, mRNAs not significantly different. **(C)** Volcano plot as in B, where mRNAs are labeled as follows: red, significant differences between ZT0 and ZT12 only (i.e. in light:dark conditions only); blue, significant differences between CT0 and CT12 as well (i.e. after 48 h of dark:dark conditions); green, significant differences between the same time points in *Bmal1*-/-clock-deficientmice after

48 h of dark:dark conditions. For visualization purposes the three significant dots were enlarged). n=3.

The two waves of transcript abundance that we detected were not only sharply segregated by phase, but entirely ontologically distinct (Fig. 4A and B; fig. S5 and Table S4). Moreover, the light and dark circadian synaptic clusters were further enriched in specific biological processes compared to the whole synaptic transcriptome (fig.S5 and Table S4), emphasizing an important temporal and local regulation. mRNAs anticipating dusk participate in cellular pathways related to synapse organization, synaptic transmission, and higher functions directly relying on them such as memory, learning and behavioral outputs (Fig. 4A). Those anticipating dawn are required for metabolism, with a high representation of lipid catabolism, translation and cell proliferation or development (Fig. 4B).

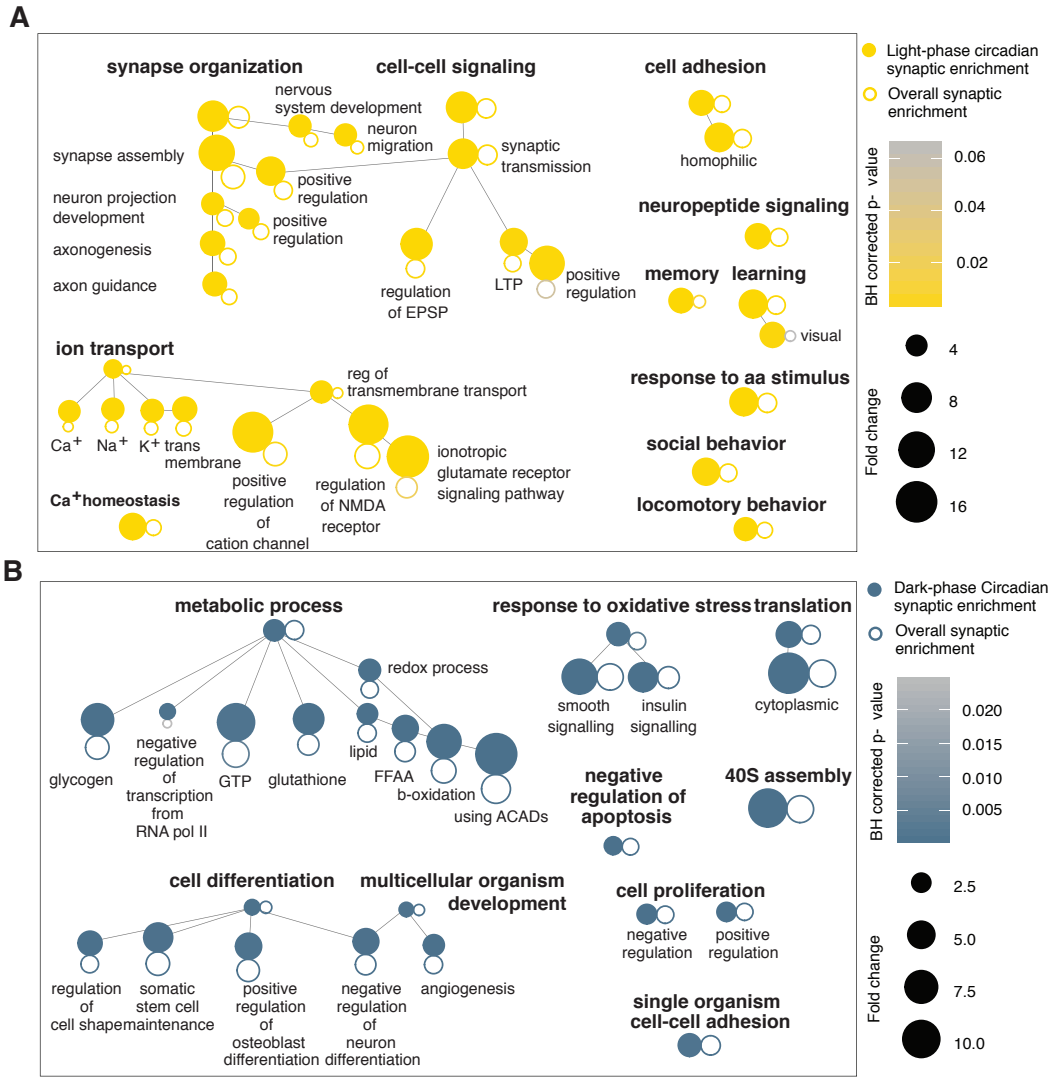


**Fig. 4. Pre-dawn and pre-dusk mRNAs relate to specific and distinct functions. (A)** Gene Ontology analysis of Biological Processes enriched in the light (pre-dusk) mRNA cluster (725 genes), grouped according to ontological hierarchy. Circle size is proportional to the fold enrichment and color is proportional to significance. Higher-level annotations are in bold. (http://www.funrich.org, BH corrected p<0.001). Open circles, enrichment for the same terms in the overall synaptic transcriptome. (Note the decrease in fold enrichment and significance for most annotations.) **(B)** Same as in A, but for the dark peaking (pre-dawn) mRNA cluster (1217 genes).

## Coordination of daily mRNA oscillations by circadian clocks and sleep cycles

The major behavioral output of the circadian oscillator in brain is the sleep-wake cycle. At the level of the whole forebrain, it has been demonstrated previously that the vast majority of "circadian" transcription is actually sleep-

wake driven (*3*). To arrive at this conclusion, the authors systematically deprived mice of sleep for the six hours preceding sacrifice at four different times of day during the circadian cycle, thereby keeping sleep pressure high across all samples (*3*, *32*). By so doing, they observed that circadian oscillations of most brain transcripts disappeared. To test whether synaptic mRNA oscillations are controlled by sleep pressure, we first derived an analogous protocol in which sleep pressure would be kept elevated across the circadian day at levels roughly equal to its normal 24h maximum under undisturbed conditions. Typically, sleep pressure is indicated by the amplitude of subsequent electroencephalogram (EEG) oscillations during sleep: the greater the sleep pressure, the greater the amplitude of "delta" oscillations (0.5-4Hz) (*32*). As can be seen in Fig. 5A and B, across six equally spaced time points during the day, four hours of prior sleep deprivation by gentle handling leaves at each time point a level of delta power approximating that maximally observed spontaneously in the day prior to the manipulation (top lines), without disrupting the circadian phase of sleep-wake behavior the following day (bottom lines). Although some fluctuation in delta power across timepoints is still observed, we estimate it to be less than a fifth what is observed under the same conditions across the normal circadian day. At some times of day (e.g. the start of the day at ZT0-4, when mice are sleeping, fig. S6A, B), this sleep deprivation results in a significant decrease in sleep latency (the time to fall asleep, fig. S6C) and increase in delta power (Fig. 5A,B) relative to control conditions. At other times (e.g. the start of the night at ZT12-16, when mice would normally be awake anyhow, fig. S6A, B), the same sleep deprivation results in almost no changes relative to control conditions (Fig.

5A,B; fig. S6C, D). In all cases, subsequent sleep and activity are completely normal, with no shift in the timing of activity (Fig. 5A,B).

We next performed this protocol preceding each time point of our synaptoneurosome transcriptomics (Fig. 5A,B). In line with observations of the whole brain transcriptome by other investigators (*3*), the rhythmicity of a large proportion of mRNAs in synaptoneurosomes was significantly altered by sleep deprivation. In general, cycling features in basal conditions (BL) showed reduced statistical significance (higher q-values) under sleep deprivation (SD) (Fig. 5C and Table S5). However, circadian oscillations of one fourth (561) of synaptic mRNAs were preserved (period 24h, $q<0.05$) and virtually unchanged in amplitude when compared to BL condition (Fig. 5D-F; fig. S7A), and of the remaining 1524 transcripts, 1271 still showed profiles with considerable time of day-dependent variation (Fig. 5G; fig. S7B). Ontologically, the analysis of rhythmic mRNAs presents a picture that is mostly unchanged (Table S6). mRNAs that encode proteins involved in synaptic transmission are enriched in the peak before the transitions to the wake phase (Fig. 6A). By contrast, mRNAs peaking before dawn, preceding the sleep phase, are involved in intracellular signaling, cell morphology, cell metabolism and translation (Fig. 6B).

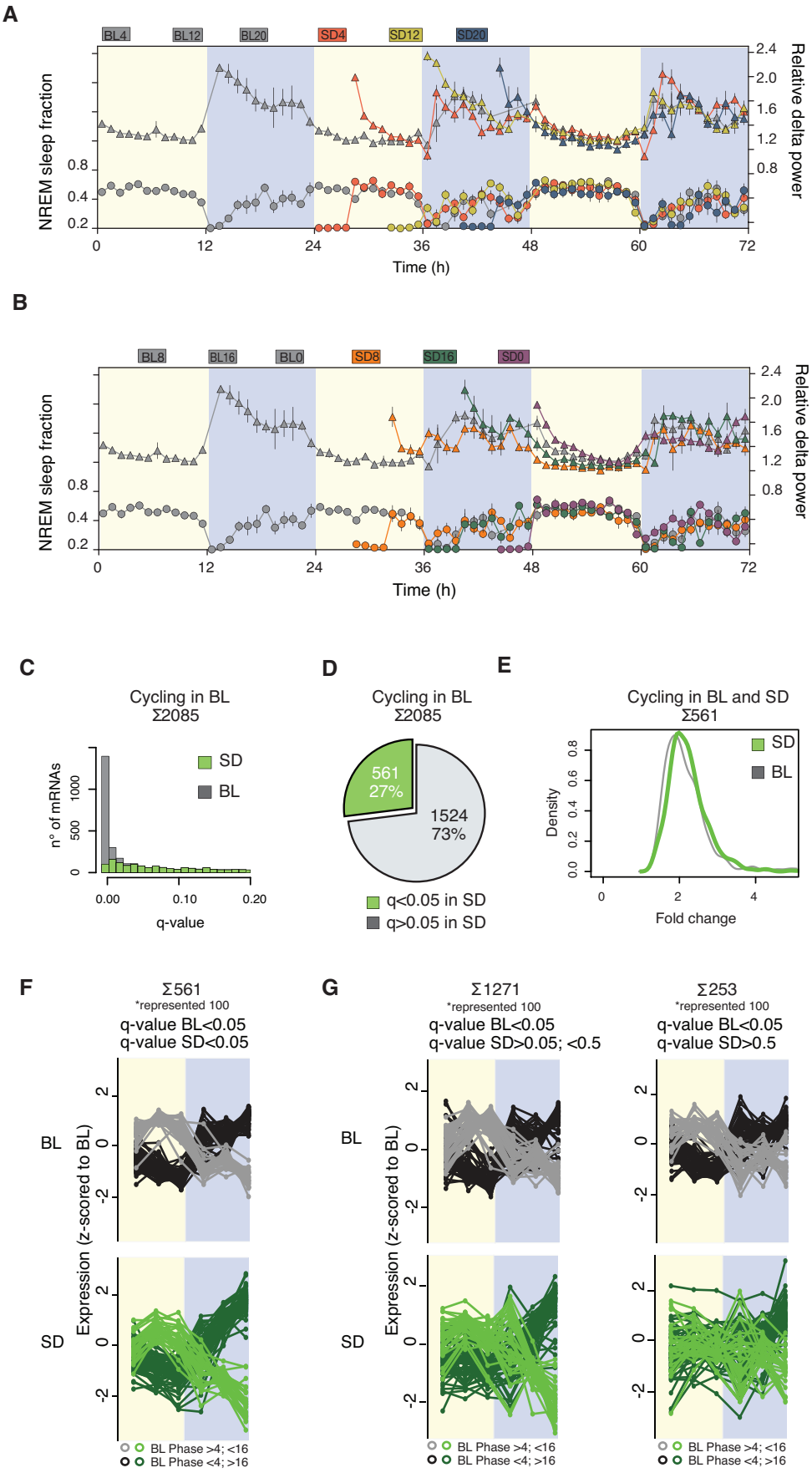
A
BL4
BL12
BL20
SD4
SD12
SD20
NREM sleep fraction
Relative delta power
Time (h)
B
BL8
BL16
BL0
SD8
SD16
SD0
NREM sleep fraction
Relative delta power
Time (h)
C
Cycling in BL
Σ2085
n° of mRNAs
SD
BL
q-value
D
Cycling in BL
Σ2085
561
27%
1524
73%
q<0.05 in SD
q>0.05 in SD
E
Cycling in BL and SD
Σ561
SD
BL
Density
Fold change
F
Σ561
*represented 100
q-value BL<0.05
q-value SD<0.05
BL
SD
Expression (z-scored to BL)
BL Phase >4; <16
BL Phase <4; >16
G
Σ1271
*represented 100
q-value BL<0.05
q-value SD>0.05; <0.5
Σ253
*represented 100
q-value BL<0.05
q-value SD>0.5

**Fig. 5. Circadian and sleep-wake regulation of synaptic mRNA abundance. (A)** and **(B)** Mean (± SEM) time course of EEG relative (to mean BL delta power; 0.5-4Hz at ZT8-12) frontal delta power during NREM sleep (triangles; % of the last 4 h of the baseline light periods) and time spent in NREM sleep (circles; min/ recording h; left y-axis) during 24-h baseline (grey symbols and lines), 24h recovery and during and after four 4-h sleep deprivations (SD) finishing either at ZT4 (red, sample name BL4/SD4), at ZT8 (orange, sample name BL8/SD8), at ZT12 (yellow, sample name BL12/SD12), at ZT16 (green, sample name BL16/SD16), at ZT20 (blue, sample name BL20/SD20) or at ZT0 (purple, sample name BL0/SD0). Grey areas delineate the dark periods. The data was divided into two panels for better visualization and note that baseline is the same in both. **(C)** Distribution of q-values for rhythmicity of the 2085 mRNAs cycling in BL (in red q-values at BL, in green q-values after SD). (q-values> 0.5 omitted). **(D)** Pie chart depicting the fraction of mRNAs that remain rhythmic (period=24h, $q<0.05$) in synaptoneurosomes of SD mice. **(E)** Density distribution of circadian amplitudes (peak/trough) of cycling synaptic transcripts that remain rhythmic after SD**.** In grey amplitude in BL and in green amplitude in SD. **(F)** Expression profiles of transcripts cycling in BL and SD (q-value BL <0.05 and q-value SD<0.05; 561 mRNAs). 100 randomly selected mRNAs are shown. **(G)** As in F but for those transcripts cycling in BL ($q<0.05$) but non-significant in SD. 1271 with lower q-values in SD (0.05<q-value<0.5; left) and 253 with higher q-values (>0.5; right) are represented separately. 100 randomly selected mRNAs are shown.

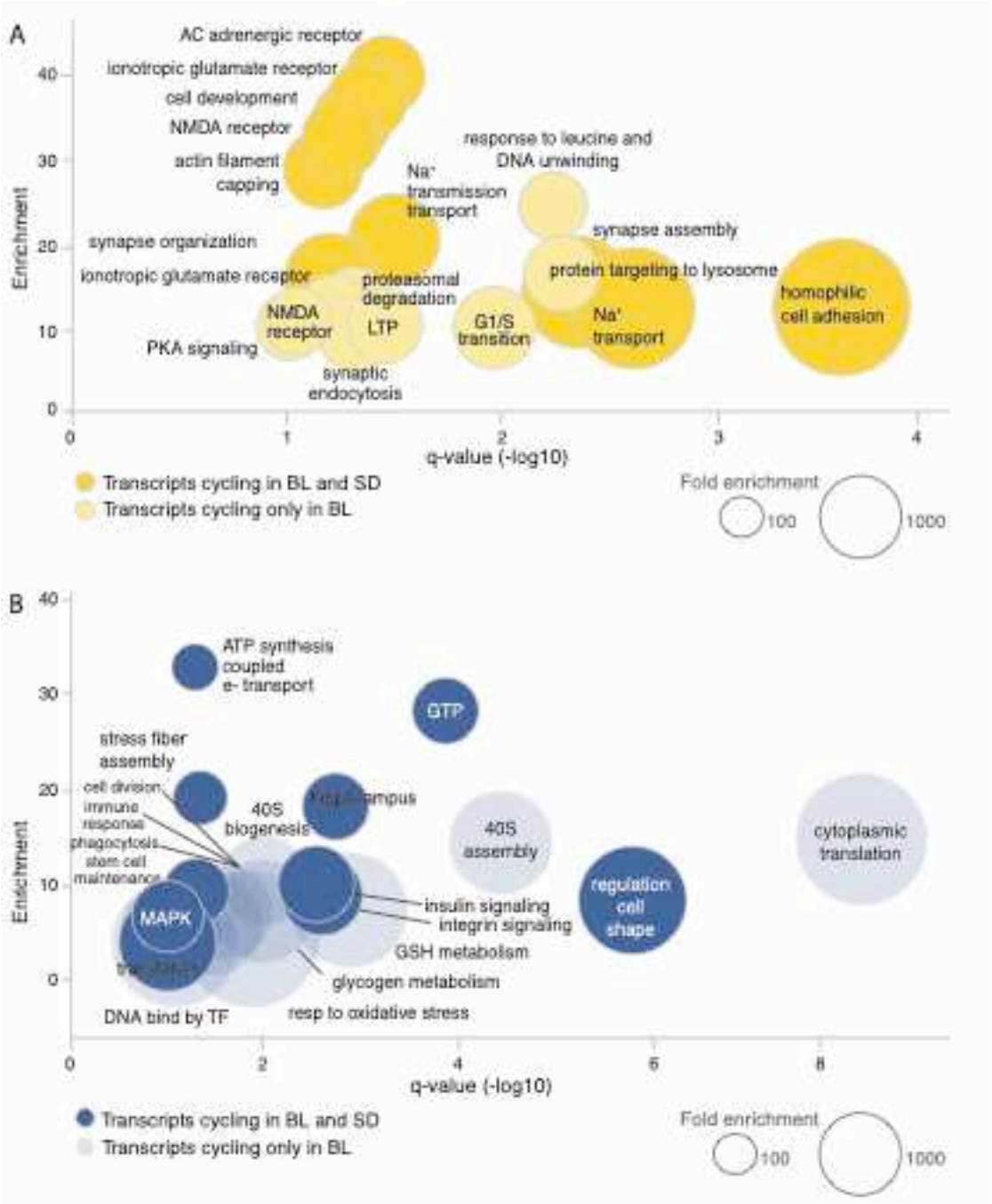


**Fig. 6. Synaptic accumulation of RNA preceding dawn and dusk is independent of sleep pressure. (A)** Gene Ontology analysis of Biological processes enriched in the light (pre-dusk) peak (according to phase in BL). Dark yellow, transcripts cycling in both BL and SD; light yellow, those cycling significantly in BL but non-significantly in SD (light yellow). Size of the circle indicates fold-enrichment in the light versus dark. **(B)** Same as in A but for the dark peak, with circle size indicating enrichment dark vs. light.

## Daily variations in the synaptic proteome are dominated by sleep-wake state

Previous studies suggest that mRNAs in the synapse are translated there, and half of these locally translated transcripts were also present in our cycling dataset (*24*)(Fig. S8). To gain further insights into the functional implication of daily oscillations of synaptic mRNAs, we performed MS-based label-free quantitative proteomics to characterize temporal patterns of the total forebrain and synaptic proteome. We measured, in a single shot manner, protein samples prepared from isolated synaptoneurosomes and total forebrain of mice (4 biological replicates) collected every 4h across 24h (see Material and Methods). Our in-depth analysis allowed us to quantify across all samples 4477 proteins in total forebrain and 4063 in synapses, with an overlap of 3710 proteins (fig. S9A). Circadian analysis revealed that in synapses 11.7% (476; Fig. 7A; Table S7A) and in total forebrain 17.2% (770; fig. S9B) of proteins were rhythmic (period=24, q-value<0.1; Table S7B). [n. b. Proteomic analyses showed lower circadian range and relative signal for less abundant components than transcriptomics; q value was chosen 0.1 at the maximum of the circadian q value distribution to assure comparable coverage and comparability with transcriptomics (fig. S9 C and D). Analyses identical to those in Fig. 7 are also presented in fig. S10 with a q value chosen at 0.05, arriving at the same conclusions with smaller numbers of proteins].

Although both the cycling synaptic and forebrain proteomes showed biphasic distributions, these were markedly different (fig. S11 A and B, Table S7C), with peak phases differing across compartments by six hours (fig. S11 C and D). Moreover, from the common proteins in both datasets (fig. S9A), only 92 were cycling in both forebrain and synapse, and these also had strikingly different phases of maximal expression (Fig. 7B and C; fig. S11 E and F) suggesting, as for

the transcriptome, totally different mechanisms for daily protein rhythm generation in the two compartments.

By contrast, the phase distribution of synaptic cycling proteins mirrored that observed for oscillating synaptic transcripts, with two clusters preceding dusk and dawn (fig. S11 B and D). We detected synaptic mRNAs for 1128 synaptic proteins (fig. S12A), and of those with daily oscillations (fig. S12B), 77.7% also had a cycling transcript predominantly with leading or sharing phase (Fig. 7D and E). As revealed for transcripts, proteins peaking before dawn are enriched in categories related to metabolism, and more specifically to lipid metabolism and mitochondria, while proteins involved in cellular signaling preceded dusk (Fig. 7F and G; Table S8). In short, under normal conditions of light and dark, synaptic proteome temporal profiles largely resembled those of the transcriptome.

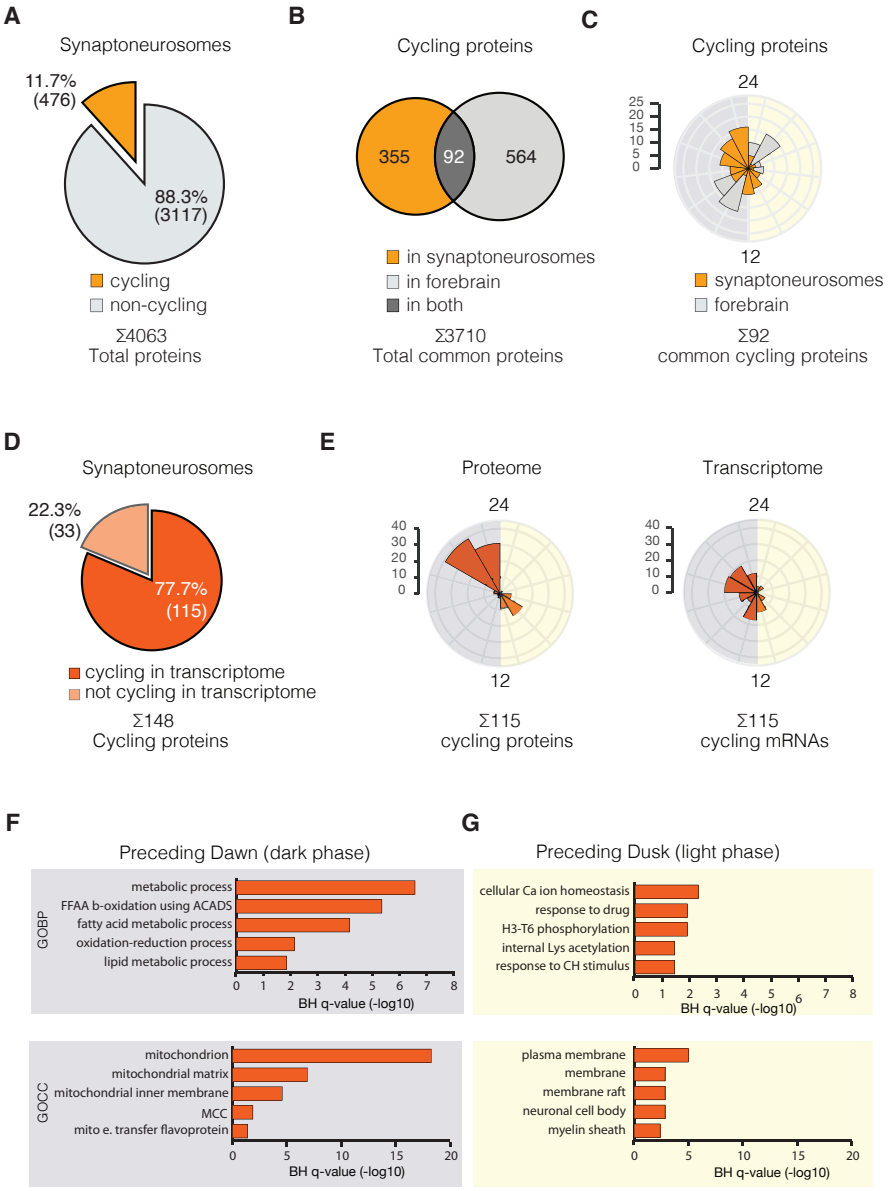


**Fig. 7. Oscillations of the synaptic proteome resemble those of the synaptic transcriptome.** **(A)** Pie chart showing the fraction of cycling proteins (period 24h, q<0.1) in synaptoneurosomes among the total 4063 quantified. **(B)** Overlap of the rhythmic proteome in synapses and in total forebrain from those quantified in both compartments (3710). **(C)** Phase distribution in synapses (orange) and forebrain (grey) of proteins cycling in both comparments. **(D)** Proportion of synaptic cycling proteins with synaptic cycling mRNAs. **(E)** Rose plots representing the frequency distribution of phases for cycling proteins and corresponding transcripts at synapses. **(F, G)** Enriched GO Biological Processes (GOBP) and Cellular Components (GOCC) in the cycling synaptic proteome with cycling transcripts separated according to protein phase; dark, anticipating dawn **(F)** and light, anticipating dusk **(G)**. (http://www.funrich.org, BH corrected p<0.01).

Analogously to the transcriptome, we next examined the daily cycles in the proteome under conditions of high sleep pressure. Here, a strikingly different picture emerged. In the time course from the serial sleep deprivation, almost all (98% with a cut-off of q<0.1 and 99.9% with a cut off of q<0.05) of the oscillating proteins in BL lost their rhythms (period=24, q-value<0.1;Fig. 8 A to C; Table S9). Our data indicate that daily changes in protein levels at the synapse are completely determined by vigilance state rather than by circadian clocks.

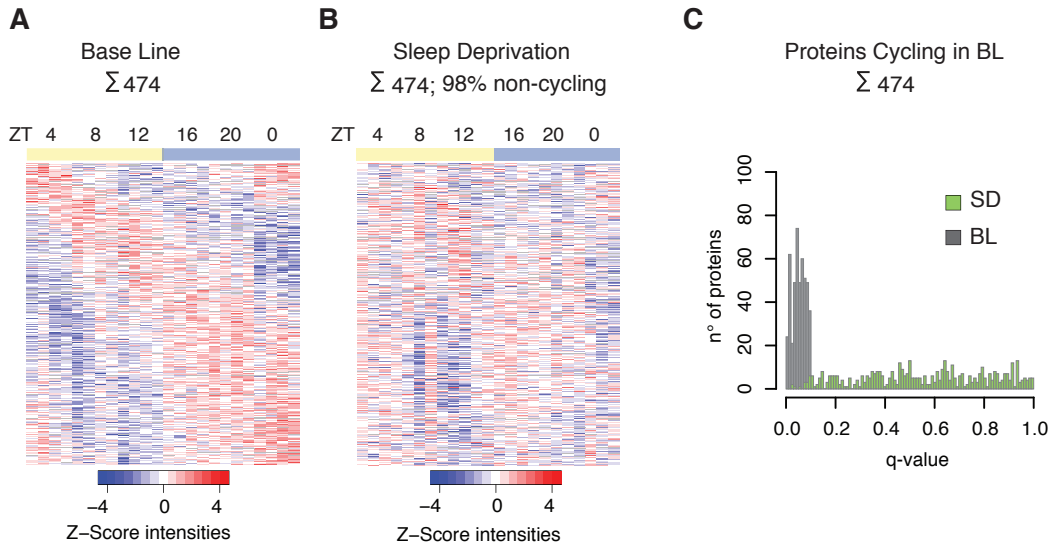


**Fig. 8. The synaptic proteome shows oscillations almost entirely dependent upon sleep-wake state. (A)** Heatmap of label free intensities of cycling proteins in BL (left) and the corresponding values in **(B)** SD (right) in all biological replicates for each sampled time point (columns). Proteins (in rows) are ordered by the estimated phase in BL, and all intensities in both conditions were z-scored to BL intensity values. Note: from the 474 proteins represented, 98% do not cycle in SD. **(C)** Distribution of the q-values of the cycling synaptic proteome in BL (grey) and the corresponding q-value in the SD dataset (green).

## Discussion

In various mammalian tissues, between 3 and 16% of total transcripts have been described as circadian until now (*33*) and our own of 6% of oscillatory mRNAs in the whole mouse forebrain is consistent with these values. However, synaptic functionality has been shown to have a strong circadian component. In the hippocampus, Long Term Potentiation (LTP) efficacy undergoes circadian

variation (*34*) and in the SCN, dynamic expression and function of ion channels or neurotransmitter receptors ensure distinct effects of light depending on time of day (*4, 35-37*). Helping to achieve this circadian functionality, we find that synaptic transcript accumulation can occur with much higher rhythmicity: 67% of enriched synaptoneurosomal transcripts show time of day variation, encompassing all aspects of synaptic function. (It should be noted that other transcripts present but not specifically enriched at synapses do not display this overwhelming degree of rhythmicity, implying differences in stability, circadian active transport, or both).

**Post-transcriptional mechanisms as a primary circadian motor**

Statistically, our results further show that this rhythmicity is generated at a post-transcriptional level, since overlap between the set of synaptic cycling transcripts and that in the whole forebrain is at levels expected by chance alone. This observation is consistent with several recent studies showing circadian variation at steps subsequent to transcription initiation (*10, 11, 38-40*). In brain, we observe rhythms of transcript abundance microscopically at equal amplitude throughout the axodendritic arbor in the *stratum radiatum* of the hippocampus, in spite of marked variation in synaptic density. Thus, spine-poor proximal regions (*30*) show the same amplitude as spine-rich distal regions. For this reason, we favor the hypothesis that the generation of synaptic transcript daily oscillations happens due to cyclical transport to synapses. Dynamics of cytoskeleton components has already been linked to the circadian clock (*39, 40*) and represent a possible regulatory node for transport in the cytoplasm, but other interesting post-transcriptional steps could be involved, including changes in the RNA degradation rate within the dendritic arbor or at

synapses. Because messenger ribonucleoproteins (mRNPs) remain docked at the nuclear basket for an uncertain time, constituting a rate-limiting step for mRNA dynamics (*41, 42*), export through the nuclear pore is also an appealing regulatory step for circadian regulation of mRNA abundance outside the nucleus.

A similar lack of parallelism between synapse and whole forebrain can be observed when examining the proteome. Three quarters of cycling synaptic proteins arose from cycling synaptic transcripts, but only 20% proteins show oscillations in the whole brain. It is difficult to draw conclusions about relative percentages of oscillatory transcripts and proteins because different platforms were used for data generation (deep sequencing vs. mass spectrometry). However, our results are consistent with the reported stability of many synaptic proteins (*19*), which would correspondingly decrease their oscillatory amplitude. Interestingly, there is also a small difference in overall phase angle between the two datasets. This phase discrepancy suggests that local translation of synaptic proteins could be a major rate-limiting step for daily changes in synaptic protein levels. Supporting this idea, a recent study in neuronal culture demonstrates that mRNA localization in the synapse is the primary mechanism contributing to the synaptic proteome compared to transport of proteins synthesized in the soma (*43*).

**A major division of biological functions preparing for sleep and wake**

In most mammalian organs, broad peaks of gene expression precede dusk and dawn (*2*). In our own study, nearly without exception both circadian transcripts and the proteins derived from them showed peak levels sharply in anticipation of dusk and dawn. Transcripts in these two phases showed a complete division

of biological function: cell-intrinsic and metabolic ontological terms preceded sleep, while terms associated with synaptic structure and function preceded wake. The division that we observe is consistent with a large literature suggesting both circadian- and sleep-dependent partition of cellular function. An inherent circadian clock is known to regulate learning and memory efficiencies diurnally (*44-47*). Mechanistically, it has being proposed that trafficking of glutamate receptors or modulation of spine densities could be involved (*48-50*). Along the same lines, synaptic homeostasis has been proposed as a major function of sleep-wake states (*20*) and others have proposed macromolecular synthesis and energy replenishment as potential functions for sleep (*51, 52*). Our synaptic gene ontology data is remarkably consistent with both suggested functions of sleep-wake cycles, neatly partitioned in circadian time. In a companion paper, we further document the role of synaptic protein phosphorylation across the circadian cycle. Again, we find a purely bimodal distribution of these ontological states, though interestingly with opposite relative proportions: whereas the majority of cycling RNAs and proteins reach peak levels at the end of the wake period in anticipation of day, the majority of circadian phosphosites reach peak levels at the end of the sleep period in anticipation of dusk (Brüning, Noya, et al., companion m.s.).

**Transcript timing dominated by clocks, protein timing by sleep-wake state**

Due to the coupling of circadian rhythms and sleep-wake cycles, distinguishing the contribution of each to cellular biology remains challenging. By depriving mice of sleep prior to each time point, one mostly dampens the normal diurnal variation of sleep need: during the light phase, SD induces an increase in sleep pressure, while during the dark phase, no significant difference occurs because

animals are already awake (Fig. 5A and fig. S6) (*32*). Under these conditions, circadian transcriptional oscillations of the mouse forebrain are strongly dampened (*3*). Surprisingly, at the synapse, the post-transcriptional mechanisms dominating diurnal transcript accumulation are less dramatically affected: while circadian rhythmicity is globally decreased, one fourth of circadian transcripts remain completely unchanged, and most others retain some evidence of time-dependent variation.

These time of day-dependent oscillations in synaptic transcript abundance persist in constant darkness, ruling out light-driven effects, but are lost in circadian clock-deficient *Bmal1*$^{-/-}$ mice in entrained light-dark conditions. It is thus tempting to attribute cyclical abundance purely to circadian clock control. However, *Bmal1*$^{-/-}$ mice (*53*) – as well as all other clock-depleted strains tested (*54*) -show markedly dampened daily variation in sleep pressure across the day, even under normal light:dark conditions. Therefore, our experiments do not rule out clock:sleep interactions, even if they demonstrate total dependence of cyclic synaptic RNA accumulation upon clock function.

It is interesting to note that ontological terms related to synaptic organization and assembly, cell adhesion, and actin cytoskeleton all retain high statistical significance and synaptic enrichment equally under conditions of sleep deprivation. Thus, sleep-wake cycle dependent changes in synaptic structure (*20, 55, 56*) appear to be preceded by a primarily circadian-driven accumulation of relevant RNAs.

Remarkably, at the protein level, virtually no circadian influence remains under conditions of high sleep pressure. While daily cycles of proteins in the synapse are detected in animals kept under a light-dark cycle, sleep deprivation completely blunts those changes.

Our findings are consistent with cellular literature suggesting activity-dependent translation at synapses: novel experience triggers the association of mRNAs to ribosomes in the synapse, synaptic activation rapidly releases the translational repression of mRNAs localized in the synapse, and local protein translation is essential for several forms of plasticity that involve active behavior (*57-60*). Similarly, evidence of synaptic downscaling during sleep has been observed ultra-structurally in mouse cortex (*55*) and likely occurs because of metabotropic Glutamate Receptor 5 (mGluR5)-dependent signaling during waking (*19*). Thus, under the serial SD protocol that we employ, as oscillations in protein levels are dampened, protein levels are mostly driven toward peak rather than nadir levels.

Many possibilities exist for the upstream signaling that drives the sleep- and circadian-dependent accumulation of RNA and proteins that we observe. Whereas the mechanism connecting cellular components of the circadian oscillator to downstream pathways are well established (*61, 62*) neither the workings of the sleep homeostat itself nor its connection to downstream sleep-dependent cellular events has been deciphered. In addition to direct synaptic activity-dependent hypotheses that we favor (*20*), indirect mechanisms like changes in brain temperature and cortisol levels are also possible. Changes in transcript abundance associated with small alterations in body temperature are believed to be mediated either by an initial post-transcriptional effect via the cold-inducible RNA-binding protein CIRBP (*63*), or by low-level activation of Heat Shock Factor 1 (*64*). We have found no overlap between mRNAs regulated by these factors and our cycling dataset, making it unlikely that temperature changes are responsible for the effects that we observe. Similarly, although cortisol elevations during wake and especially during sleep deprivation are

well-documented, adrenalectomy experiments establish that cortisol is not responsible for most of the transcriptional effects of SD (*65*). Therefore, we also disfavor this indirect cue as a primary signal.

Overall, our results are consistent with anticipatory circadian delivery of synaptic mRNAs prior to dawn and dusk, followed by "need-dependent" local translation linked to sleep and wake states. These spatiotemporal dynamics across the synaptic landscape likely play a critical role in diurnally regulating all aspects of forebrain function.

**References**

1. K. F. Storch *et al.*, Intrinsic circadian clock of the mammalian retina: importance for retinal processing of visual information. *Cell* **130**, 730-741 (2007).
2. R. Zhang, N. F. Lahens, H. I. Ballance, M. E. Hughes, J. B. Hogenesch, A circadian gene expression atlas in mammals: implications for biology and medicine. *Proc Natl Acad Sci U S A* **111**, 16219-16224 (2014).
3. S. Maret *et al.*, Homer1a is a core brain molecular correlate of sleep loss. *Proc Natl Acad Sci U S A* **104**, 20090-20095 (2007).
4. S. Panda *et al.*, Coordinated transcription of key pathways in the mouse by the circadian clock. *Cell* **109**, 307-320 (2002).
5. N. Koike *et al.*, Transcriptional architecture and chromatin landscape of the core circadian clock in mammals. *Science* **338**, 349-354 (2012).
6. D. Feng *et al.*, A circadian rhythm orchestrated by histone deacetylase 3 controls hepatic lipid metabolism. *Science* **331**, 1315-1319 (2011).

7. I. Schmutz, J. A. Ripperger, S. Baeriswyl-Aebischer, U. Albrecht, The mammalian clock component PERIOD2 coordinates circadian output by interaction with nuclear receptors. *Genes Dev* **24**, 345-357 (2010).

8. G. Rey *et al.*, Genome-wide and phase-specific DNA-binding rhythms of BMAL1 control circadian output functions in mouse liver. *PLoS Biol* **9**, e1000595 (2011).

9. M. S. Robles, J. Cox, M. Mann, In-vivo quantitative proteomics reveals a key contribution of post-transcriptional mechanisms to the circadian regulation of liver metabolism. *PLoS Genet* **10**, e1004047 (2014).

10. B. G. Robinson, D. M. Frim, W. J. Schwartz, J. A. Majzoub, Vasopressin mRNA in the suprachiasmatic nuclei: daily regulation of polyadenylate tail length. *Science* **241**, 342-344 (1988).

11. V. Bélanger, N. Picard, N. Cermakian, The circadian regulation of Presenilin-2 gene expression. *Chronobiol Int* **23**, 747-766 (2006).

12. C. Vollmers *et al.*, Time of feeding and the intrinsic circadian clock drive rhythms in hepatic gene expression. *Proc Natl Acad Sci U S A* **106**, 21453-21458 (2009).

13. K. S. Kosik, Life at Low Copy Number: How Dendrites Manage with So Few mRNAs. *Neuron* **92**, 1168-1180 (2016).

14. A. R. Buxbaum, G. Haimovich, R. H. Singer, In the right place at the right time: visualizing and understanding mRNA localization. *Nat Rev Mol Cell Biol* **16**, 95-109 (2015).

15. J. L. Dynes, O. Steward, Dynamics of bidirectional transport of Arc mRNA in neuronal dendrites. *J Comp Neurol* **500**, 433-447 (2007).

16. R. B. Knowles *et al.*, Translocation of RNA granules in living neurons. *J Neurosci* **16**, 7812-7820 (1996).

17. S. Miller *et al.*, Disruption of dendritic translation of CaMKIIalpha impairs stabilization of synaptic plasticity and memory consolidation. *Neuron* **36**, 507-519 (2002).

18. S. Hutten, T. Sharangdhar, M. Kiebler, Unmasking the messenger. *RNA Biol* **11**, 992-997 (2014).

19. G. H. Diering *et al.*, Homer1a drives homeostatic scaling-down of excitatory synapses during sleep. *Science* **355**, 511-515 (2017).

20. G. Tononi, C. Cirelli, Sleep and the price of plasticity: from synaptic and cellular homeostasis to memory consolidation and integration. *Neuron* **81**, 12-34 (2014).

21. S. Ray, A. B. Reddy, Cross-talk between circadian clocks, sleep-wake cycles, and metabolic networks: Dispelling the darkness. *Bioessays* **38**, 394-405 (2016).

22. P. R. Dunkley, P. E. Jarvie, P. J. Robinson, A rapid Percoll gradient procedure for preparation of synaptosomes. *Nat Protoc* **3**, 1718-1728 (2008).

23. I. J. Cajigas *et al.*, The local transcriptome in the synaptic neuropil revealed by deep sequencing and high-resolution imaging. *Neuron* **74**, 453-466 (2012).

24. R. Ouwenga *et al.*, Transcriptomic Analysis of Ribosome-Bound mRNA in Cortical Neurites. *J Neurosci* **37**, 8688-8705 (2017).

25. S. Tyanova *et al.*, The Perseus computational platform for comprehensive analysis of (prote)omics data. *Nat Methods* **13**, 731-740 (2016).

26. M. E. Hughes, J. B. Hogenesch, K. Kornacker, JTK_CYCLE: an efficient nonparametric algorithm for detecting rhythmic components in genome-scale data sets. *J Biol Rhythms* **25**, 372-380 (2010).

27. R. T. Fremeau, S. Voglmaier, R. P. Seal, R. H. Edwards, VGLUTs define subsets of excitatory neurons and suggest novel roles for glutamate. *Trends Neurosci* **27**, 98-103 (2004).

28. A. Karlén *et al.*, Nogo receptor 1 regulates formation of lasting memories. *Proc Natl Acad Sci U S A* **106**, 20476-20481 (2009).

29. A. Jilg *et al.*, Temporal dynamics of mouse hippocampal clock gene expression support memory processing. *Hippocampus* **20**, 377-388 (2010).

30. M. Megías, Z. Emri, T. F. Freund, A. I. Gulyás, Total number and distribution of inhibitory and excitatory synapses on hippocampal CA1 pyramidal cells. *Neuroscience* **102**, 527-540 (2001).

31. M. K. Bunger *et al.*, Mop3 is an essential component of the master circadian pacemaker in mammals. *Cell* **103**, 1009-1017 (2000).

32. P. Franken, D. Chollet, M. Tafti, The homeostatic regulation of sleep need is under genetic control. *J Neurosci* **21**, 2610-2621 (2001).

33. D. Bell-Pedersen *et al.*, Circadian rhythms from multiple oscillators: lessons from diverse organisms. *Nat Rev Genet* **6**, 544-556 (2005).

34. H. Nakatsuka, K. Natsume, Circadian rhythm modulates long-term potentiation induced at CA1 in rat hippocampal slices. *Neurosci Res* **80**, 1-9 (2014).

35. T. A. Wang *et al.*, Circadian rhythm of redox state regulates excitability in suprachiasmatic nucleus neurons. *Science* **337**, 839-842 (2012).

36. C. M. Pennartz, R. Hamstra, A. M. Geurtsen, Enhanced NMDA receptor activity in retinal inputs to the rat suprachiasmatic nucleus during the subjective night. *J Physiol* **532**, 181-194 (2001).

37. K. Richter *et al.*, VGLUT1 Binding to Endophilin or Intersectin1 and Dynamin Phosphorylation in a Diurnal Context. *Neuroscience* **371**, 29-37 (2018).

38. G. Benegiamo, S. A. Brown, S. Panda, RNA Dynamics in the Control of Circadian Rhythm. *Adv Exp Med Biol* **907**, 107-122 (2016).

39. S. Kojima, M. Hirose, K. Tokunaga, Y. Sakaki, H. Tei, Structural and functional analysis of 3' untranslated region of mouse Period1 mRNA. *Biochem Biophys Res Commun* **301**, 1-7 (2003).

40. E. Y. Kim *et al.*, Drosophila CLOCK protein is under posttranscriptional control and influences light-induced activity. *Neuron* **34**, 69-81 (2002).

41. B. L. Timney *et al.*, Simple kinetic relationships and nonspecific competition govern nuclear import rates in vivo. *J Cell Biol* **175**, 579-593 (2006).

42. T. Dange, D. Grünwald, A. Grünwald, R. Peters, U. Kubitscheck, Autonomy and robustness of translocation through the nuclear pore complex: a single-molecule study. *J Cell Biol* **183**, 77-86 (2008).

43. A. Zappulo *et al.*, RNA localization is a key determinant of neurite-enriched proteome. *Nat Commun* **8**, 583 (2017).

44. O. Rawashdeh *et al.*, PERIOD1 coordinates hippocampal rhythms and memory processing with daytime. *Hippocampus* **24**, 712-723 (2014).

45. W. Hauber, A. Bareiss, Facilitative effects of an adenosine A1/A2 receptor blockade on spatial memory performance of rats: selective enhancement of reference memory retention during the light period. *Behav Brain Res* **118**, 43-52 (2001).

46. Y. Takahashi, K. Sawa, T. Okada, The diurnal variation of performance of the novel location recognition task in male rats. *Behav Brain Res* **256**, 488-493 (2013).

47. K. L. Eckel-Mahan *et al.*, Circadian oscillation of hippocampal MAPK activity and cAmp: implications for memory persistence. *Nat Neurosci* **11**, 1074-1082 (2008).

48. J. J. Zhu, Y. Qin, M. Zhao, L. Van Aelst, R. Malinow, Ras and Rap control AMPA receptor trafficking during synaptic plasticity. *Cell* **110**, 443-455 (2002).

49. P. Chen, Z. Gu, W. Liu, Z. Yan, Glycogen synthase kinase 3 regulates N-methyl-D-aspartate receptor channel trafficking and function in cortical neurons. *Mol Pharmacol* **72**, 40-51 (2007).

50. M. Ikeda *et al.*, Hippocampal spine changes across the sleep-wake cycle: corticosterone and kinases. *J Endocrinol* **226**, M13-27 (2015).

51. J. H. Benington, H. C. Heller, Restoration of brain energy metabolism as the function of sleep. *Prog Neurobiol* **45**, 347-360 (1995).

52. M. Mackiewicz *et al.*, Macromolecule biosynthesis: a key function of sleep. *Physiol Genomics* **31**, 441-457 (2007).

53. A. Laposky *et al.*, Deletion of the mammalian circadian clock gene BMAL1/Mop3 alters baseline sleep architecture and the response to sleep deprivation. *Sleep* **28**, 395-409 (2005).

54. J. P. Wisor *et al.*, A role for cryptochromes in sleep regulation. *BMC Neurosci* **3**, 20 (2002).

55. L. de Vivo *et al.*, Ultrastructural evidence for synaptic scaling across the wake/sleep cycle. *Science* **355**, 507-510 (2017).

56. M. Jasinska *et al.*, Circadian rhythmicity of synapses in mouse somatosensory cortex. *Eur J Neurosci* **42**, 2585-2594 (2015).

57. J. A. Ainsley, L. Drane, J. Jacobs, K. A. Kittelberger, L. G. Reijmers, Functionally diverse dendritic mRNAs rapidly associate with ribosomes following a novel experience. *Nat Commun* **5**, 4510 (2014).

58. S. Hüttelmaier *et al.*, Spatial regulation of beta-actin translation by Src-dependent phosphorylation of ZBP1. *Nature* **438**, 512-515 (2005).

59. K. M. Huber, M. S. Kayser, M. F. Bear, Role for rapid dendritic protein synthesis in hippocampal mGluR-dependent long-term depression. *Science* **288**, 1254-1257 (2000).

60. K. C. Martin *et al.*, Synapse-specific, long-term facilitation of aplysia sensory to motor synapses: a function for local protein synthesis in memory storage. *Cell* **91**, 927-938 (1997).

61. S. A. Brown, A. Azzi, Peripheral circadian oscillators in mammals. *Handb Exp Pharmacol*, 45-66 (2013).

62. M. Brancaccio *et al.*, Network-mediated encoding of circadian time: the suprachiasmatic nucleus (SCN) from genes to neurons to circuits, and back. *J Neurosci* **34**, 15192-15199 (2014).

63. J. Morf *et al.*, Cold-inducible RNA-binding protein modulates circadian gene expression posttranscriptionally. *Science* **338**, 379-383 (2012).

64. A. Neueder *et al.*, HSF1-dependent and -independent regulation of the mammalian in vivo heat shock response and its impairment in Huntington's disease mouse models. *Sci Rep* **7**, 12556 (2017).

65. V. Mongrain *et al.*, Separating the contribution of glucocorticoids and wakefulness to the molecular and electrophysiological correlates of sleep homeostasis. *Sleep* **33**, 1147-1157 (2010).

66. I. Tobler, K. Jaggi, Sleep and EEG spectra in the Syrian hamster (Mesocricetus auratus) under baseline conditions and following sleep deprivation. *J Comp Physiol A* **161**, 449-459 (1987).

67. A. M. Bolger, M. Lohse, B. Usadel, Trimmomatic: a flexible trimmer for Illumina sequence data. *Bioinformatics* **30**, 2114-2120 (2014).

68. B. Li, C. N. Dewey, RSEM: accurate transcript quantification from RNA-Seq data with or without a reference genome. *BMC Bioinformatics* **12**, 323 (2011).

69. M. D. Robinson, D. J. McCarthy, G. K. Smyth, edgeR: a Bioconductor package for differential expression analysis of digital gene expression data. *Bioinformatics* **26**, 139-140 (2010).

70. N. Nagaraj *et al.*, System-wide perturbation analysis with nearly complete coverage of the yeast proteome by single-shot ultra HPLC runs on a bench top Orbitrap. *Mol Cell Proteomics* **11**, M111.013722 (2012).

**Acknowledgments**

We are grateful to the Functional Genomics Center Zürich (FGCZ) for transcriptomics services, and to Juergen Cox and the Max Planck Institute of Biochemistry, Münich for proteomics services. Funding: SAB and SBN were supported by the Swiss National Science Foundation, the Velux Foundation, the Human Frontiers Science Program, and the Zürich Clinical Research Priority Project "Sleep and Health". SBN and SKT were further supported by a PhD grant from the Zürich Neurozentrum. All three are members of the Neurosciences program within the Life Sciences Zürich Graduate School. M.S.R., F.B. and M.M. were supported the Max-Planck Society for the Advancement of Sciences and the German Research Foundation

(DFG/Gottfried Wilhelm Leibniz Prize) and from the European Union Horizon ERC-2012-SyG 318987 CToPAG. In addition, M.S.R. was supported by the Volkswagen Foundation (93 071) and the DFG (Projektnummer 329628492 – SFB 1321 and INST 86/1800-1 FUGG). Author contributions: S.A.B., S.T., D.M. and S.B.N. initiated the project; S.A.B and S.B.N. designed experiments; S.B.N. performed mice experimental work, sample preparation and bioinformatics analysis of data with the advice and under the supervision of S.A.B.; D.C., performed single molecule mRNA FISH experiments and analysis; F.B. performed sample preparation, mass spectrometry experiments and data processing under the supervision of M.S.R. who also did the proteomic data analysis and advised and supervised the evaluation of circadian analysis of both the transcriptomic and proteomic data; A.S. performed sleep analysis; L.O. performed data processing of transcriptomic data; M.M., supported and provisioned resources for the mass spectrometry experiments; S.B.N wrote the manuscript with editing input from M.S.R and S.A.B. **Data and materials availability:** RNA-seq data have been deposited in the ArrayExpress database at EMBL-EBI (www.ebi.ac.uk/arrayexpress) under accession number E-MTAB-7347. Images from the mRNA in situ have been deposited in the ZENODO repository and are accessible at the ZENODO DOI Badge 10.5281/zenodo.2546770. The mass spectrometry proteomics data have been deposited to the ProteomeXchange Consortium via the PRIDE (Vizcaino, Csordas et al. 2016) partner repository with the dataset identifier PXD010697 (Username: reviewer90747@ebi.ac.uk and Password: CVJBkoUs, during review). Script for FISH image analysis (https://github.com/dcolam/Cluster-Analysis-Plugin).

**Supplementary Content (see Appendix)**

Materials. And Methods

Fig. S1-S12.

Tables S1-S9.

Databases 1-3.

Script for FISH image analysis.

## 1.5. Manuscript 2. Sleep-wake Cycles Drive Daily Dynamics of Synaptic Phosphorylation

Franziska Brüning*, Sara B. Noya*, Tanja Bange, Stella Koutsouli, Jan D. Rudolph, Shiva K. Tyagarajan, Jürgen Cox, Matthias Mann, Steven A. Brown, Maria S. Robles.

***These authors contributed equally to this work.**

**INTRODUCTION**: Globally, circadian clock–driven protein phosphorylation is a key mechanism to temporally compartmentalize biological processes across the day in peripheral tissues. In the brain, phosphorylation of several proteins has been reported to correlate with sleep pressure, itself regulated in a circadian fashion. Locally in neurons, phosphorylation plays a critical role in the regulation of synaptic function by allowing rapid modulation of protein activity and could thus dynamically scale synaptic strength in response to circadian or sleep-driven cues. Understanding the magnitude and origin of phosphorylation dynamics within synaptic proteins on a system level would be of great value to mechanistically assess synaptic function deficiencies and to understand temporal contributions to brain pathologies.

**RATIONALE**: Little is known about whether and how global phosphorylation signaling in synapses is shaped in a time dependent manner. To comprehensively characterize phosphorylation rhythms in the synaptic compartment driven by circadian and sleepwake– dependent cues, we biochemically isolated isolated synaptoneurosomes from mouse forebrain and analyzed them with advanced mass spectrometry–based proteomics.

RESULTS: Of more than 8000 phosphopeptides in almost 2000 proteins accurately quantified in the synaptoneurosome compartment across 24 hours, 30% oscillated in abundance. The phases of rhythmic phosphopeptides were

distributed in two major clusters, corresponding to the transition from wake to sleep at dawn and sleep to wake at dusk. In addition to important synaptic constituents such as ion channels, receptors, and scaffolds, a large number of kinases were among the synaptic proteins modulated by phosphorylation in a time-dependent manner. More than half of the detected phosphorylated kinases in synapses show rhythmic phosphorylation at one or more residues. Predictive and experimental data demonstrate that widespread dynamic regulation of kinase activity is a core phospho-dependent functional process at synapses. Together, our data uncover molecular processes in synapses whose activity is temporally gated by phosphorylation, such as synaptic inhibition at dawn and excitation at dusk. We further assessed circadianand sleep-driven signals by interfering with the sleep-wake cycle by applying 4 hours of sleep deprivation at different times of the day. Sleep deprivation resulted in the loss of 98% of rhythmic phosphorylation in forebrain synapses but left circadian cycles unaffected in a core of 41 phosphoproteins that function in synaptic transport and scaffolding.

**CONCLUSION**: This global rhythmic phosphoproteome of isolated synaptoneurosomes reveals a major reorganization of the synaptic molecular compartment concomitant with changes in activity. Our results indicate that phospho-dependent activation of kinases in response to sleep and wake is a core driver of these synaptic phosphorylation dynamics. Together, our data point toward an association of synaptic potentiation with wakefulness (activity) and down scaling with sleep (rest). High sleep pressure induced through sleep deprivation almost completely abrogates both peaks of daily phosphorylation cycles in synapses. We thus hypothesize that modulation of phosphorylation-

mediated synaptic signaling could be a key driver underlying sleep- and wake-dependent mechanisms to regulate synaptic homeostasis and function.

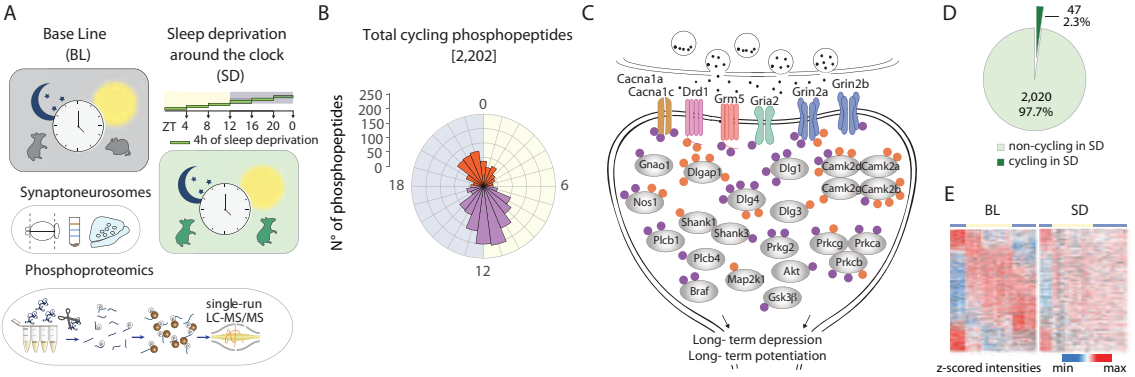


**Daily dynamics of global phosphorylation in forebrain synaptoneurosomes under basal and sleep-deprived conditions. (A)** Quantitative phosphoproteomics analyses of isolated synaptoneurosomes from rested and sleep-deprived mice around the clock. **(B and C)** More than 30% of phosphorylations in many synaptic components and numerous kinases cycle daily with peaks at the sleep-wake-sleep transitions. **(D and E)** Sleep deprivation abolished 98% of all phosphorylation cycles in synaptoneurosomes.

### 4.1.2. Entire manuscript 2

**Abstract**

The circadian clock drives daily changes of physiology, including sleep-wake cycles, by regulating transcription, protein abundance and function. Circadian phosphorylation controls cellular processes in peripheral organs, but little is known about its role in brain function and synaptic activity. We applied advanced quantitative phosphoproteomics to mouse forebrain synaptoneurosomes isolated across 24h, accurately quantifying almost 8,000 phosphopeptides. Remarkably, half of the synaptic phosphoproteome, including numerous kinases, had large-amplitude rhythms peaking at rest-activity and activity-rest transitions. Bioinformatic analyses revealed global temporal control of synaptic function via phosphorylation, including synaptic transmission, cytoskeleton reorganization and excitatory/inhibitory balance. Remarkably, sleep deprivation abolished 98% of all phosphorylation cycles in synaptoneurosomes, indicating that rest-activity cycles rather than circadian signals are main drivers of synaptic phosphorylation, responding to both sleep and wake pressures.

**One Sentence Summary**: Sleep and wake pressure shape synaptic phosphorylation dynamics and function.

**Introduction**

Circadian clocks are endogenous oscillators present in virtually every mammalian cell. The molecular mechanism of the clock drives cycles of transcription, translation and protein activity to regulate daily changes in physiology and behavior. Mass spectrometry (MS) - based quantitative proteomics has importantly contributed to our understanding how circadian

post-transcriptional mechanisms temporally shape metabolic processes in peripheral tissues (*1, 2*). Interestingly, circadian phosphorylation changes by far eclipse the regulation at the transcriptional and proteome levels in amplitude (*3*). Temporal characterization of proteome and phosphoproteome changes in the central nervous system, in contrast, has been challenging due to the sensitivity, dynamic range and throughput required to capture the regional, cellular and synaptic heterogeneity. However, recent advances in MS in combination with spatial isolation methods allow the deep characterization of proteomes from different brain regions and cell populations (*4, 5*). In addition, high-throughput phosphoproteomic technologies are now suitable for the global characterization of phosphorylation signaling dynamics in different brain areas (*6*).

Numerous synaptic features, like diffusion of receptors in membranes, channel conductance or cytoskeleton remodeling, depend on fast phosphorylation-based control mechanisms. In particular, synaptic plasticity and scaling have been linked to phosphorylation of receptors, scaffolding, cytoskeletal and other synaptic proteins (*7, 8*). Although quantitative phosphoproteomics has been applied to the synaptic compartment, technical limitations have so far precluded accurate quantification that would allow the precise characterization of global phosphorylation dynamics associated with synaptic function (*7*). It is thus unknown whether daily changes in synaptic activity are coupled to global dynamics of phosphorylation in synapses, and moreover, whether daily rhythms of phosphorylation temporally segregate synaptic processes. Two recent reports have addressed these technical limitations by either fractionating post-synaptic density (*9*) or by mapping whole-brain phosphoproteomics to synaptic protein annotations (*10*). Both highlight a role for sleep pressure in

driving synaptic phosphorylation changes associated with the kinase (SIK3) and downstream effectors (HOMER1a).

Here we apply state-of-the-art quantitative MS-based proteomics to characterize *in vivo* phosphorylation dynamics across the day in isolated synaptoneurosomes from mouse forebrain, resulting in by far the most comprehensive time-resolved phosphoproteome of synapses to date. Combination with in depth proteomics (see accompanying paper (*11*)) reveals that more than one fourth of the individual phosphorylation sites in synaptic proteins oscillate daily and independently of protein abundance. We bioinformatically analyze dynamic synaptic process and the regulatory protein classes modulated by phosphorylation.

Temporally modulated phosphorylation networks gate synaptic processes at both dawn and dusk, suggesting a potential association with activity-rest cycles. To test this, we interfere with the sleep cycle and investigate the effect on the synaptic phosphoproteome. This leads to a dramatic ablation of global phosphorylation cycles, suggesting a dominant role of both sleep and wake pressure in synaptic phosphorylation dynamics.

## Results

### In-depth phosphoproteomic profiling of synaptoneurosomes

To characterize daily dynamics of phosphorylation abundance specifically in synapses, we biochemically isolated synaptoneurosomes from mouse forebrains (*11*). Mice were kept in 12h:12h (light : dark) schedules and then sacrificed in biological quadruplicates at six time points, every 4 h, across 24 h (n=24 mice). We used a rapid method based on Percoll gradients to prepare synaptoneurosomes from forebrains, containing both pre- and post-synaptic

components (*12*) and immediately flash-froze them to prevent de-phosphorylation. To achieve sufficient throughput for our time-dependent experiments, we employed the EasyPhos method (*13*) to enrich phosphopeptides from only 1 mg of proteome homogenate for each synaptoneurosome preparation. Figure 1A depicts the MS-based quantitative phosphoproteomics workflow consisting of single runs on a high-resolution, high sensitivity quadrupole-Orbitrap HF-X mass spectrometer. Across all samples this resulted in a total of 10,439 unique phosphosites in 14,462 phosphopeptides, mapping to more than 2,000 proteins (Fig. 1B and table S1). Comparing phosphorylated amino acids in synapses to our previous circadian study in the liver (*3*) revealed similar proportions (83.6 % pS, 15.7% pT, 0.6% pY; Fig. 1B). Phosphopeptide intensities between measurements were highly reproducible in both biological replicates and time points (Pearson $r = 0.88$ and 0.83, respectively; Fig. 1C). Synaptic phosphopeptide intensities ranged over five orders of magnitude (fig. S1A), similar to what we found in liver, indicating that the synaptic compartment still has a wide quantitative range of phosphorylation levels. To indirectly evaluate our isolation method, we performed a Fisher's exact test on the total phosphoproteome dataset. Of all keywords, the top two are "Synapse" and "Cell junction" ($p < 10e\text{-}40$ for both) and the other highly enriched ones are also all relevant to synaptic function, even when analyzing every time point separately (Fig. 1D fig. S1B and S1C and see Methods). Our data show the power of combining high-throughput phosphoproteomics with biochemical isolation of synaptoneurosomes to deeply

profile phosphorylation in this discrete neuronal compartment.

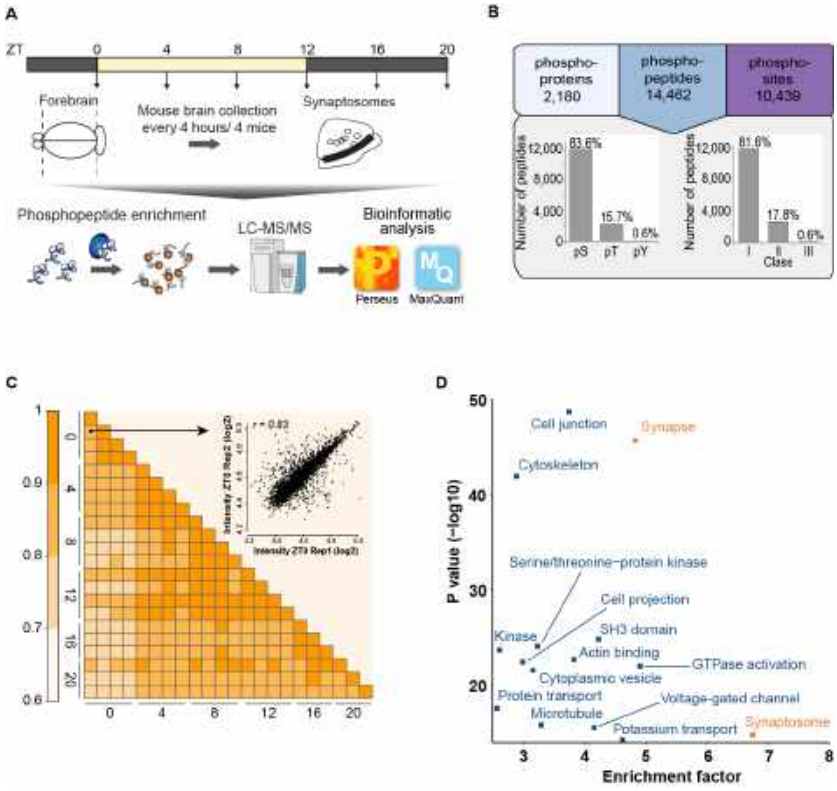


Fig. 1 Phosphoproteome characterization of synaptoneurosomes isolated across the day from mouse forebrains. (A) Experimental workflow. (B) Number of identified phosphoproteins, phosphopeptides and phosphosites in all measured samples. Lower left: distribution of phosphorylated amino acids (Serine (pS), Threonine (pT) and Tyrosine (pY)). Lower right: number of phosphorylated residues from different classes according to localization probability -- Class I (probability > 75%), Class II (probability = 50 - 75%) and Class III (localization probability < 50%). (C) Heatmap representation of Pearson correlation coefficients calculated among phosphoproteomes. Inset: Example scatterplot of phosphopeptide intensities between two biological replicates of ZT0. (D) Scatterplot shows protein annotations (UniprotKB keywords) statistically enriched (Fisher's exact test FDR < 0.02) in the total synaptoneurosome phosphoproteome compared to an in-silico mouse gene list.

## Daily rhythms of the synaptic phosphoproteome

Next we performed statistical cycling analysis in the circadian module of the Perseus software (*2*, *3*, *14*), to filter and cosine-fit the phosphopeptide intensities. A total of 2,202 (30.4%) of the 7,257 phosphopeptides accurately quantified in at least 50% of the samples oscillate in abundance with a rhythm of 24h (q-value < 0.05, see Methods, Fig. 2 A and B and table S2). We detected

rhythmic phosphorylation for more than half of the synaptic phosphoproteins (838 out of the total 1,655, Fig. 2C). These rhythmic sites were localized with high probability to a single residue (mean 0.97) and their amino acid distribution was similar to the total dataset (Fig. 1C and fig. S2A). Cycling phosphopeptides had a similar intensity distribution as the total phosphoproteome (fig. S2B), implying that circadian phospho-regulation is not biased by abundance. Little is known about the magnitude of dynamic phosphorylation changes in the synaptic compartment and our data now revealed that these changes are substantial: the mean amplitude changes are more than three-fold, with hundreds of sites at more than 10-fold (Fig. 2D).

To assess to which extent these phosphorylation dynamics depend on protein abundance changes, we quantitatively compared the levels of phosphopeptides with the abundance of the corresponding protein. Almost 90% of proteins with cycling phosphopeptides were quantified at the protein level in our companion study (*11*), and of these only 5% significantly oscillate in abundance ($q < 0.05$, 24h period, Fig. 2E). Even the small fraction of rhythmic proteins with oscillating phosphorylation generally displays different phases across the day, and furthermore, multiple sites in the same protein generally behaved differently (Fig. 2F, fig. S2C). In the minor population of rhythmic proteins carrying cycling phosphorylation, the mean amplitudes at the phosphorylation level were ten-fold larger than those at the protein level (Fig. 2G). Our data clearly establish that protein phosphorylation in forebrain synaptoneurosomes is highly dynamic across the day and almost completely independent of protein abundance, suggesting another layer of synaptic functional regulation.

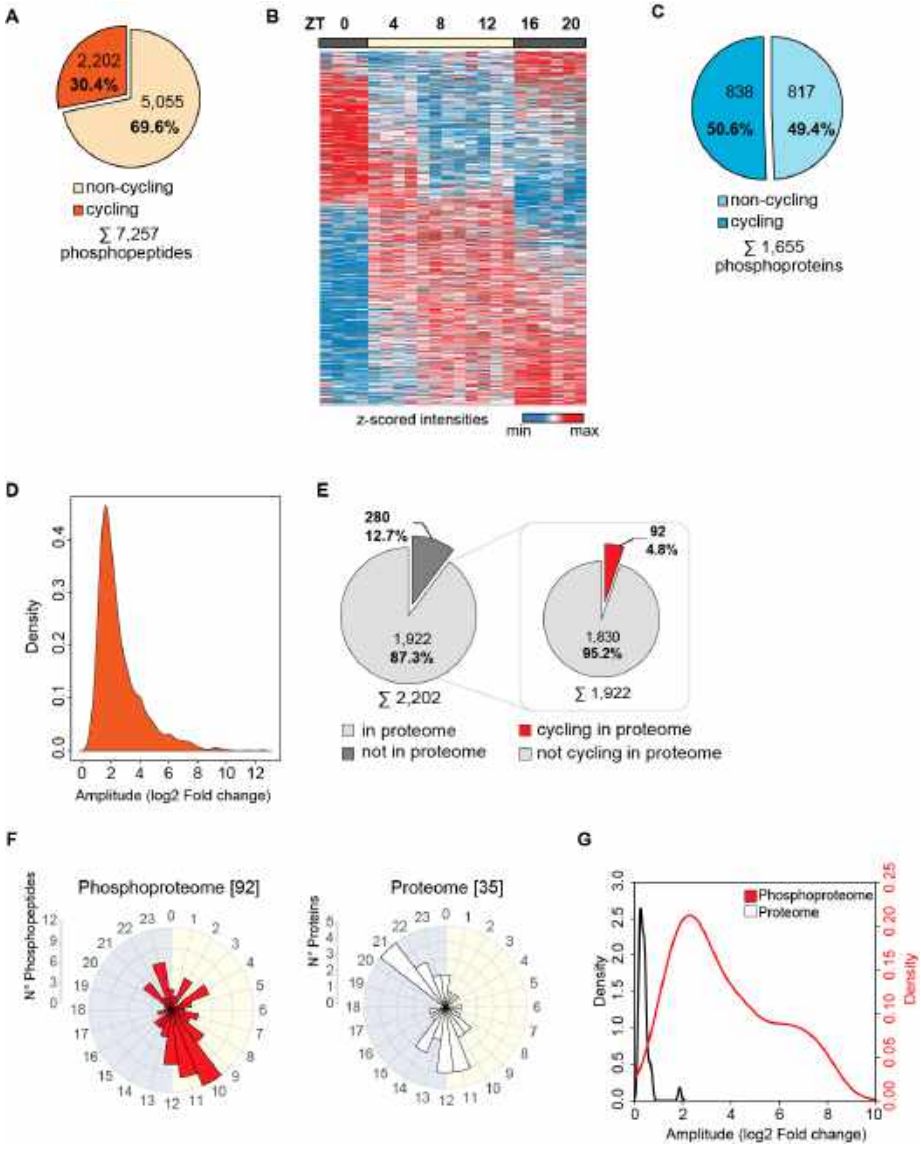


**Fig. 2 Daily rhythms of the synaptic phosphoproteome. (A)** Pie chart showing the percentage of phosphopeptides oscillating daily in synaptoneurosomes. (**B)** Heat map with the intensities (log2 z-scored) of each cycling phosphopeptide (rows) across the measure samples (columns) ordered by peak of abundance. **(C)** Pie chart with the percentage of phosphoproteins oscillating daily in synaptoneurosomes. **(D)** Density plot showing the calculated amplitudes of rhythmic phosphopeptides in synaptoneurosomes. **(E)** Pie charts showing the percentage of cycling phosphopeptides from proteins quantified in our proteome study (left) and the fraction of cycling phosphopeptides from rhythmic proteins (right). **(F)** Rose plots representing the phase distribution of rhythmic phosphopeptides (left) and their corresponding oscillating proteins (right). **(G)** Density plots comparing the amplitudes of the rhythmic phosphopeptides and the corresponding oscillating proteins.

## Temporal compartmentalization of synaptic protein phosphorylation

Our previous study in liver revealed that dynamic phosphorylation drives daily organ functions to an previously unappreciated degree (*3*). Examining the phosphorylation rhythms in the synaptic compartment showed that the phases of rhythmic phosphopeptides gathered in two distinct clusters. The larger one, at the light to dark transition when mice start to be active, contains two thirds of them, whereas the remaining largely clusters at the end of the night, preceding the resting phase (Fig. 3A). This phase distribution indicates a major rewiring of protein phosphorylation and presumably synaptic function at the activity-to-rest and rest-to-activity transitions. In order to identify synaptic functions that are temporally compartmentalized by protein phosphorylation, we searched for statistically enriched protein annotations in each of the two defined phase clusters (Fisher's exact test $p<0.05$, see Methods). At the end of the resting phase, our analysis found keywords representing Cell adhesion and Cell junction as well as Ion channels, Ion transporters, Hydrolases and Kinases highly enriched. In contrast, Cell projection, Cytoskeleton and Ubiquitin conjugation proteins are rhythmically phosphorylated in the cluster at the end of the activity phase (Fig. 3, B and C, table S3). This highlights the temporal regulatory nodes involved in the remodeling processes that are known to occur at synapses (*15*). Proteins involved in Cell division and Mitosis were also overrepresented in the phosphorylation cluster at the end of the activity phase. Although far from the nucleus, the localization and function of some proteins with key roles in cell division, e.g. CDK5, are also important for synaptic activity (*16*), and such unexpected connections may be true for other proteins. We suggest that the combination of an in-depth, quantitative workflow with spatial isolation can enable the identification of phosphorylation events in proteins not traditionally associated with synaptic function.

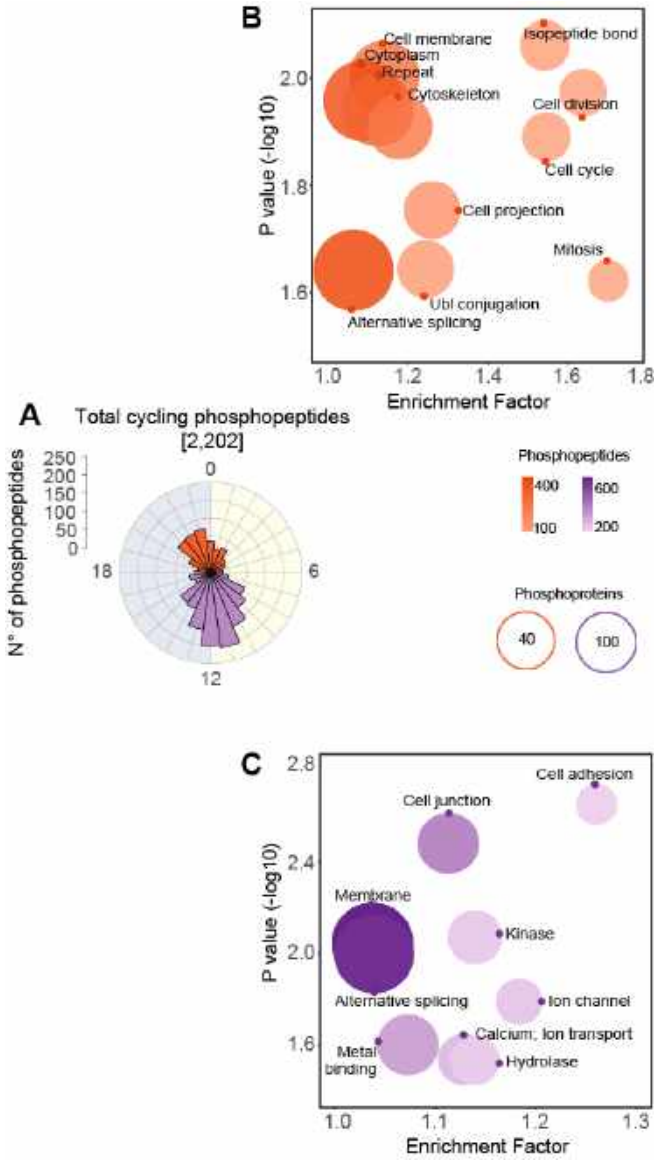


Fig. 3 Phosphorylation-dependent temporal control of synaptic functions. (A) Rose plot showing the distribution of phases from cycling phosphopeptides of the total phosphoproteome. (B) Scatter plot showing the significantly enriched (Fisher's exact test $p < 0.05$) Uniprot Keywords protein annotations showing peak of phosphorylation cycles in the activity-rest transition (ZT18 to ZT6). Size of geometric points is proportional to the number of cycling phosphoproteins in the annotation and color intensity to the total number of phosphosites. (C) As in B but for the phosphopeptide cluster in the transition of rest-activity (ZT6 to ZT18).

## Synapses are hubs of kinases

We next focused our attention on the major and specific enrichment of kinases, key regulators of almost all cellular process, at the end of the resting phase.

Almost 500 phosphorylated peptides from a total of 128 kinases from all major families. Thus a fifth of the total mouse kinome is not only present in the synaptic compartment but also detectable in a phosphorylated form (fig. S3A). More than half of these kinases show at least one rhythmic phosphorylation with the same overall phase distribution as the total cycling synaptic phosphoproteome ($q < 0.05$, Fig. 4A, fig. S3B, 3C and table S4). They belong to all major kinase families with a higher representation of AGC threonine/serine kinases (Fig. 4B and fig. S3D). All of the 66 kinases with rhythmic phosphorylation were also quantified at the protein level in this compartment (*11*), however, only four of them cycled in protein abundance (fig S3E). Therefore, phosphorylation, rather than protein abundance, regulates temporal kinase function at synapses across the day.

Since site-specific phosphorylation does not always imply changes in activity, we set out to identify temporally activated kinases with an unbiased workflow that uses high-confidence protein-protein interaction networks and large-scale phosphorylation data to retrieve protein signaling functionality. This PHOTON pipeline assigns a score to each protein based on the phosphorylation status of their interacting proteins (*17*). As these scores reflect the changes in phosphorylation levels of their substrates/interactors, kinases that are activated rather than only phosphorylated should have PHOTON scores cycling across the 24h, with the maximum score indicating the peak of kinase activity. From all synaptic kinases with rhythmic phosphorylation, this analysis resulted in rhythmic activity patterns for 13 of them (see Methods). Of these, 11 are active at the rest-activity transition, including protein kinase C (PRKCA, PRKCB, PRKCG) and Ca2+/calmodulin-dependent kinase 2 (CAMK2B, CAMK2G). Conversely, the tyrosine-protein kinase ABL2 and the serine/threonine-protein

kinase DCLK1 showed the opposite behavior, peaking at the activity-rest transition (Fig 4, C and D). Interestingly, the kinases activated at the end of the rest phase are associated with excitatory synaptic activity (*8*) while those activated at the end of the activity phase are associated with inhibitory synaptic activity (*18, 19*). PHOTON scores were also used to predict temporally regulated synaptic processes by means of phosphorylation dynamics (see Methods). In line with our kinase activity results, we inferred that the triggering of inhibitory synaptic mechanism, involving GABA, happens at the end of the activity period, while glutamate-mediated synaptic excitatory activity was predominantly associated to the rest-activity transition (Fig. 4E). These data are consistent with the roles of these synaptic types in rest and activity, respectively (*20, 21*). While the existing network data are sufficient to associate rhythmic activity with a substantial subset of the kinases, more complete networks will likely establish activity changes for a much larger fraction of the cycling synaptic phosphoproteome in the future. Together the combination of predictive and experimental data places extensive temporal regulation of kinases activity at the core phospho-dependent functional processes at the synapse.

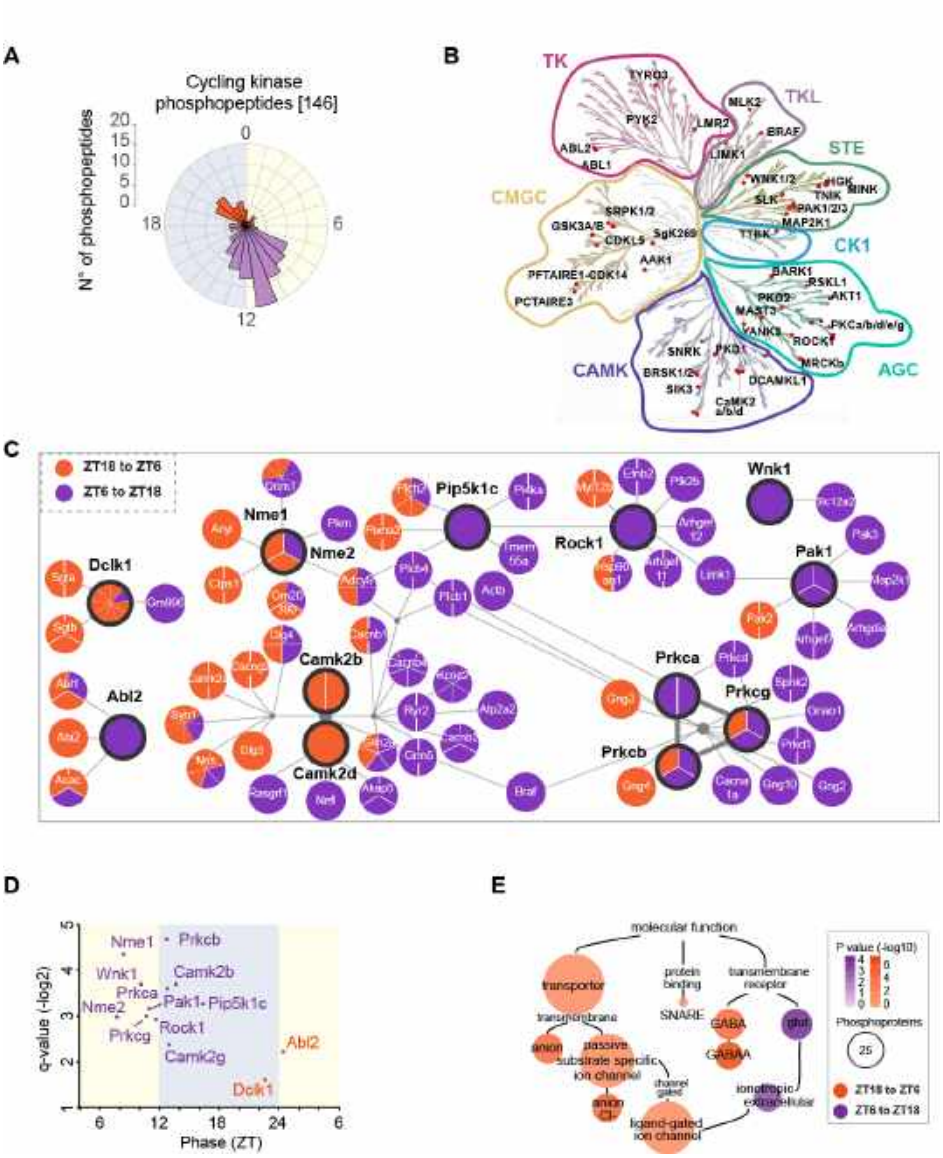


Fig. 4 Rhythmic phosphorylation and activation of synaptic kinases. (A) Rose plot with the phases of cycling phosphopeptides in kinases of synaptoneurosomes. Colors denote the clusters of activity-rest transition (ZT18-ZT6, orange) and rest-activity transition (ZT6-ZT18, purple). (B) Kinases with at least one phosphorylation cycling annotated to the major kinase families (52 out of the total 66 cycling) using http://www.kinhub.org. Tyrosine Kinases (TK), Tyrosine Kinase-Like (TKL), Homologs of the yeast STE7, STE11 and STE20 genes (STE), Casein/cell kinase 1 family (CK1), Protein Kinase A, G, C families (AGC), Calmodulin/Calcium regulated kinases and some non-calcium regulated families (CAMK), CDK, MAPK, GSK3 and CLK kinase families (CMGC). Atypical kinases are not shown. (C) Protein interaction network of PHOTON predicted cycling kinases (q <0.05) with rhythmic phosphorylations with their cycling phosphorylated interactors. Nodes are divided based on the number of cycling phosphorylations color coded based on the clusters in A. (D) Scatter plot showing the PHOTON predicted peak of activation of kinases from C color coded based on the transition clusters shown in A. Phases are represented in the X-axis and the q-value obtained in the cycling

analysis of the PHOTON scores in the Y-axis. (E) Representation of the GO Molecular Function annotations statistically enriched in a phase dependent manner using the PHOTON scores (phase dependent enrichment test $q < 0.05$, see Methods). Color indicates the phase of the annotation based on the cluster colors of A. Size of circles is proportional to the number of cycling phosphoproteins in the annotation and color intensity to the p-value of the enrichment test.

**Sleep deprivation abrogates synaptic phosphorylation rhythms**

We hypothesized that the sharp distribution of synaptic phosphorylation patterns concomitant with the activity transitions may reflect sleep pressure (a sleep homeostat) in addition or alternatively to circadian (time-of-day) mechanisms. To test their relative contribution, we subjected mice to 4h sleep deprivation (SD) by gentle handling (*22*) prior to each timepoint, and collected brains every 6h in 24h (n=4/time point; Fig. 5A). This protocol of SD across the 24h time course equalizes the sleep pressure to keep it constantly high (*23*). Synaptoneurosomes from forebrain were prepared from SD mice, and phosphopeptides enriched prior to MS analysis as above (Fig. 5A, see Methods). We accurately quantified 7,021 phosphopeptides in at least 50% of the measured samples, very similar values to those in the base-line experiment, with more than 90% overlap between them (fig. S4A). Strikingly, cycling analysis of the 6,526 phosphopeptides revealed almost complete abrogation of rhythmic phosphorylation in the synaptic compartment of SD mice. Only 2.3% (47 phosphopeptides corresponding to 41 proteins) cycled in SD (period=24h, $q < 0.05$, see Methods, Fig. 5, B and C, fig. S4B-D, table S5). These few remaining cycling phosphopeptides oscillated with similar amplitudes and with comparable phases in both conditions (Fig. 6A-C).

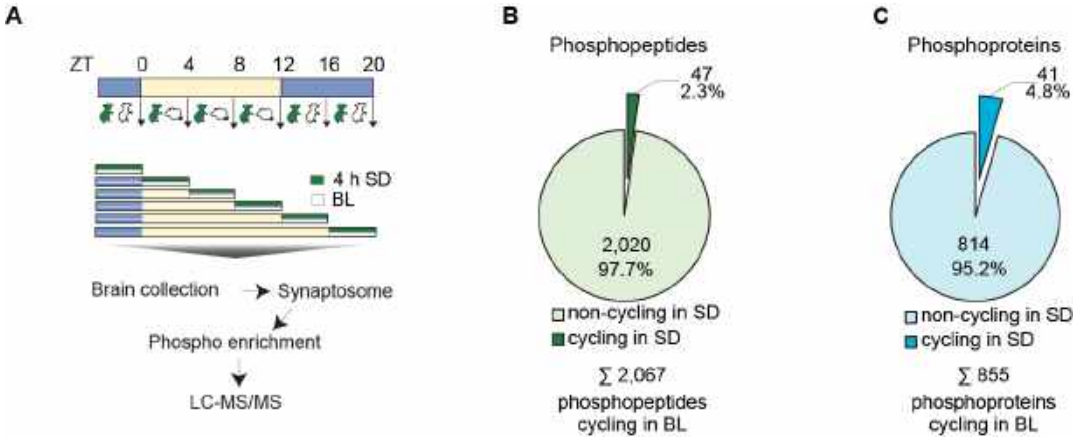


**Fig. 5 Sleep deprivation abrogates synaptic phosphorylation rhythms.** **(A)** Experimental workflow used to profile the synaptoneurosome phosphoproteome under sleep deprivation across 24h. Sleep deprived (SD) animals were kept awake for 4h (green window) before being euthanized together with base line controls (BL). Blue and yellow indicate the light conditions during the protocol. Note that SD animals are awake regardless of the light conditions whereas BL mice rest during the light phase and are active in the dark. **(B)** Pie chart representing the fraction of cycling phosphopeptides (period=24h, $q<0.05$) in forebrain synaptoneurosomes from SD mice out of the 2,067 rhythmic in BL mice. **(C)** Pie chart representing the fraction of proteins with at least one cycling (period=24h, $q<0.05$) phosphopeptide in synaptoneurosomes of SD mice out of the 855 oscillating under BL conditions.

Since sleep pressure did not affect the pattern of the remaining rhythmic phosphopeptides, they appear to only be driven by the circadian clock. Of the corresponding 41 synaptic phosphoproteins, 31 form a protein interaction network with SHANK3, RTN4, MTAP1B, STX1, MYO5A and HSP90 at the core, much more than expected by chance (see Methods, fig. S5). They belong to interconnected cellular structures such as cytoskeleton, synaptic scaffolding, membrane, vesicle trafficking, and ubiquitin mechanisms, all important for synaptic integrity and function (*24-26*). Almost a third are cytoskeletal proteins with molecular motors such as MTAP1B and MYO5A and other microtubule associated proteins (MTAP4, KIF21A, STMN3, STMN1, ABI1). Furthermore, under SD rhythmic phosphorylation is also preserved on proteins involved in synaptic vesicle formation and exocytosis, which is essential for chemical

neurotransmission (CHGB, STX1A, STXBP5). Cell adhesion (RTN4, PGRMC1, BASP1, NRCAM, CADM1) and scaffolding proteins (SHANK3, PICCOLO, BASSOON) are likewise unaffected, commensurate with the crucial role of these proteins in the regulation of synaptic integrity. Finally, the rhythmic phosphorylation of chaperone HSP90A, important in the synapse for trafficking of AMPA receptors (*24*), persisted. Thus only a very small number of phosphorylation sites in key synaptic components remain cycling under high sleep pressure, perhaps because of indispensable regulatory roles. Our results clearly establish that sleep deprivation severely affects synaptic phosphorylation across the day, leading to a dramatic loss in rhythmicity.

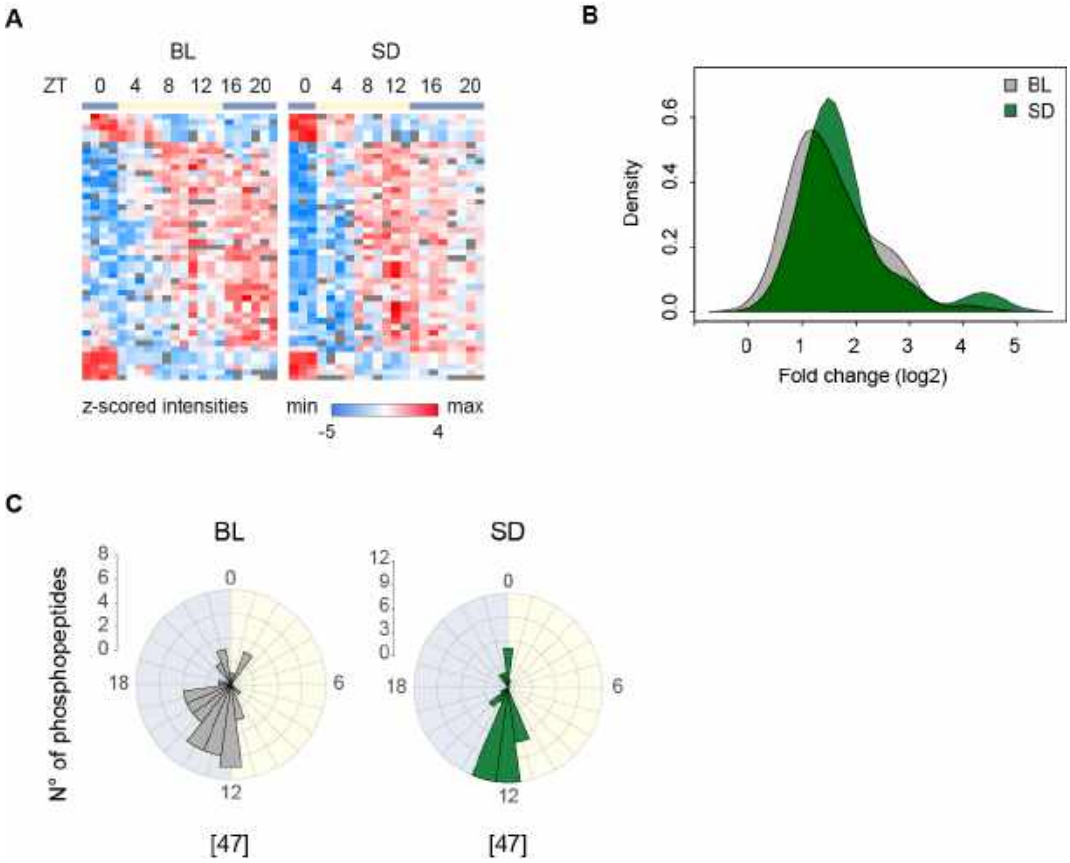


**Fig. 6 Synaptic phosphoproteome cycling under sleep deprivation.** **(A)** Heat maps of the intensities (z-scored log2) of the 47 cycling phosphopeptides in BL (left) and SD (right) synaptoneurosomes ordered by peak of abundance. **(B)** Density plot with the fold change of the 47 phosphopeptides rhythmic in both conditions, calculated for BL (grey) and SD (green)

conditions. **(C)** Rose plots showing the phase distribution in BL (left) and SD (right) for the 47 cycling phosphopeptides.

## Discussion

Synaptic plasticity and function dynamically change across the day (*27*). It was already known that changes in synaptic activity are associated with the phosphorylation of several signaling proteins (*8, 26*). However, our large-scale quantitative phosphoproteomes of isolated synaptoneurosomes resulted in the first comprehensive time-resolved map of synaptic phosphorylation across the entire activity and rest phases. We detected cycles on 30% of phosphorylation events in the synaptic compartment, a fraction far exceeding the 5% reported in total mouse hippocampus (*28*). The phosphoproteome is much more dynamic than the proteome (50% of proteins oscillating on at least one site vs. only 5% of oscillating proteins). Similar to our previous finding in the liver (*3*), mean fold-changes of the phosphoproteome are more than three-fold higher than in the proteome. At 7,000 accurately quantified phosphopeptides, the depth of our analysis allowed in depth bioinformatic analysis, retrieving many known but also highlighting novel temporally regulated processes at synapses. Overall, the phases of cycling phosphorylation fall into two main clusters at the boundaries of activity-rest transitions, implying a major role of synaptic phosphorylation in this process.

Numerous kinases are expressed in the brain, and some of them have been also localized to the synaptic compartment (*29*). However, our study clearly now classifies the synapse as a major kinase hub. Indeed, we detect more than 100 phosphorylated kinases (20% of the total kinome) and found that 50% cycle on at least one phosphoresidue. Combining protein interaction network data with

our quantitative phosphoproteome revealed that these phosphorylation changes regulate the activity of at least a subset of them.

Together, our predictive and experimental data suggest phosphorylation-dependent temporal segregation of long-term potentiation (LTP) and long-term depression (LTD). Kinases with higher activity at the end of the rest period are involved in LTP, such as CAMK and PRKC, which function directly downstream of NMDARs receptor Ca2+ signaling (*8*). In contrast, ABL2 and DCLK1, two kinases modulating structural synaptic plasticity (*18, 19*) peak in activity at the transition to the rest period. Lack of ABL2 leads to elevated NMDAR synaptic currents (*19*), therefore ABL2 activation at the beginning of the resting phase may mediate synaptic downscaling. At the beginning of the active phase, GSK3b is phosphorylated on its inhibitory site S389. This blocks LTD and GABAR trafficking (*30*), further indicating a role of phosphorylation in the temporal segregation of LTP and LTD. Figure 7 summarizes the complex phosphorylation pattern of many key components of these processes.

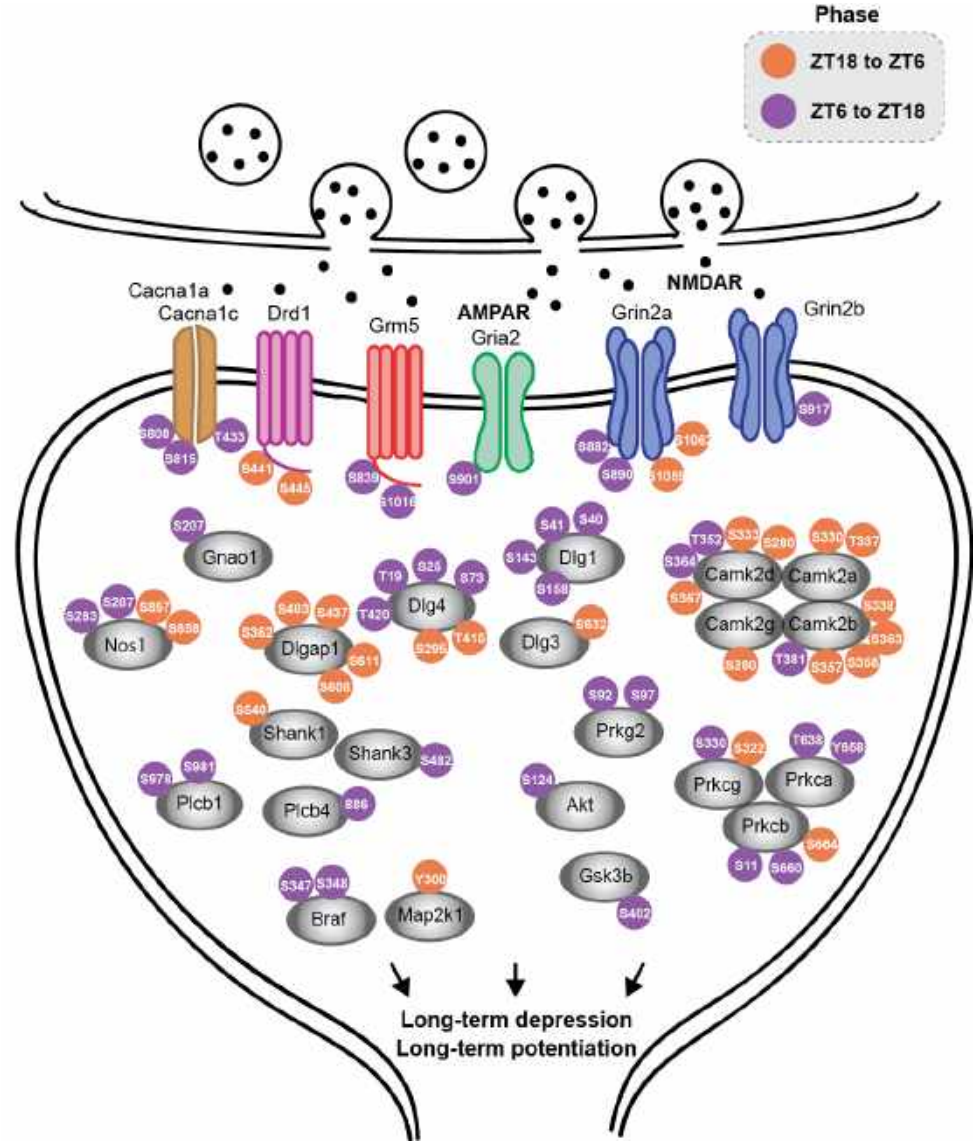


**Fig. 7 Dynamic phosphorylation of synaptic plasticity mediators.** Schematic map of an excitatory synapse showing rhythmic phosphorylated sites detected in proteins involved in long term depression and potentiation. Number in the circle represents the phosphorylated amino acid and the color refers to the peak of the phosphorylation cycle as in Fig. 3A (orange from ZT18 to ZT6 and purple from ZT6 to ZT18).

Together, our data point towards an association of synaptic potentiation with wakefulness (activity) while synaptic downscaling with rest. This supports the general synaptic homeostasis hypothesis for sleep – that synaptic downscaling is a critical function of sleep (*31*) at the molecular level and provides starting points for a multitude of mechanistic investigations.

To directly test the contribution of sleep and circadian cycles on phospho-dependent synaptic function, we sleep deprived mice at different times during the rest period. We observed that sleep pressure almost entirely abrogates global diurnal oscillation of phosphorylation in the synaptic compartment. This discovery establishes the importance of the homeostatic regulation of sleep over any other mechanism in generating daily rhythms of phosphorylation to modulate synaptic function.

Independent studies examining phosphorylation and sleep pressure support our findings. A very recent analysis in total mouse brain showed that increasing hours of sleep deprivation resulted in increasing average phosphorylation levels of 80 synaptic proteins (*10*). Based on these results, we examined our data and found phosphorylations in all of those 80 proteins. Our data also show rhythms over the day in 69 of them, although our site-specific data reveal a more nuanced picture than a simple overall increase in phosphorylation. Nevertheless, the fact that two completely different experimental approaches find concordant regulation on a subset of synaptic proteins provides validation, whereas our rhythmic data support the hypothesis that these phosphorylation sites are indeed part of the signatures of sleep.

Another recent phosphoproteomics study in the synaptic compartment showed that sleep regulates dephosphorylation of AMPA receptors in response to HOMER1a-dependent immediate early transcriptional signaling (*9*). Our data independently support these findings, extend them to several other neurotransmitter receptors and supply their diurnal rhythms of phosphorylation in response to sleep and activity pressure (Fig. 7).

Although the vast majority of protein phosphorylation appears to be regulated by sleep or wake states, a small number of circadian phosphorylations remain

unchanged in amplitude and phase under sleep deprivation. These phosphorylations occur in a highly connected node of proteins involved in both synaptic vesicle trafficking (molecular motors, microtubule-associated proteins) and synaptic scaffold (SHANK3, PICCOLO, BASSOON), overall regulating excitatory synaptic strength, apparently irrespective of sleep-wake pressure. The fact that circadian rhythmicity regulates cortical function is already well documented at both behavioral and molecular levels (*32*). Together with our data, this makes it likely that even as sleep-wake pressures dynamically reconfigure synaptic structure and function, an underlying circadian rhythmicity continues at the molecular level, accounting for sleep-independent, circadian rhythms in cortical function.

In conclusion, this study represents the first *in vivo* evidence of orchestration of thousands of phosphorylation events in synapses across the day. These extensive phosphorylation rhythms temporally segregate synaptic activity in response to activity changes. Our study demonstrates a central role for rest-activity cycles in regulating phospho-dependent synaptic homeostasis in response to both sleep and wake pressure, potentially modulating inhibitory and excitatory synaptic plasticity. Interfering with rest-activity cycles almost completely abolished rhythms of phosphorylation in synaptic proteins, which may lead to dysfunctional synaptic plasticity associated with sleep deprivation.

**References**

1. D. Mauvoisin *et al.*, Circadian clock-dependent and -independent rhythmic proteomes implement distinct diurnal functions in mouse liver. *Proceedings of the National Academy of Sciences of the United States of America* 111, 167-172 (2014).

2. M. S. Robles, J. Cox, M. Mann, In-vivo quantitative proteomics reveals a key contribution of post-transcriptional mechanisms to the circadian regulation of liver metabolism. *PLoS genetics* 10, e1004047 (2014).

3. M. S. Robles, S. J. Humphrey, M. Mann, Phosphorylation Is a Central Mechanism for Circadian Control of Metabolism and Physiology. *Cell Metab*, (2016).

4. F. Hosp, M. Mann, A Primer on Concepts and Applications of Proteomics in Neuroscience. *Neuron* 96, 558-571 (2017).

5. K. Sharma *et al.*, Cell type- and brain region-resolved mouse brain proteome. *Nature neuroscience* 18, 1819-1831 (2015).

6. J. J. Liu *et al.*, In vivo brain GPCR signaling elucidated by phosphoproteomics. *Science* 360, (2018).

7. D. C. Dieterich, M. R. Kreutz, Proteomics of the Synapse--A Quantitative Approach to Neuronal Plasticity. *Molecular & cellular proteomics : MCP* 15, 368-381 (2016).

8. K. M. Woolfrey, M. L. Dell'Acqua, Coordination of Protein Phosphorylation and Dephosphorylation in Synaptic Plasticity. *The Journal of biological chemistry* 290, 28604-28612 (2015).

9. G. H. Diering *et al.*, Homer1a drives homeostatic scaling-down of excitatory synapses during sleep. *Science* 355, 511-515 (2017).

10. Z. Wang *et al.*, Quantitative phosphoproteomic analysis of the molecular substrates of sleep need. *Nature*, (2018).

11. S. B. Noya *et al.*, The Cortical Synaptic Transcriptome is Organized by Clocks, but its Proteome is Driven by Sleep (2018).

12. P. R. Dunkley, P. E. Jarvie, P. J. Robinson, A rapid Percoll gradient procedure for preparation of synaptosomes. *Nature protocols* 3, 1718-1728 (2008).

13. S. J. Humphrey, S. B. Azimifar, M. Mann, High-throughput phosphoproteomics reveals in vivo insulin signaling dynamics. *Nature biotechnology* 33, 990-995 (2015).

14. S. Tyanova *et al.*, The Perseus computational platform for comprehensive analysis of (prote)omics data. *Nat Methods* 13, 731-740 (2016).

15. V. M. Ho, J. A. Lee, K. C. Martin, The cell biology of synaptic plasticity. *Science* 334, 623-628 (2011).

16. K. O. Lai, Z. Liang, E. Fei, H. Huang, N. Y. Ip, Cyclin-dependent Kinase 5 (Cdk5)-dependent Phosphorylation of p70 Ribosomal S6 Kinase 1 (S6K) Is Required for Dendritic Spine Morphogenesis. *The Journal of biological chemistry* 290, 14637-14646 (2015).

17. J. D. Rudolph, M. de Graauw, B. van de Water, T. Geiger, R. Sharan, Elucidation of Signaling Pathways from Large-Scale Phosphoproteomic Data Using Protein Interaction Networks. *Cell Syst* 3, 585-593 e583 (2016).

18. E. Shin *et al.*, Doublecortin-like kinase enhances dendritic remodelling and negatively regulates synapse maturation. *Nature communications* 4, 1440 (2013).

19. X. Xiao, A. D. Levy, B. J. Rosenberg, M. J. Higley, A. J. Koleske, Disruption of Coordinated Presynaptic and Postsynaptic Maturation Underlies the Defects in Hippocampal Synapse Stability and Plasticity in Abl2/Arg-Deficient Mice. *The Journal of neuroscience : the official journal of the Society for Neuroscience* 36, 6778-6791 (2016).

20. C. Cirelli, C. M. Gutierrez, G. Tononi, Extensive and divergent effects of sleep and wakefulness on brain gene expression. *Neuron* 41, 35-43 (2004).

21. V. V. Vyazovskiy, C. Cirelli, M. Pfister-Genskow, U. Faraguna, G. Tononi, Molecular and electrophysiological evidence for net synaptic

potentiation in wake and depression in sleep. *Nature neuroscience* 11, 200-208 (2008).

22. I. Tobler, T. Deboer, M. Fischer, Sleep and sleep regulation in normal and prion protein-deficient mice. *The Journal of neuroscience : the official journal of the Society for Neuroscience* 17, 1869-1879 (1997).

23. S. Maret *et al.*, Homer1a is a core brain molecular correlate of sleep loss. *Proceedings of the National Academy of Sciences of the United States of America* 104, 20090-20095 (2007).

24. N. Z. Gerges *et al.*, Independent functions of hsp90 in neurotransmitter release and in the continuous synaptic cycling of AMPA receptors. *The Journal of neuroscience : the official journal of the Society for Neuroscience* 24, 4758-4766 (2004).

25. D. Ivanova, A. Dirks, A. Fejtova, Bassoon and piccolo regulate ubiquitination and link presynaptic molecular dynamics with activity-regulated gene expression. *J Physiol* 594, 5441-5448 (2016).

26. J. Li *et al.*, Long-term potentiation modulates synaptic phosphorylation networks and reshapes the structure of the postsynaptic interactome. *Science signaling* 9, rs8 (2016).

27. G. Tononi, C. Cirelli, Sleep and the price of plasticity: from synaptic and cellular homeostasis to memory consolidation and integration. *Neuron* 81, 12-34 (2014).

28. C. K. Chiang *et al.*, Phosphoproteome Profiling Reveals Circadian Clock Regulation of Posttranslational Modifications in the Murine Hippocampus. *Front Neurol* 8, 110 (2017).

29. L. L. Baltussen, F. Rosianu, S. K. Ultanir, Kinases in synaptic development and neurological diseases. *Prog Neuropsychopharmacol Biol Psychiatry* 84, 343-352 (2018).

30. C. A. Bradley *et al.*, A pivotal role of GSK-3 in synaptic plasticity. *Front Mol Neurosci* 5, 13 (2012).

31. G. Tononi, C. Cirelli, Sleep function and synaptic homeostasis. *Sleep Med Rev* 10, 49-62 (2006).

32. R. Iyer, T. A. Wang, M. U. Gillette, Circadian gating of neuronal functionality: a basis for iterative metaplasticity. *Front Syst Neurosci* 8, 164 (2014).

33. J. A. Vizcaino *et al.*, 2016 update of the PRIDE database and its related tools. *Nucleic Acids Res* 44, D447-456 (2016).

34. P. R. Dunkley, P. E. Jarvie, P. J. Robinson, A rapid Percoll gradient procedure for preparation of synaptosomes. *Nature protocols* 3, 1718-1728 (2008).

35. M. S. Robles, S. J. Humphrey, M. Mann, Phosphorylation Is a Central Mechanism for Circadian Control of Metabolism and Physiology. *Cell Metab*, (2016).

36. S. Tyanova, T. Temu, J. Cox, The MaxQuant computational platform for mass spectrometry-based shotgun proteomics. *Nature protocols* 11, 2301-2319 (2016).

37. S. Tyanova *et al.*, The Perseus computational platform for comprehensive analysis of (prote)omics data. *Nat Methods* 13, 731-740 (2016).

38. M. S. Robles, J. Cox, M. Mann, In-vivo quantitative proteomics reveals a key contribution of post-transcriptional mechanisms to the circadian regulation of liver metabolism. *PLoS genetics* 10, e1004047 (2014).

**Acknowledgments**: We thank K. Mayr, I. Paron and G. Sowa for technical assistance with the MS measurements, B. Collins for critical reading of the manuscript and B. Splettstößer for technical help with experimental workflow.

Funding: This work was supported by the Max-Planck Society for the Advancement of Sciences and the German Research Foundation (DFG/Gottfried Wilhelm Leibniz Prize) funded this study. S.A.B. and S.B.N. were supported by the Swiss National Science Foundation, the Velux Foundation, the Human Frontiers Science Program, and the Zürich Clinical Research Priority Project "Sleep and Health" and are members of the Neurosciences program within the Life Sciences Zürich Graduate School; Author contributions: S.B.N., M.S.R. and S.A.B. conceived and initiated the project and designed experiments; S.B.N., M.S.R. and F.B performed sample preparation and mass spectrometry experiments; M.S.R. and F.B. performed bioinformatic and data analysis with help from S.B.N. and T.B.; J.D.R. performed PHOTON analysis under supervision of J.C.; S.B.N., F.B., M.S.R., S.A.B. and M.M. wrote the manuscript with editing and input from T.B. and J.D.R.

# 5. Discussion and Outlook

In this thesis, I demonstrate a major daily molecular reorganization of the rhythmic transcriptome, proteome and phosphoproteome in synaptoneurosomes. In a way distinctive from the brain as a whole, molecules oscillate daily to reach peak levels at dawn and dusk. These peaks reflect control of different aspects of cellular physiology, since mRNAs, proteins and phosphoproteins from each participate in very distinctive biological processes. Controlling those rhythms, a circadian clock mostly dictates temporal abundance of transcripts, but sleep-wake cycles participate in the regulation with a more profound effect on proteins and phosphorylations. It could be that mRNA is provisioned in two phases anticipating the requirements of the time that follows. This would create a basis for proteins to be translated as needed when wake and sleep happen, thereby facilitating the brain functions that accompany these two behavioral states. Likely, the dynamics of both these processes are signaled at the synpase through phosphorylation of synaptic proteins to drive homeostasis.

The comprehensive catalog of mRNAs, proteins and phosphorylations in forebrain synapses that I created was obtained with poly(A) RNA sequencing and LC-MS/MS. The elements found and enriched in synaptoneurosome fractions clearly classified the samples as synapses according to Gene Ontology analysis, but cycling datasets diverged always in identity and abundance of elements in each phase. Therefore, significant dissimilarities exist in cellular function across time. Particularly impressive was that 78% of all transcripts were cycling in the transcriptome of synapses, a pervasiveness that is larger than that of the companion proteome and phosphoproteome as well as any other circadian transcriptome published to date. Moreover, these daily cycles of transcripts, proteins and phosphorylations were independent of those in the soma.

## 1.6. The mechanism behind synaptic rhythms

In principle, variations in temporal abundance of synaptic components could be achieved by transport from the soma, local degradation or local production. In our analysis we saw that rhythms in the soma are different from those of the synapses therefore some of the three processes listed above must be controlled by circadian clocks. Quantifying single mRNAs along dendrites demonstrated rhythms with equal amplitudes at different distances from the soma. Nevertheless, synaptic density increases in distal regions. This observation favors the idea of circadian transport rather than circadian stability of transcripts at synapses: if transport was constant but mRNA stability at synapses were circadian, one would predict increased circadian amplitude as synaptic density increased. Supporting the idea of circadian transport of mRNA to synapses, I have obtained preliminary data looking at the RBP Staufen1 indicating that it participates in the transport of a set of circadian synaptic mRNAs. Mice expressing a truncated Staufen1 protein that lacks the ability to bind RNA are viable but their neurons show a defect in RNA transport (Vessey et al., 2008). From the first manuscript we know that at synapses, transcripts that oscillate daily have significantly high levels at dawn versus dusk or vice versa. Looking at mRNA levels of those two phases from Staufen1 mutant synapses would show if the transport defects linked to the truncated STAU1 participate in time of day accumulation of mRNAs in the synapse.

Stau1 mutant and wild type (WT) littermates (n=6) were maintained in a regular LD scheduled and released in constant darkness 48 h before the isolation of synapses that happened at the subjective dawn (ZT0) and dusk (ZT12). A total of 16440 mRNAs were identified as expressed in synapses of mutant and wild type collected at the two circadian times. Of them, 845 features showed significant differences in at least one group ($q<=0.05$). Hierarchical clustering separated the dusk and dawn samples but

differences between wild type and mutant mice were only present in the dawn samples (Figure 3. A). 490 RNAs were low at dusk in both genotypes but different at dawn between wild type and mutant. Those differences between the genotypes indicate that Staufen1 participates in a time of day dependent accumulation of transcripts at the synapse. Due to the role of Staufen1 in dendritic transport of mRNAs (Vessey et al., 2008), this preliminary experiments further support the circadian transport hypothesis.

These preliminary data represent only the beginning of experiments that might decipher the mechanisms underlying the processes that I have characterized in this thesis. Taking the approach describe above, one could test complementary RBPs. In addition to RBPs, other key molecules of the neuronal transport mechanism are motor proteins that allow a rapid translocation of cargoes along microtubules. Cycling mRNAs encode both pre- and postsynaptic components. Therefore kinesins are more likely involved in circadian transport to synapses than dyneins, which only mediate anterograde transport in axons. A siRNA screening in neuronal cultures served to identify kinesins that are involved in axonal length sensing (Rishal et al., 2012). The same technique could serve to identify which kinesins are involved in circadian mRNA transport to synapses.

Such experiments will help to characterize the details of a complex mechanism responsible for the circadian synaptic transcriptome, where I propose that the clock would regulate multiple RBPs, motor proteins, and possibly other different post-transcriptional steps.

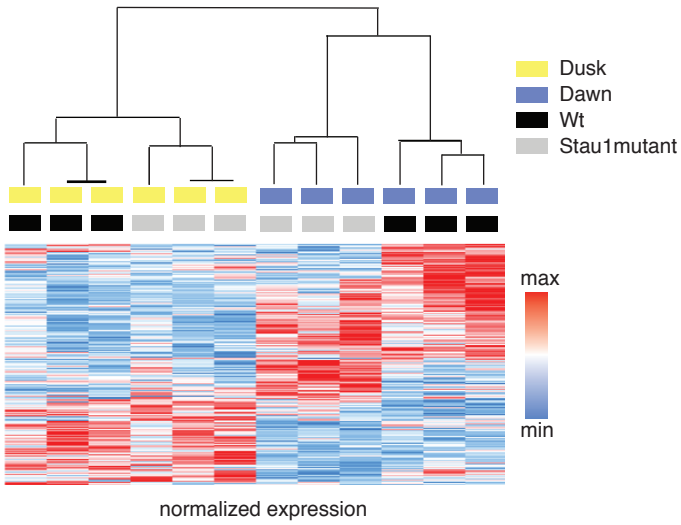


Figure 3. A. Heatmap of mRNA levels of 845 of transcripts (in rows) significantly different between groups (ANOVA, q<=0.05). Biological replicates of the for conditions (columns) are ordered according to hierarchical clustering.

As is the case for mRNAs, daily oscillations of proteins and their phosphorylations are also different between the synapses and the whole brain. In the first manuscript it was suggested that oscillations of mRNAs might be determining oscillations of a fraction of synaptic proteins. This again does not rule out a daily regulation of protein transport or local protein synthesis. Indeed, this thesis presents solid data that support as well the latter. Cycles in the synaptic proteome are abolished in a high sleep pressure time course. This might be the result of variations in synaptic local protein synthesis and protein phosphorylation due to the synaptic activity adjustments that come along with sleep deprivation. To confirm that hypothesis, studies of local protein translation rates in a time scale that resolves the daily oscillations become essential, and these studies are now more feasible after recent advances in the field (Hafner et al., 2019, Biever et al., 2020). As for proteins, cycles in synaptic phosprorylation are also dramatically affected with changes in sleep pressure. These changes could be due to alteration in protein abundance. However, in basal conditions, the dynamics of phosphopeptides are independent and of higher amplitudes than dynamics of the proteome. Beyond

translation, another mechanistic step must be discovered to explain synaptic cycles of phosphorylation in a normal day or under high sleep pressure. In manuscript 2, it is shown that at the synapse, a fifth of all mouse kinases are detected and half of them with cycling phosphorylations that match the phase of the whole synaptic phosphoproteome. Therefore, it could be that temporal phosphoregulation of kinases is the mechanism behind the synaptic phosphoproteome. To test this hypothesis, CamK2 and PKC isoforms, predicted to be temporally activated in the second manuscript, could be immunoprecipitated from synapses at different times of day and under different sleep pressure scenarios to evaluate their "in vitro" activity. To complement these experiments, temporal characterization of synaptic phosphoproteome from mouse models deficient in kinases that localize or have a predominant role at the synapse would be of great interest (Maier et al., 2009, Ukai et al., 2017).

## 1.7. The extent of the Sleep-wake contribution to synaptic oscillations

The results of the thesis in numbers: 2085 cycling transcripts, 946 proteins and 2202 phosphopeptides. These are rich time-resolved datasets to look for key molecules involved in dynamics of neuronal communication. For example, it would be quite interesting to seek molecular correlates of the slow wave activity that reflects homeostatic sleep pressure, and both I and other authors have begun to do this.

From the mRNAs, under conditions of high sleep pressure, a fourth had identical oscillations and the others preserved some degree of circadian rhythmicity. These data suggest that there is a circadian control of the oscillations that can be modified to different extents by sleep. A contemporary study derived 6 mathematical models of gene expression dynamics to determine the relative contributions of both circadian and

sleep processes and identified mRNAs in the mouse cortex for 6 possible groups (Hor et al., 2019). Using similar mathematical models, the synaptic mRNA dynamics of the first manuscript might also fit to several dynamics with relative circadian and sleep contribution of mRNA dynamics in the synapse. Indeed, in whole forebrain, from the six models, the one that parallels EEG delta power dynamics had the largest number of genes assigned (Hor et al., 2019). Similarly, another study found that about 80% transcripts of the mouse cortex undergoing diurnal changes depend on sleep pressure and cortical levels of a single transcript, *Homer1a*, was identified as a near-perfect biomarker of sleep loss (Maret et al., 2007). Yet another study focused on neurons that express Homer1a to select those cells activated by sleep deprivation. This allowed the authors to conclude that the response to sleep loss involves the regulation of intracellular calcium to recover from glutamate-dependent neuronal hyperactivity. Interestingly, while in the whole forebrain Homer1a protein decreases with sleep, it increases at synapses (Diering et al., 2017) indicating once more that is necessary to consider the polarization of neurons to study the mechanism of sleep homeostasis. In this case, following the increase of Homer1a during sleep, the authors found dephosphorylation of AMPA receptors that promotes its removal from the postsynaptic density and a subsequent synaptic scaling-down (Diering et al., 2017). In the other hand, for a scale-up, targeting this receptors to the membrane depends on its phosphorylation mediated by the kinase PKA (Diering et al., 2014). In a more recent study, an evolutionarily conserved PKA phosphorylation site was identified in the kinase SIK3 that is crucial for the regulation of sleep need (Honda et al., 2018). If this phosphorylation in SIK3 doesn't happen, mice have increased NREM amounts and inherent sleep need. Follow-up studies showed that inhibition of SIK3 reduces the phosphorylation of 80 synaptic proteins concomitantly with a decrease in slow wave

activity during sleep (Wang et al., 2019). The correlation between the phosphorylation state of these 80 proteins and measured sleep pressure made the authors call them "SNIPPs"; synaptic sleep-need-index phosphoproteins.

In the two manuscripts presented here the dynamics of the synaptic proteome and phosphoproteome were dramatically affected by the constant high sleep pressure since almost all daily oscillations were abrogated. Phosphorylations in SNIPPs were also detected in this cycling phosphoproteome . Of them, some were peaking with time spent awake but surprisingly there are phosphorylations in these proteins that increase with time spent asleep (Figure 4). Indeed, two thirds of cycling phosphorylations in the synapse peak at dusk, at the end of the rest phase of mice. Can these be "SSIPPs"? sleep-surplus-index phopshopeptides that increase with time spent asleep and after extended sleep time?

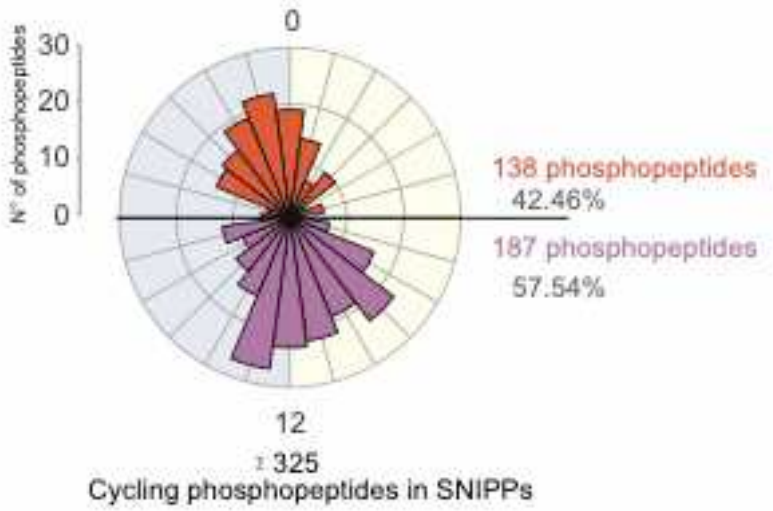


Figure 4. Rose plot of cycling phosphopeptides in SNIPPs from Wang et al. 2019 detected in the phosphoproteome of synapses presented in the second manuscript. As can be appreciated, in the Sleep Need Index Phosphoproteins, phosphorylations that increase with both time awake (orange) and time asleep (purple) are detected.

In the Manuscript 2 there is a proof for the first statement: many rhythmic phosphopeptides accumulate at synapses with time spent asleep. The proof of the second requires additional experiments. Something that could be done would be to

obtain the proteome and phosphoproteome of synapses in a time course of normal circadian timing but constant low sleep pressure, where the opposite behavior of SSIPs would be predicted. The idea for this came from forced dessynchrony studies in human and mice were sleep was monitored under cycles with different lengths (add here, Hassan et al., 2018). For example, a T20, with 10 h of light and 10 hours of dark allows that the clock runs free, meaning circadian time is unchanged (Wyatt et al., 1999, Derk-Jan Dijk et al., 1999, Braguer et al., 2013, Hassan et al., 2018). By contrast, the study showed that the 24-hour rhythmic distribution of sleep in terms of amount and intensity was abolished, and instead followed a disturbed 20-hour rhythmicity. Of interest for the experiments to come is that in subsequent cycles of the T20 one can find 6 circadian times across 24 h where sleep pressure is at its normal lowest daily level (Figure 5). Those times would become the low sleep pressure time course from which “SSIPPs” could be identified. The sleep field had focused so far in the identification of correlates of the homeostat that indicate sleep need. The low sleep pressure experiment would try to find anti-correlates indicating sleep surplus.

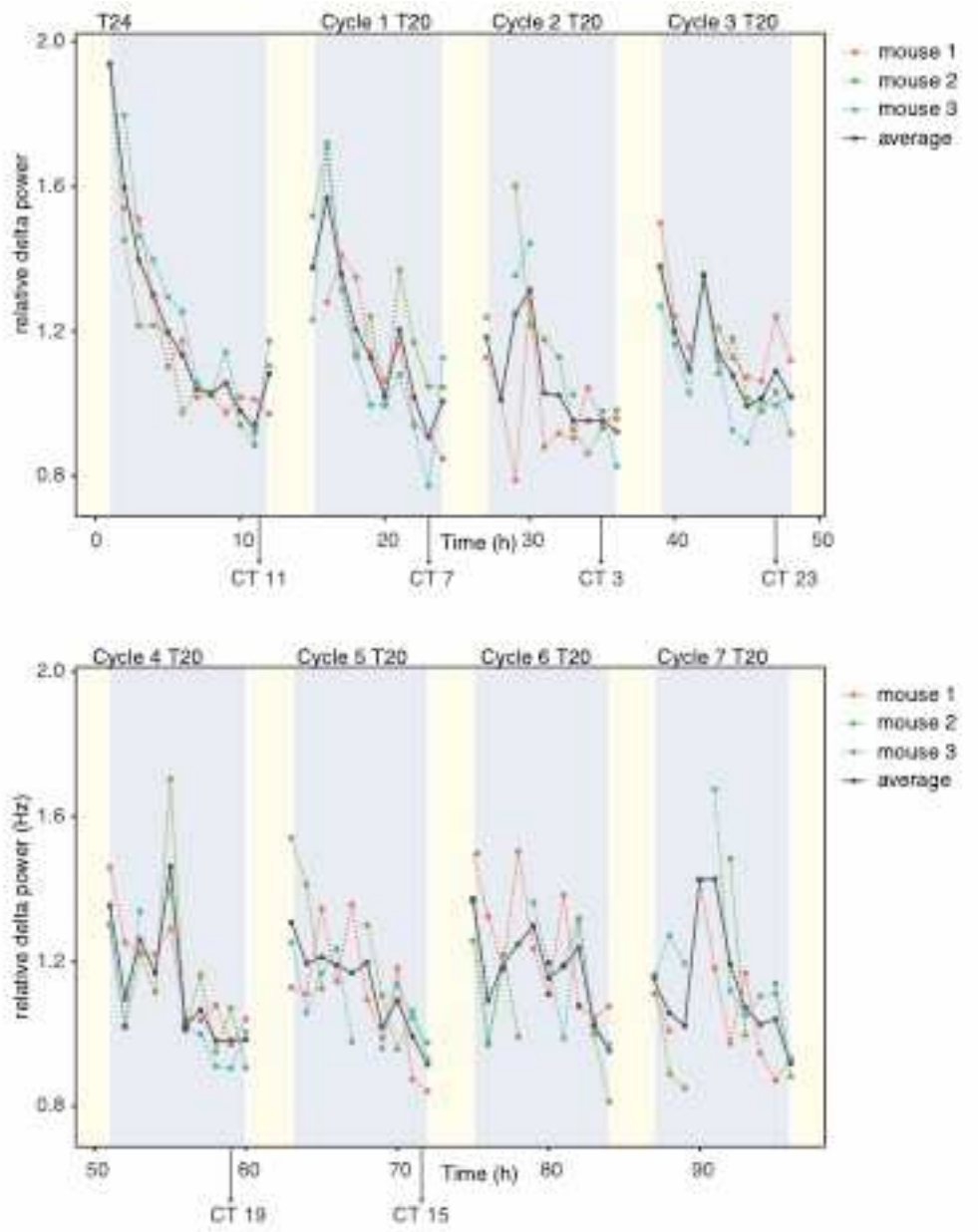


Figure 5 Time course of EEG delta power (individual biological replicates in color and dashed lines and mean in black) during one T24 cycle and 7 T20 cycles. For visualization purposes only the dark phase is shown. In squares are indicated the ideal collection times to generate a low sleep pressure time course around the clock.

## 1.8. Circadian and sleep modulation of ribosomal oxidation and translation

This multi-omics approach shows the complexity of synapses, and raises the question of how synapses might carry out their functions in such confined spaces. Despite the fact

that dendritic arbor volume represents about 30 to 60 times that of the soma, synapses are small. For example, it was estimated that synaptic spines are less than 100 nm3 (Harris and Stevens, 1989). It is tempting to suggest that the pervasiveness of daily rhythms in synapses facilitates function in the small available space. Compartmentalization of synaptic functions can be very well appreciated in the prediction analysis that came along with the three -omics datasets I obtained. In anticipation of daily activity RNAs, proteins and phosphopeptides contributing to synaptic transmission show peak levels. This goes in line with the idea that during wakefulness, while engaging with the external world, neurons increase the speed of their firing rates and strengthen. By contrast, in anticipation of sleep, synapses show peak levels of molecules that serve to a variety of cellular processes such as lipid catabolism, response to redox stress, ribosomal function and translation. According to the Synaptic Homeostasis Hypothesis, together with an overall downscaling, replenishment and restoration of neurons happen during sleep (Cirelli and Tononi, 2003 and reviewed in Tononi and Cirelli, 2014). Replenishment is represented in the Gene Ontology analysis from the first manuscript by Translation related annotations; repair by the Response to Oxidative Stress. Interestingly, my preliminary experiments link both with ribosomal structure, our third significant ontology annotation of the dusk peak. In E. coli reactive oxygen species (ROS) can oxidize ribosomal RNA at specific positions of the ribosome's catalytic center, inhibiting protein translation (Willi et al., 2018). In a pilot study, similar oxidation marks in the catalytic domain of ribosomal RNA from the mouse brain were found and many of them were significantly different among samples collected at dawn, dusk or when mice were sleep-deprived (Figure 5).

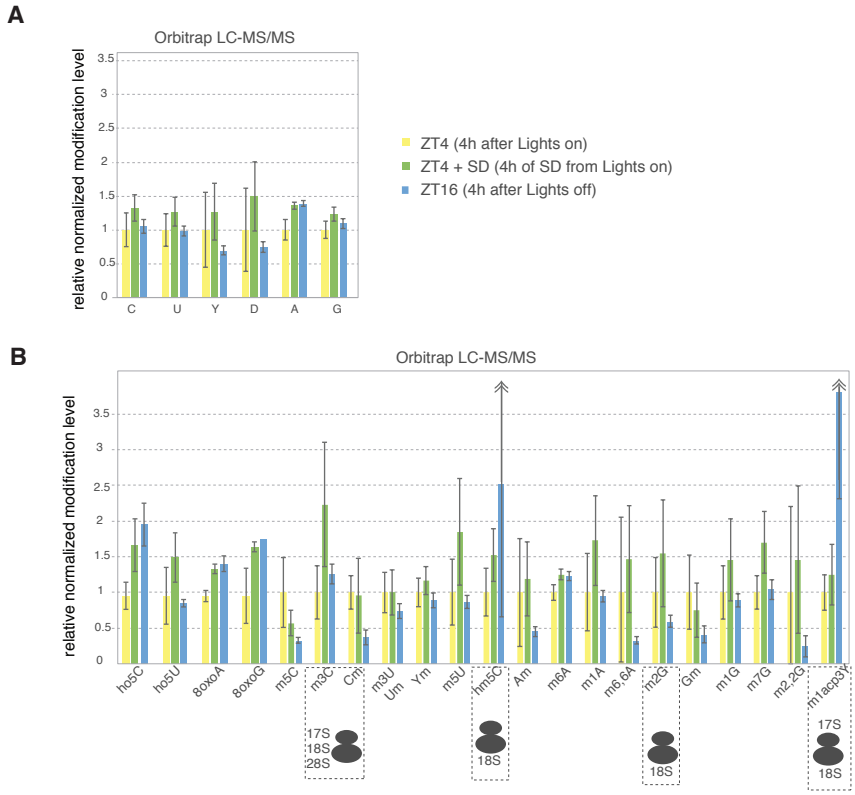


Figure 5. Relative normalized values (average of 4 biological replicates divided by average of replicates of BL4) of RNA oxidation marks measured with the Orbitrap LC-MS/MS system. A double arrow indicates standard deviations higher than the axis value levels. Modifications previously identified on rRNAs of eukaryotic ribosomal subunits are indicated.

To follow up that preliminary result, oxidation in synaptic ribosomal RNAs will be measured as well as the "in vitro" translation capacity of synaptic ribosomes. If circadian differences in oxidation were found, that will imply a circadian degradation of ribosomes that would require a temporal coupling of ribosome biogenesis. In the liver, ribosome biogenesis is under control of the clock (Jouffe et al., 2013), so such a hypothesis is plausible. If sleep need changes oxidation and degradation of ribosomes independently of time of day, the same experiment will establish redox state as a new sensor of sleep homeostasis.

## 1.9. Final conlusion

In this dissertation, transcriptomics, proteomics and phosphoprotomics show that mouse brain synapses are hubs of daily rhythms of accumulation of mRNAs, proteins and phosphorylation that are distinct from the neurons as a whole. Mechanisms to achieve this temporal compartmentalisation are new potential research avenues for the circadian and neuroscience fields.

Cycles in the three datasets show strong peak levels at only two specific times of day; some molecules reaching peaks of accumulation at dawn and others at dusk. Functionally, the two clusters represent biological processes related unambiguously to sleep and wake functions. This indicates that daily rhythms of synaptic molecular landscape are mainly linked to sleep and wake physiology and behavior as predicted by the Synaptic Homeostasis hypothesis of sleep. Indeed, the daily oscillations are shown to be controlled by both circadian clocks and sleep homeostasis. Clocks dictate mRNA rhythmic oscillations that can be modulated to certain extent by sleep homeostasis. However, the sleep-wake modulation of protein and phosphorylation dynamics overrides any underlying daily control. In agreement with the most recent findings searching for markers of sleep loss, in the present unbiased screening I confirm that phosphorylation at synapses is globally affected by sleep homeostasis disruptions, and indeed synaptic phosphorylation may therefore represent a potential diganostic and therapeutic target for sleep-wake-related dysfuctions.

Combining all the findings, the overall picture is one of circadian anticipation wake by synaptic provisioning of mRNAs to support synaptic transmission, and anticipation of sleep by provisioning of mRNAs to support restoration. These mechanisms are followed by a sleep-homeostatic control of protein

accumulation and phosphorylation to support synaptic potentiation and downscaling.

# 6. References

Adamantidis AR, Gutierrez Herrera C, Gent TC. Oscillating circuitries in the sleeping brain. *Nat Rev Neurosci*. 2019;20(12):746-762. doi:10.1038/s41583-019-0223-4

Allada R, White NE, So W V, Hall JC, Rosbash M. A mutant Drosophila homolog of mammalian Clock disrupts circadian rhythms and transcription of period and timeless. *Cell*. 1998;93(5):791-804. doi:10.1016/s0092-8674(00)81440-3

Allada R, White NE, So W V, Hall JC, Rosbash M. A mutant Drosophila homolog of mammalian Clock disrupts circadian rhythms and transcription of period and timeless. *Cell*. 1998;93(5):791-804. doi:10.1016/s0092-8674(00)81440-3

Archer SN, Laing EE, Möller-Levet CS, et al. Mistimed sleep disrupts circadian regulation of the human transcriptome. *Proc Natl Acad Sci U S A*. 2014;111(6):E682-E691. doi:10.1073/pnas.1316335111

Archer SN, Laing EE, Möller-Levet CS, et al. Mistimed sleep disrupts circadian regulation of the human transcriptome. *Proc Natl Acad Sci U S A*. 2014;111(6):E682-E691. doi:10.1073/pnas.1316335111

Astiz M, Heyde I, Oster H. Mechanisms of communication in the Mammalian Circadian timing system. *Int J Mol Sci*. 2019;20(2). doi:10.3390/ijms20020343

Barclay JL, Husse J, Bode B, et al. Circadian desynchrony promotes metabolic disruption in a mouse model of shiftwork. *PLoS One*. 2012;7(5). doi:10.1371/journal.pone.0037150

Barnes, CA, McNaughton BL, Goddard, GV, Douglas RM, Adamec R. Circadian rhythm of synaptic excitability in rat and monkey CNS. *Science (80- )*. 1977;197(4298):91-92. doi:10.1038/098448b0

Bauer KE, Segura I, Gaspar I, et al. Live cell imaging reveals 3′-UTR dependent mRNA sorting to synapses. *Nat Commun*. 2019;10(1). doi:10.1038/s41467-019-11123-x

Biever A, Glock C, Tushev G, et al. Monosomes actively translate synaptic mRNAs in neuronal processes. *Science (80- )*. 2020;367(6477). doi:10.1126/science.aay4991

Borbely AA. A two process model of sleep regulation. *Hum Neurobiol*. 1982;1(3):195-204.

Borbély AA, Daan S, Wirz-Justice A, Deboer T. The two-process model of sleep regulation: A reappraisal. *J Sleep Res*. 2016;25(2):131-143. doi:10.1111/jsr.12371

Brager AJ, Ehlen JC, Castanon-Cervantes O, et al. Sleep Loss and the Inflammatory Response in Mice Under Chronic Environmental Circadian Disruption.

Mistlberger RE, ed. *PLoS One*. 2013;8(5):e63752. doi:10.1371/journal.pone.0063752

Bray M. The influence of soil cryostructure on the creep and long term strength properties of frozen soils. 2008. doi:http://proquest.umi.com/pqdweb?did=1710343731&Fmt=7&clientId=4671&RQT=309&VName=PQD

Brown SA, Kowalska E, Dallmann R. (Re)inventing the Circadian Feedback Loop. *Dev Cell*. 2012;22(3):477-487. doi:10.1016/j.devcel.2012.02.007

Burgess HJ. Partial sleep deprivation reduces phase advances to light in humans. *J Biol Rhythms*. 2010;25(6):460-468. doi:10.1177/0748730410385544

Buxbaum AR, Wu B, Singer RH. Single β-actin mRNA detection in neurons reveals a mechanism for regulating its translatability. *Science (80- )*. 2014;343(6169):419-422. doi:10.1126/science.1242939

Challet E, Turek FW, Laute M, Van Reeth O. Sleep deprivation decreases phase-shift responses of circadian rhythms to light in the mouse: role of serotonergic and metabolic signals. *Brain Res*. 2001;909(1-2):81-91. doi:10.1016/s0006-8993(01)02625-7

Chang JW, Arnold MM, Rozenbaum A, et al. The Local Transcriptome in the Synaptic Neuropil Revealed by Deep Sequencing and High-Resolution Imaging. *Neuron*. 2012;74(3):453-466. doi:10.1016/j.jneumeth.2012.09.005

Chiang CK, Mehta N, Patel A, et al. The Proteomic Landscape of the Suprachiasmatic Nucleus Clock Reveals Large-Scale Coordination of Key Biological Processes. *PLoS Genet*. 2014;10(10):e1004695. doi:10.1371/journal.pgen.1004695

Cirelli C, Tononi G. Sleep and synaptic homeostasis. In: *Current Advances in Sleep Biology*. Vol 38. Nova Science Publishers, Inc.; 2009:123-139. doi:10.5665/sleep.4348

Crowe SA, Døssing LN, Beukes NJ, et al. Atmospheric oxygenation three billion years ago. *Nature*. 2013;501(7468):535-538. doi:10.1038/nature12426

Daan S, Beersma DGM, Borbely AA. Timing of human sleep: Recovery process gated by a circadian pacemaker. *Am J Physiol - Regul Integr Comp Physiol*. 1984;15(2). doi:10.1152/ajpregu.1984.246.2.r161

Damiola F, Le Minli N, Preitner N, Kornmann B, Fleury-Olela F, Schibler U. Restricted feeding uncouples circadian oscillators in peripheral tissues from the central pacemaker in the suprachiasmatic nucleus. *Genes Dev*. 2000;14(23):2950-2961. doi:10.1101/gad.183500

Davies SK, Ang JE, Revell VL, et al. Effect of sleep deprivation on the human metabolome. *Proc Natl Acad Sci U S A*. 2014;111(29):10761-10766. doi:10.1073/pnas.1402663111

de Juan-Sanz J, Holt GT, Schreiter ER, de Juan F, Kim DS, Ryan TA. Axonal Endoplasmic Reticulum Ca2+ Content Controls Release Probability in CNS Nerve Terminals. *Neuron*. 2017;93(4):867-881.e6. doi:10.1016/j.neuron.2017.01.010

Diering GH, Gustina AS, Huganir RL. PKA-GluA1 coupling via AKAP5 controls AMPA receptor phosphorylation and cell-surface targeting during bidirectional homeostatic plasticity. *Neuron*. 2014;84(4):790-805. doi:10.1016/j.neuron.2014.09.024

Diering GH, Nirujogi RS, Roth RH, Worley PF, Pandey A, Huganir RL. Homer1a drives homeostatic scaling-down of excitatory synapses during sleep. *Science (80- )*. 2017;355(6324):511-515. doi:10.1126/science.aai8355

Dieterich DC, Kreutz MR. Proteomics of the synapse - A quantitative approach to neuronal plasticity. *Mol Cell Proteomics*. 2016;15(2):368-381. doi:10.1074/mcp.R115.051482

Dijk DJ, Duffy JF, Kiel E, Shanahan TL, Czeisler CA. Ageing and the circadian and homeostatic regulation of human sleep during forced desynchrony of rest, melatonin and temperature rhythms. *J Physiol*. 1999;516(2):611-627. doi:10.1111/j.1469-7793.1999.0611v.x

Doyle M, Kiebler MA. Mechanisms of dendritic mRNA transport and its role in synaptic tagging. *EMBO J*. 2011;30(17):3540-3552. doi:10.1038/emboj.2011.278

Dunlap JC. Molecular bases for circadian clocks. *Cell*. 1999;96(2):271-290. doi:10.1016/S0092-8674(00)80566-8

Ebbinghaus H. Memory: A Contribution to Experimental Psychology. *Ann Neurosci*. 2013;20(4). doi:10.5214/ans.0972.7531.200408

Edgar DM, Dement WC, Fuller CA. Effect of SCN lesions on sleep in squirrel monkeys: Evidence for opponent processes in sleep-wake regulation. *J Neurosci*. 1993;13(3):1065-1079. doi:10.1523/jneurosci.13-03-01065.1993

Franken P, Dijk DJ. Circadian clock genes and sleep homeostasis. *Eur J Neurosci*. 2009;29(9):1820-1829. doi:10.1111/j.1460-9568.2009.06723.x

Franken P, Tobler I, Borbély AA. Sleep homeostasis in the rat: Simulation of the time course of EEG slow-wave activity. *Neurosci Lett*. 1991;130(2):141-144. doi:10.1016/0304-3940(91)90382-4

Fultz NE, Bonmassar G, Setsompop K, et al. Coupled electrophysiological, hemodynamic, and cerebrospinal fluid oscillations in human sleep. *Science (80- )*. 2019;366(6465):628-631. doi:10.1126/science.aax5440

Funato H, Miyoshi C, Fujiyama T, et al. Forward-genetics analysis of sleep in randomly mutagenized mice. *Nature*. 2016;539(7629):378-383. doi:10.1038/nature20142

Garces RG, Wu N, Gillon W, Pai EF. Anabaena circadian clock proteins KaiA and KaiB reveal a potential common binding site to their partner KaiC. *EMBO J*. 2004;23(8):1688-1698. doi:10.1038/sj.emboj.7600190

Gekakis N, Staknis D, Nguyen HB, et al. Role of the CLOCK protein in the mammalian circadian mechanism. *Science (80- )*. 1998;280(5369):1564-1569. doi:10.1126/science.280.5369.1564

Goo MS, Sancho L, Slepak N, et al. Activity-dependent trafficking of lysosomes in dendrites and dendritic spines. *J Cell Biol*. 2017;216(8):2499-2513. doi:10.1083/jcb.201704068

Greenwell BJ, Trott AJ, Beytebiere JR, Finegan P, Hernandez C, Menet Correspondence JS. Rhythmic Food Intake Drives Rhythmic Gene Expression More Potently than the Hepatic Circadian Clock in Mice. 2019. doi:10.1016/j.celrep.2019.03.064

Hablitz LM, Vinitsky HS, Sun Q, et al. Increased glymphatic influx is correlated with high EEG delta power and low heart rate in mice under anesthesia. *Sci Adv*. 2019;5(2). doi:10.1126/sciadv.aav5447

Hafner AS, Donlin-Asp PG, Leitch B, Herzog E, Schuman EM. Local protein synthesis is a ubiquitous feature of neuronal pre- And postsynaptic compartments. *Science (80- )*. 2019;364(6441). doi:10.1126/science.aau3644

Hanus C, Schuman EM. Proteostasis in complex dendrites. *Nat Rev Neurosci*. 2013;14(9):638-648. doi:10.1038/nrn3546

Hardin PE. Molecular genetic analysis of circadian timekeeping in Drosophila. In: *Advances in Genetics*. Vol 74. Academic Press Inc.; 2011:141-173. doi:10.1016/B978-0-12-387690-4.00005-2

Harris KM, Teyler TJ. Age differences in a circadian influence on hippocamapl LTP. *Brain Res*. 1983;261(1):69-73. doi:10.1016/0006-8993(83)91284-2

Hasan S, Foster RG, Vyazovskiy V V., Peirson SN. Effects of circadian misalignment on sleep in mice. *Sci Rep*. 2018;8(1):1-13. doi:10.1038/s41598-018-33480-1

Hasan S, van der Veen DR, Winsky-Sommerer R, Dijk DJ, Archer SN. Altered sleep and behavioral activity phenotypes in PER3-deficient mice. *Am J Physiol - Regul Integr Comp Physiol*. 2011;301(6):R1821-30. doi:10.1152/ajpregu.00260.2011

Hirokawa N. mRNA transport in dendrites: RNA granules, motors, and tracks. *J Neurosci*. 2006;26(27):7139-7142. doi:10.1523/JNEUROSCI.1821-06.2006

Honda T, Fujiyama T, Miyoshi C, et al. A single phosphorylation site of SIK3 regulates daily sleep amounts and sleep need in mice. *Proc Natl Acad Sci U S A*. 2018;115(41):10458-10463. doi:10.1073/pnas.1810823115

Honma A, Revell VL, Gunn PJ, et al. Effect of acute total sleep deprivation on plasma melatonin, cortisol and metabolite rhythms in females. *Eur J Neurosci*. 2020;51(1):366-378. doi:10.1111/ejn.14411

Hor CN, Yeung J, Jan M, et al. Sleep–wake-driven and circadian contributions to daily rhythms in gene expression and chromatin accessibility in the murine cortex. *Proc Natl Acad Sci U S A*. 2019;116(51):25773-25783. doi:10.1073/pnas.1910590116

Hosp F, Mann M. A Primer on Concepts and Applications of Proteomics in Neuroscience. *Neuron*. 2017;96(3):558-571. doi:10.1016/j.neuron.2017.09.025

Huber R, Deboer TOM, Tobler I. Topography of EEG dynamics after sleep deprivation in mice. *J Neurophysiol*. 2000;84(4):1888-1893. doi:10.1152/jn.2000.84.4.1888

Huber R, Deboer T, Tobler I. Effects of sleep deprivation on sleep and sleep EEG in three mouse strains: Empirical data and simulations. *Brain Res*. 2000;857(1-2):8-19. doi:10.1016/S0006-8993(99)02248-9

Ikeda M, Hojo Y, Komatsuzaki Y, et al. Hippocampal spine changes across the sleep-wake cycle: Corticosterone and kinases. *J Endocrinol*. 2015;226(2):M13-M27. doi:10.1530/JOE-15-0078

Jasińska M, Grzegorczyk A, Jasek E, et al. Daily rhythm of synapse turnover in mouse somatosensory cortex. *Acta Neurobiol Exp (Wars)*. 2014;74(1):104-110.

Johnson EM, Kinoshita Y, Weinreb DB, et al. Role of Pur alpha in targeting mRNA to sites of translation in hippocampal neuronal dendrites. *J Neurosci Res*. 2006;83(6):929-943. doi:10.1002/jnr.20806

Jouffe C, Cretenet G, Symul L, et al. The Circadian Clock Coordinates Ribosome Biogenesis. Hardin PE, ed. *PLoS Biol*. 2013;11(1):e1001455. doi:10.1371/journal.pbio.1001455

King DP, Zhao Y, Sangoram AM, et al. Positional cloning of the mouse circadian Clock gene. *Cell*. 1997;89(4):641-653. doi:10.1016/S0092-8674(00)80245-7

Kojima S, Gatfield D, Esau CC, Green CB. MicroRNA-122 modulates the rhythmic expression profile of the circadian deadenylase Nocturnin in mouse liver. *PLoS One*. 2010;5(6). doi:10.1371/journal.pone.0011264

Kondo T, Strayer CA, Kulkarni RD, et al. Circadian rhythms in prokaryotes: Luciferase as a reporter of circadian gene expression in cyanobacteria. *Proc Natl Acad Sci U S A*. 1993;90(12):5672-5676. doi:10.1073/pnas.90.12.5672

Konopka RJ, Benzer S. Clock mutants of Drosophila melanogaster. *Proc Natl Acad Sci U S A*. 1971;68(9):2112-2116. doi:10.1073/pnas.68.9.2112

Kornmann B, Schaad O, Bujard H, Takahashi JS, Schibler U. System-Driven and Oscillator-Dependent Circadian Transcription in Mice with a Conditionally Active Liver Clock. O'Rahilly S, ed. *PLoS Biol*. 2007;5(2):e34. doi:10.1371/journal.pbio.0050034

Kosik KS. Life at Low Copy Number: How Dendrites Manage with So Few mRNAs. *Neuron*. 2016;92(6):1168-1180. doi:10.1016/j.neuron.2016.11.002

Laposky A, Easton A, Dugovic C, Walisser J, Bradfield C, Turek F. Deletion of the Mammalian Circadian Clock Gene BMAL1/Mop3 Alters Baseline Sleep Architecture and the Response to Sleep Deprivation. *Sleep*. 2005;28(4):395-410. doi:10.1093/sleep/28.4.395

Li JZ, Bunney BG, Meng F, et al. Circadian patterns of gene expression in the human brain and disruption in major depressive disorder. *Proc Natl Acad Sci U S A*. 2013;110(24):9950-9955. doi:10.1073/pnas.1305814110

Liu AC, Welsh DK, Ko CH, et al. Intercellular Coupling Confers Robustness against Mutations in the SCN Circadian Clock Network. *Cell*. 2007;129(3):605-616. doi:10.1016/j.cell.2007.02.047

Maier B, Wendt S, Vanselow JT, et al. A large-scale functional RNAi screen reveals a role for CK2 in the mammalian circadian clock. *Genes Dev*. 2009;23(6):708-718. doi:10.1101/gad.512209

Marchand V, Gaspar I, Ephrussi A. An Intracellular Transmission Control Protocol: Assembly and transport of ribonucleoprotein complexes. *Curr Opin Cell Biol*. 2012;24(2):202-210. doi:10.1016/j.ceb.2011.12.014

Maret S, Dorsaz S, Gurcel L, et al. Homer1a is a core brain molecular correlate of sleep loss. *Proc Natl Acad Sci U S A*. 2007;104(50):20090-20095. doi:10.1073/pnas.0710131104

Martin KC, Ephrussi A. mRNA Localization: Gene Expression in the Spatial Dimension. *Cell*. 2009;136(4):719-730. doi:10.1016/j.cell.2009.01.044

Mauvoisin D, Wang J, Jouffe C, et al. Circadian clock-dependent and -independent rhythmic proteomes implement distinct diurnal functions in mouse liver. *Proc Natl Acad Sci U S A*. 2014;111(1):167-172. doi:10.1073/pnas.1314066111

Milev NB, Reddy AB. Circadian redox oscillations and metabolism. *Trends Endocrinol Metab*. 2015;26(8):430-437. doi:10.1016/j.tem.2015.05.012

Miller S, Yasuda M, Coats JK, Jones Y, Martone ME, Mayford M. Disruption of dendritic translation of CaMKIIα impairs stabilization of synaptic plasticity and memory consolidation. *Neuron*. 2002;36(3):507-519. doi:10.1016/S0896-6273(02)00978-9

Milos P, Morse D, Hastings JW. Circadian control over synthesis of many Gonyaulax proteins is at a translational level. *Naturwissenschaften*. 1990;77(2):87-89. doi:10.1007/BF01131782

Mrosovsky N. Phase response curves for social entrainment. *J Comp Physiol A*. 1988;162(1):35-46. doi:10.1007/BF01342701

Mure LS, Le HD, Benegiamo G, et al. Diurnal transcriptome atlas of a primate across major neural and peripheral tissues. *Science (80- )*. 2018;359(6381). doi:10.1126/science.aao0318

Myung J, Schmal C, Hong S, et al. The choroid plexus is an important circadian clock component. *Nat Commun*. 2018;9(1). doi:10.1038/s41467-018-03507-2

Nagoshi E, Saini C, Bauer C, Laroche T, Naef F, Schibler U. Circadian gene expression in individual fibroblasts: Cell-autonomous and self-sustained oscillators pass time to daughter cells. *Cell*. 2004;119(5):693-705. doi:10.1016/j.cell.2004.11.015

Nakatsuka H, Natsume K. Circadian rhythm modulates long-term potentiation induced at CA1 in rat hippocampal slices. *Neurosci Res*. 2014;80(1):1-9. doi:10.1016/j.neures.2013.12.007

Noya SB, Colameo D, Brüning F, et al. The forebrain synaptic transcriptome is organized by clocks but its proteome is driven by sleep. *Science (80- )*. 2019;366(6462). doi:10.1126/science.aav2642

O-Neill JS, Reddy AB. Circadian clocks in human red blood cells. *Nature*. 2011;469(7331):498-504. doi:10.1038/nature09702

Palacios IM, Johnston D St. Getting the Message Across: The Intracellular Localization of mRNAs in Higher Eukaryotes. *Annu Rev Cell Dev Biol*. 2001;17(1):569-614. doi:10.1146/annurev.cellbio.17.1.569

Panda S, Antoch MP, Miller BH, et al. Coordinated transcription of key pathways in the mouse by the circadian clock. *Cell*. 2002;109(3):307-320. doi:10.1016/S0092-8674(02)00722-5

Patke A, Young MW, Axelrod S. Molecular mechanisms and physiological importance of circadian rhythms. *Nat Rev Mol Cell Biol*. 2020;21(2):67-84. doi:10.1038/s41580-019-0179-2

Preitner N, Damiola F, Luis-Lopez-Molina, et al. The orphan nuclear receptor REV-ERBα controls circadian transcription within the positive limb of the mammalian

circadian oscillator. *Cell*. 2002;110(2):251-260. doi:10.1016/S0092-8674(02)00825-5

Raab-Graham KF, Haddick PCG, Jan YN, Jan LY. Activity- and mTOR-dependent suppression of Kv1.1 channel mRNA translation in dendrites. *Science (80- )*. 2006;314(5796):144-148. doi:10.1126/science.1131693

Reddy AB, Karp NA, Maywood ES, et al. Circadian Orchestration of the Hepatic Proteome. *Curr Biol*. 2006;16(11):1107-1115. doi:10.1016/j.cub.2006.04.026

Reppert SM, Weaver DR. Coordination of circadian timing in mammals. *Nature*. 2002;418(6901):935-941. doi:10.1038/nature00965

Rhizobium GE. Complete Genome Sequence of the Sesbania Symbiont and Rice. *Nucleic Acids Res*. 2013;1(1256879):13-14. doi:10.1093/nar

Rishal I, Kam N, Perry RBT, et al. A Motor-Driven Mechanism for Cell-Length Sensing. *Cell Rep*. 2012;1(6):608-616. doi:10.1016/j.celrep.2012.05.013

Robles MS, Cox J, Mann M. In-Vivo Quantitative Proteomics Reveals a Key Contribution of Post-Transcriptional Mechanisms to the Circadian Regulation of Liver Metabolism. *PLoS Genet*. 2014;10(1). doi:10.1371/journal.pgen.1004047

Robles MS, Humphrey SJ, Mann M. Phosphorylation Is a Central Mechanism for Circadian Control of Metabolism and Physiology. *Cell Metab*. 2017;25(1):118-127. doi:10.1016/j.cmet.2016.10.004

Rossi MJ, Pekkurnaz G. Powerhouse of the mind: mitochondrial plasticity at the synapse. *Curr Opin Neurobiol*. 2019;57:149-155. doi:10.1016/j.conb.2019.02.001

Rutila JE, Suri V, Le M, So W V, Rosbash M, Hall JC. CYCLE is a second bHLH-PAS clock protein essential for circadian rhythmicity and transcription of Drosophila period and timeless. *Cell*. 1998;93(5):805-814. doi:10.1016/s0092-8674(00)81441-5

Sato TK, Panda S, Miraglia LJ, et al. A functional genomics strategy reveals rora as a component of the mammalian circadian clock. *Neuron*. 2004;43(4):527-537. doi:10.1016/j.neuron.2004.07.018

Schieweck R, Ang F yee, Fritzsche R, Kiebler MA. Isolation and characterization of endogenous RNPs from Brain tissues. In: *Methods in Molecular Biology*. Vol 1649. Humana Press Inc.; 2018:419-426. doi:10.1007/978-1-4939-7213-5_28

Schmidt C, Collette F, Cajochen C, Peigneux P. A time to think: Circadian rhythms in human cognition. *Cogn Neuropsychol*. 2007;24(7):755-789. doi:10.1080/02643290701754158

Sehgal A, Price JL, Man B, Young MW. Loss of circadian behavioral rhythms and per RNA oscillations in the Drosophila mutant timeless. *Science (80- )*. 1994;263(5153):1603-1606. doi:10.1126/science.8128246

Sharangdhar T, Sugimoto Y, Heraud-Farlow J, et al. A retained intron in the 3'-UTR of Calm3 mRNA mediates its Staufen2- and activity-dependent localization to neuronal dendrites. *EMBO Rep*. 2017;18(10):1762-1774. doi:10.15252/embr.201744334

Shiromani PJ, Xu M, Winston EM, Shiromani SN, Gerashchenko D, Weaver DR. Sleep rhythmicity and homeostasis in mice with targeted disruption of mPeriod genes. *Am J Physiol - Regul Integr Comp Physiol*. 2004;287(1 56-1):R47-57. doi:10.1152/ajpregu.00138.2004

Snider KH, Sullivan KA, Obrietan K. Circadian Regulation of Hippocampal-Dependent Memory: Circuits, Synapses, and Molecular Mechanisms. 2018. doi:10.1155/2018/7292540

Steward O, Levy WB. Preferential localization of polyribosomes under the base of dendritic spines in granule cells of the dentate gyrus. *J Neurosci*. 1982;2(3):284-291. doi:10.1523/jneurosci.02-03-00284.1982

Susaki EA, Ukai H, Ueda HR. Next-generation mammalian genetics toward organism-level systems biology. *npj Syst Biol Appl*. 2017;3(1):1-11. doi:10.1038/s41540-017-0015-2

Tao CL, Liu YT, Sun R, et al. Differentiation and characterization of excitatory and inhibitory synapses by cryo-electron tomography and correlative microscopy. *J Neurosci*. 2018;38(6):1493-1510. doi:10.1523/JNEUROSCI.1548-17.2017

Tei H, Okamura H, Shigeyoshi Y, et al. Circadian oscillation of a mammalian homologue of the Drosophila period gene. *Nature*. 1997;389(6650):512-516. doi:10.1038/39086

Tobler I, Borbély AA, Groos G. The effect of sleep deprivation on sleep in rats with suprachiasmatic lesions. *Neurosci Lett*. 1983;42(1):49-54. doi:10.1016/0304-3940(83)90420-2

Tolino M, Köhrmann M, Kiebler MA. RNA-binding proteins involved in RNA localization and their implications in neuronal diseases. *Eur J Neurosci*. 2012;35(12):1818-1836. doi:10.1111/j.1460-9568.2012.08160.x

Tomita J, Nakajima M, Kondo T, Iwasaki H. No transcription-translation feedback in circadian rhythm of KaiC phosphorylation. *Science (80- )*. 2005;307(5707):251-254. doi:10.1126/science.1102540

Tononi G, Cirelli C. Sleep and the Price of Plasticity: From Synaptic and Cellular Homeostasis to Memory Consolidation and Integration. *Neuron*. 2014;81(1):12-34. doi:10.1016/j.neuron.2013.12.025

Tononi G, Cirelli C. Sleep and synaptic homeostasis: A hypothesis. *Brain Res Bull*. 2003;62(2):143-150. doi:10.1016/j.brainresbull.2003.09.004

Tononi G, Cirelli C. Modulation of brain gene expression during sleep and wakefulness: A review of recent findings. *Neuropsychopharmacology*. 2001;25(5):S28-S35. doi:10.1016/S0893-133X(01)00322-0

Ueda HR, Chen W, Adachi A, et al. A transcription factor response element for gene expression during circadian night. *Nature*. 2002;418(6897):534-539. doi:10.1038/nature00906

Ueda HR, Hayashi S, Chen W, et al. System-level identification of transcriptional circuits underlying mammalian circadian clocks. *Nat Genet*. 2005;37(2):187-192. doi:10.1038/ng1504

Van Der Horst GTJ, Muijtjens M, Kobayashi K, et al. Mammalian Cry1 and Cry2 are essential for maintenance of circadian rhythms. *Nature*. 1999;398(6728):627-630. doi:10.1038/19323

Vessey JP, Macchi P, Stein JM, et al. A loss of function allele for murine Staufen1 leads to impairment of dendritic Staufen1-RNP delivery and dendritic spine morphogenesis. *Proc Natl Acad Sci U S A*. 2008;105(42):16374-16379. doi:10.1073/pnas.0804583105

Vollmers C, Schmitz RJ, Nathanson J, Yeo G, Ecker JR, Panda S. Circadian oscillations of protein-coding and regulatory RNAs in a highly dynamic mammalian liver epigenome. *Cell Metab*. 2012;16(6):833-845. doi:10.1016/j.cmet.2012.11.004

Wang Z, Ma J, Miyoshi C, et al. Quantitative phosphoproteomic analysis of the molecular substrates of sleep need. *Nature*. 2018;558(7710):435-439. doi:10.1038/s41586-018-0218-8

Warner JR. The economics of ribosome biosynthesis in yeast. *Trends Biochem Sci*. 1999;24(11):437-440. doi:10.1016/S0968-0004(99)01460-7

Welsh DK, Logothetis DE, Meister M, Reppert SM. Individual neurons dissociated from rat suprachiasmatic nucleus express independently phased circadian firing rhythms. *Neuron*. 1995;14(4):697-706. doi:10.1016/0896-6273(95)90214-7

Welsh DK, Yoo SH, Liu AC, Takahashi JS, Kay SA. Bioluminescence imaging of individual fibroblasts reveals persistent, independently phased circadian rhythms of clock gene expression. *Curr Biol*. 2004;14(24):2289-2295. doi:10.1016/j.cub.2004.11.057

Welz PS, Zinna VM, Symeonidi A, et al. BMAL1-Driven Tissue Clocks Respond Independently to Light to Maintain Homeostasis. *Cell*. 2019;177(6):1436-1447.e12. doi:10.1016/j.cell.2019.05.009

Williams SB, Vakonakis I, Golden SS, LiWang AC. Structure and function from the circadian clock protein KaiA of Synechococcus elongatus: A potential clock input mechanism. *Proc Natl Acad Sci U S A*. 2002;99(24):15357-15362. doi:10.1073/pnas.232517099

Wilsbacher LD, Takahashi JS. Circadian rhythms: Molecular basis of the clock. *Curr Opin Genet Dev*. 1998;8(5):595-602. doi:10.1016/S0959-437X(98)80017-8

Wisor JP, O'Hara BF, Terao A, et al. A role of cryptochromes in sleep regulation. *BMC Neurosci*. 2002;3. doi:10.1186/1471-2202-3-20

Wyatt JK, Ritz-De Cecco A, Czeisler CA, Dijk DJ. Circadian temperature and melatonin rhythms, sleep, and neurobehavioral function in humans living on a 20-h day. *Am J Physiol - Regul Integr Comp Physiol*. 1999;277(4 46-4). doi:10.1152/ajpregu.1999.277.4.r1152

Xie L, Kang H, Xu Q, et al. Sleep drives metabolite clearance from the adult brain. *Science (80- )*. 2013;342(6156):373-377. doi:10.1126/science.1241224

Yamanaka Y, Honma S, Honma K. Daily exposure to a running wheel entrains circadian rhythms in mice in parallel with development of an increase in spontaneous movement prior to running-wheel access. *Am J Physiol Regul Integr Comp Physiol*. 2013;305(11):R1367-75. doi:10.1152/ajpregu.00389.2013

Yang G, Gan W-B. Sleep contributes to dendritic spine formation and elimination in the developing mouse somatosensory cortex. *Dev Neurobiol*. 2012;72(11):1391-1398. doi:10.1002/dneu.20996

Zhang R, Lahens NF, Ballance HI, Hughes ME, Hogenesch JB. A circadian gene expression atlas in mammals: Implications for biology and medicine. *Proc Natl Acad Sci U S A*. 2014;111(45):16219-16224. doi:10.1073/pnas.1408886111

# 7. Curriculum Vitae

Sara Bernardez Noya

PhD Student

University of Zürich Faculty of Science

Professional +41 44 635 59 63 Private +34 618 43 09 12

sara.bernardez@pharma.uzh.ch sarabnoya@gmail.com

EDUCATION

OCT 2015 - PRESENT **PHD IN NEUROSCIENCE** UNIVERSITY OF ZÜRICH

Supervised by Prof. Steven A. Brown and Shiva K. Tyagarajan. Thesis Title: Circadian Rhythms at the Synapse. Keywords: Circadian Rhythms – Sleep – Neuroscience.

2013 – 2014 **MASTER IN MOLECULAR BIOMEDICINE** UNIVERSIDAD AUTONOMA DE MADRID (UAM). Thesis Title: p38δ: a starting point to understand diet-induced phenotypes through Akt and Fgf21. Keywords: Metabolism – MAPK kinases.

2008 – 2013 **DEGREE IN BIOLOGY** UNIVERSIDAD DE SANTIAGO DE COMPOSTELA (USC). Grade: 9,4123 (over 10. Protocol SUG according RD 1125/2003). 3rd of 141 students.

2006 - 2008 **INTERNATIONAL BACCALOUREATE® DIPLOMA PROGRAMME** IES ROSALIA DE CASTRO.

RESEARCH EXPERIENCE

2015-PRESENT **INSTITUTE OF PHARMACOLOGY AND TOXICOLOGY, UNIVERSITY OF ZÜRICH**. PhD Candidate. Laboratory: Chronobiology and sleep research, Supervisor: Steven A. Brown.

2013 **CENTRO NACIONAL DE INVESTIAGACIONES CARDIOVASCULARES (CNIC),** MADRID. CICERONE Program. Laboratory: Stress kinases in Diabetes, Cancer and Cardiovascular Disease, Supervisor: Antonia Tomas Loba.

2012 **NSTITUTO DE INVESTIGACION SANITARIA DE SANTIAGO (IDIS).** Internship. Laboratory: Grupo de Obesidomica ("Obesidomics Group"). Supervisor: Maria Pardo.

2012 **CENTER FOR RESEARCH IN MOLECULAR MEDICINE AND CHRONOC DISEASES (CiMUS),** SANTIAGO DE COMPOSTELA. Internship. Laboratory: Cellular Signalling and Stress. Supervisor: Celia Maria Pombo Ramos.

## HONORS AND RECOGNITIONS

2008 **Mention of 1st Price XXI Certamen de jóvenes investigadores, Instituto de Juventud INJUVE (Joung Reserchers Contest, Ministery of Health, Social Services and Equeality)** with the work "Wine… long life elixir? Quantitation of polyphenol content in wines from different Galician regionswith high longevity rates

## PUBLICATIONS

S. B. Noya et al., The forebrain synaptic transcriptome is organized by clocks but its proteome is driven by sleep. Science 366, Issue 6462, DOI: 10.1126/science.aav2642.

F. Brüning et al., Sleep-wake cycles drive daily dynamics of synaptic phosphorylation. Science 366, Issue 6462, DOI: 10.1126/science.aav3617.

## ATTENDANCE AT CONFERENCES AND SEMINARS

**GRC Chronobiology Conference.** 2019. Short Talk.

**ESRS Conference** 2018. Short Talk.

**SRBR Conference** 2018. Poster.

**EBRS Conference** 2017. Short Talk; 2019. 2019. Prize to the best poster.

**CRPP** 2017. Short Talk.

**ZNZ Symposium** 2016 Poster. 2017 Poster.

**Swiss RNA Workshop**. 2016 Poster-2017 Short Talk-2018. Poster.

**Swiss Chronobiology Meeting**. 2016 Poster- 2017 Poster – 2018 Poster.

**GABA Meeting** 2018 (emerging mechanisms for inhibitory synapse plasticity). Poster.

## EXTRACURRICULAR ACTIVITIES

ArtLab. Project Leader. 2017 and 2019. https://www.sciencexploresuisse.org/

EBRS Trainee Day 2017 and 2019. Committee member.

EBRS Career Mentorship Program. Founder.

## REFERENCES

Steven Brown steven.brown@pharma.uzh.ch

Shiva Tyagarajan tyagarajan@pharma.uzh.ch

Maria Robles charo.robles@med.uni-muenchen.de

Antonia Tomas Loba atomas200@hotmail.com

Maria Pardo maruxapardo@hotmail.com

# 8. Appendix

## 1.10. Additional material from manuscript 1

**This section includes:**
Materials. And Methods

Fig. S1-S12.

**Other Supplementary Materials** for this manuscript that can be accessed in the link below include the following:

Tables S1-S9.

Databases 1-3.

Script for FISH image analysis.

https://science.sciencemag.org/content/suppl/2019/10/09/366.6462.eaav2642.DC1

**Materials and Methods**

**Animals and Tissue Collection**

All experiments were performed in accordance with institutional guidance of the University of Zürich and veterinary authorities of the Canton of Zürich. Ten-week-old male C57BL/6 mice were housed with free access to food and water and entrained to a 12 h/12 h light-dark schedule (LD) for 14 days. Mice were sacrificed at 4 h intervals over 1 day (ZT0, ZT4, ZT8, ZT12, ZT16 and ZT20; n=3 for transcriptome and n=4 for proteome). At the time points overlapping with light transitions (ZT0 and ZT12), euthanasia was performed right before the light change. For the around-the-clock sleep deprivation, mice were allowed to acclimatize to a 12-h light/12-h dark cycle for 14 days. Six groups of mice were sleep deprived for 4 hours by gentle handling (cage exchange and introduction of novel objects as described previously(*66*)) at different times of day (SD4 [sleep deprivation from ZT0 to ZT4], SD8, SD12, SD16, SD20 and SD0; n=3 for transcriptome and n=4 for proteome). To collect synaptoneurosomes from mice kept in constant darkness, and from *Bmal1*-/-

mice, animals were kept in LD for 2 weeks and then transferred to constant darkness (DD) 48 hours before euthanasia at circadian times (CT) CT0 and CT12 respectively (n=3).

**EEG recording and Sleep data analysis**

Adult C57BL/6 mice were used for surgery (8-10 weeks old at surgery). Mice were implanted epidurally under isoflurane anesthesia for EEG recording. Right before and 24h after surgery mice were treated with an analgesic (Temgesic, 0.1 mg/kg, intraperitoneal). Gold-plated miniature screws (0.9 mm diameter) were used as EEG electrodes and positioned on the left hemisphere above the frontal cortex (1.5 mm anterior to bregma, 1.5 mm lateral to the midline) and the parietal cortex (2 mm posterior to bregma and 2 mm lateral to the midline). The reference electrode was placed above the cerebellum (2 mm posterior to lambda, 0 mm lateral to the midline). Screws were connected to copper wires and fixed to the skull with dental cement (Paladur 2-component system). Electromyography (EMG) was recorded using two gold wires (0.2 mm diameter) inserted bilaterally in the neck muscle. After 1 week of recovery EEG-EMG was recorded continuously for 7 days. 2 cohorts of 6 and 8 mice, respectively, underwent a BL days recording and 3 SD days with 48h of recovery in between. Cohort 1 underwent SD at ZT4-8, ZT12-16 and ZT 16-20. Cohort 2 underwent SD at ZT0-4, ZT8-12 and ZT20-24. SD was performed by gentle handling as described previously (*66*). Both EEG and EMG signals were amplified (factor 2000), analogue filtered (high-pass filter: -3 dB at 0.016 Hz; low-pass filter: -3 dB at 40 Hz, less than -35 dB at 128 Hz), sampled with 512 Hz, digitally filtered (EEG: low-pass FIR filter 25 Hz; EMG: band-pass FIR 20-50 Hz) and stored with a 128 Hz resolution. EEG power spectra were computed for 4-s epochs by a Fast Fourier Transform routine within the frequency range of 0.5 –

25 Hz. Between 0.5 Hz and 5 Hz, 0.5 Hz bins were used, and between 5 and 25 Hz 1 Hz bins were used. The corresponding slow-wave-activity (SWA) was calculated using the raw parietal and frontal EEG, as well as the raw and integrated EMG to visually score three vigilance states (NREM sleep, rapid eye-movement sleep (REM) and wake) for 4-s epochs. Epochs containing artifacts were identified and excluded from the spectral analysis. Data analysis was carried out using MATLAB version R2015a (The Math Works, Inc., Natick, MA, USA). Relative frontal SWA was calculated relative to the mean SWA at ZT8-12 during the BL day. Sleep loss was calculated by comparing NREM sleep amount in each 4h SD slot to the sleep amount in the same time of day of the corresponding BL day. 1-way ANOVA, $p<0.05$. Sleep latency was analyzed by measuring the time each mouse stayed awake after the end of each 4h SD until it slept for more than 1 min. 1-way ANOVA, $p<0.05$.

**Purification of Synaptoneurosomes**

Synaptoneurosomes from mouse forebrain were prepared as described previously (22). In brief, brain was isolated and rapidly cooled to 4°C, washed in ice-cooled sucrose buffer (320 mM Sucrose, 5 mM HEPES, pH 7.4) followed by homogenization with a Teflon-glass tissue grinder using a motor-driven pestle keeping samples cooled. Homogenate was centrifuged at 1000 g for 10 min. 2 ml of the supernatant were loaded over discontinuous Percoll gradients (3%, 10% and 23% Percoll in sucrose buffer) and centrifuged at 31000 g for 5 minutes. The fraction at the interfaces between 3-10% and 10-23% were collected and further centrifuged at 20000 g to pellet synaptoneurosomes. All centrifugation steps were performed at 4°C. All solutions were supplemented with complete protease inhibitor cocktail (Roche®), 0.05mM DTT, 0.1mM PMSF and RNaseOUT 20 U/10 µl (Invitrogen®).

**RNA Sample Preparation**

200 µl of homogenate were used for total RNA extraction. Briefly, tissue lysate in QIAzol Lysis Reagent (Quiagen ®) was vortexed for few seconds. 0.2 ml of chloroform was added to lysate and mixed by vigorous shaking for 15 sec. The mixture was incubated at room temperature for 10 min and centrifuged at 18,000 g for 20 min at 4°C to separate phases. The upper aqueous phase containing RNA was carefully aspirated to a fresh, nuclease-free tube. The RNA was then precipitated by adding one volume of isopropanol and centrifuged at 18,000 g for 20 min at 4°C. The RNA pellet was washed with 70% ethanol, air-dried and dissolved in nuclease-free water.

Frozen synaptoneurosome pellets (approximately 500 µl) were processed with High Pure RNA Isolation Kit Roche®. Samples were mixed with 600 µl of Lysis Binding buffer and further steps were carried out according to the manufacturer's instructions. The dissolved total RNA was quantified by NanoDrop (NanoDrop Technologies) and Qubit® (1.0) Fluorometer (Life Technonologies, California, USA). The quality was assessed with Agilent 2100 Bioanalyzer (Agilent Technologies, Waldbronn, Germany).

**Library Preparation, Sequencing and Data Processing**

PolyA RNA sequencing was performed using 500 µg total RNA. Strand-specific cDNA libraries were prepared using Illumina's TruSeq stranded Sample Prep Kit (125 bp single-read mode) following the manufacturer's directions, then sequenced on an Illumina HiSeq 4000 (Illumina Inc., California, USA). The raw reads were first cleaned by removing adapter sequences, trimming low quality ends, and filtering reads with low quality (phred quality <20) using Trimmomatic (Versions 0.33 & 0.36) (*67*). Specific quality control measures were evaluated and we excluded the following samples: replicates number 3 in ZT16

BL due to degradation during the library preparation, 1 from ZT8 BL due to reduced read counts (less than 10 million), 2 from ZT4 SD, 3 ZT16 SD and 3 from ZT20 SD, due to signs of contamination with external material. Sequence alignment of the resulting high-quality reads to the Mouse reference genome (build GRCm38) and quantification of gene level expression was carried out using RSEM (Versions 1.2.22 & 1.3.0) (*68*). For downstream analysis, the mRNA features were filtered according to normalized (logMean) featureCounts , which represents aggregated raw counts of mapped reads at the gene level (RSEM). We determined a threshold for minimum gene expression based on the assumption that a transcript with more than 10 counts in 2 out of 3 replicates is expressed (linear signal threshold of 10).

**Bioinformatic and Statistical Analyses of Transcriptomics Data**

To search for transcripts that are enriched in neuronal synapses, we did a differential gene expression analysis using a pairwise comparison between synaptoneurosomes and whole brain at two time points (ZT0 and ZT12). The threshold to consider a gene Enriched in the synapse was a fold change (of the synaptic samples versus the whole forebrain samples) larger than 1.5 in one of the two time points.

Cycling analysis was performed using the computational platform Perseus (*25*). We fit the normalized mRNA counts to a cosine with a fixed period of 24 h and with amplitude and phase as free parameters (*9*). Profiles were ranked by their variance ratio. This was the part of the variance explained by the fit divided by the contribution to the variance that was not accounted for by the fit. Based on this ranking, we determined a permutation-based FDR by repeating the same procedure 1,000 times on the same profiles but with randomized time labels. We used a statistical cut-off of $q < 0.05$ to define the cycling transcriptome.

Hierarchical clustering was performed in a phase-preserving manner, by restricting the order of elements to that determined by the output of the cosine model-based fitting. Amplitudes were calculated as the log2 of the fold change of counts. To evaluate the effect of constant darkness and the lack of a functional clock on the generation of the peaks of synaptic transcript accumulation, we compared the following conditions ZT0 vs. CT0; ZT0 vs. CT0 *Bmal*$^{+/+}$; ZT12 vs. CT12; and ZT12 vs. CT12 *Bmal1*-/- by applying a count based negative binomial model implemented in the software package EdgeR (R version: 3.4.2, EdgeR version: 3.20.1) (*69*). The differential expression was assessed using an exact test adapted for over-dispersed data. Genes showing altered expression with adjusted (Benjamin and Hochberg method) p-value < 0.05 were considered differentially expressed.

**Protein Sample Preparation**

For protein extraction, 4% SDS was added to each synaptoneurosomal sample or to the homogenate followed by 5 min incubation at 95°C. Samples were flash frozen and stored at -80°C until used. Samples were lysed (0.1 mM Tris-HCl [pH 7.6], and 4 % SDS), sonicated in a bioruptor (4 °C for 15 min or until homogenous suspension was formed) and boiled at 95 °C for 5 min. Protein lysates were treated first with 1 µl DTT (1 M) followed by 10 µl 2-Chloroacetamide (0.5 M). Each treatment was performed at room temperature (RT, 22 °C) for 20 min. The lysates were precipitated with acetone as described (*9*). In detail, pellets were resuspended in 500 µl TFE digestion buffer. For protein digestion 1:100 (protein:enzyme) trypsin as well as LysC were added and samples incubated overnight at 37 °C with rapid agitation (1,500 rpm). Digested peptides were concentrated in a SpeedVac for 15 min at 45 °C followed by acidification using 10 µl of 10% Trifluoroacetic acid (TFA). Peptides were then desalted using stageTips with two layers of styrenedivinylbenzene–

reversed phase sulfonated (SDB-RPS; 3M Empore), washed twice with wash buffer (0.2% TFA) and one with isopropanol containing 1 % TFA. Peptides were eluted by adding 60 µl SDB-RPS elution buffer (80 % ACN, 1.25 % $NH_4OH$ (25 % HPLC grade)) and immediately concentrated in a SpeedVac for 30 min at 45 °C. Concentrated peptides were then resuspended in a buffer containing 2 % ACN and 0.1 % TFA prior to chromatography-tandem mass spectrometry (LC-MS/MS) analysis.

**LC-MS/MS Analysis and Data Processing**

Samples were measured in a single-shot (*70*), loading approximately 2µg of peptide mixture onto a 50 cm reversed-phase column (diameter 75 µM; packed in-house with 1.9 µM C18 ReproSil particles [Dr. Maisch GmbH]). The temperature of the homemade column oven was maintained at 60 °C. The column was mounted to the EASY-nLC 1200 system (Thermo Fisher Scientific). The peptides were eluted with a binary buffer system consisting out of buffer A (0.1 % formic acid) and buffer B (80 % ACN and 0.1 % formic acid). A gradient length of 140 min was chosen (5 %-65 % buffer B for 130 min followed by 10 min 80 % buffer B) with a flow rate of 300 nl/min. Peptides were then electrosprayed into a Q Exactive HF mass spectrometer (MS) (Thermo Fisher Scientific) obtaining full scans (300-1,650 m/z, R = 60,000 at 200 m/z) at a target of 3e6 ions. The 15 most abundant ions were selected and fragmented with higher-energy collisional dissociation (HCD) (target 1e5 ions, maximum injection time 60 ms, isolation window 1.4 m/z, underfill ratio 1 %) followed by the detection in the Orbitrap (R = 15,000 at 200 m/z). Raw MS data files were processed using MaxQuant (version 1.5.5.6, (24)) to calculate label free intensities with the Andromeda search engine with FDR < 0.01 at protein and peptide level. The default settings were used with the following modifications: (1) the variable modification methionine (M), acetylation (protein N-term) and

the fixed modification carbamidomethyl (C) were selected, (2) only peptides with a minimal length of seven amino acids were considered, and (3) the "match between run" option was enabled with a matching time window of 0.7 min. For protein and peptide identification the UniProt database from mouse (September 2014) including 51,210 entries was used. Each raw file and replicate was treated as one independent experiment.

**Bioinformatic and Statistical Analyses of Proteomics Data**

Processed data was uploaded in the Perseus software (*25*). First, reverse sequences and potential contaminants were removed. Then the total data set was log2 transformed and label free intensities were normalized in each sample by substracting the media of all intensities in the same sample. Proteins without label free intensities in <10 samples were removed in each data set synaptoneurosomes (SD/BL) and total forebrain. Replicates 1 and 4 of ZT4, 4 of ZT8 and 1 of ZT12 of the total brain homogenate were not considered since the protein quantification in theses samples was limited.

Cycling analysis was done as for the transcriptomic data in this case using protein intensity values. Amplitudes were as well calculated as the log2 fold change. For comparison of transcriptome and the proteome data we matched datasets by Gene name or Uniprot ID.

**Gene Ontology Analysis**

All Ontological Analyses were done with the Enrichment Analysis Tool FunRich using the Hgcn gene symbols. For analysis of synaptic enriched mRNAs (3104 of which 2954 were available in database) Gene ontology options GOTERM Cellular Component was selected. A maximum p-value of 0.001 was chosen to select only significant categories. For the evaluation of synaptic enrichment, we filtered for annotations containing the following terms; synap*, project*, dendr*, axon or spine. The percentage of genes for each annotation and

the fold enrichment in the three categories (Identified, expressed and enriched features) were used to validate the enrichment strategy. Only the top ten annotations according to p-value were included in the graphical representation; all returned annotations are visible in supplementary tables. Enriched Biological Processes of the cycling transcriptome were identified separately for light (752 of which 725 were available in Biological process database features found in database) or dark phases (1263 of which 1217 were available in Biological process database found in database). Features were ascribed to each group using hierarchical clustering according to the temporal expression profile. Annotation with BH corrected p-value<0.001 were included. Enrichment for Biological Processes in the synaptic enriched dataset was also performed for comparison of the common annotations. To compare the annotation enrichment between the light and dark clusters we performed a Fold enrichment analysis between both datasets and obtained a Fold value (included in Table S4). To analyze the gene datasets obtained after the SD experiment we followed similar steps. 4 groups of features were independently analyzed according to phase or cycling behavior in SD (Light and q<0.05, 149 features; light and q>0.05, 603 features; dark and q<0.05, 393 features; dark and q>0.05, 863 features). For representation, the top ten enriched annotations (ranked by Fold value between phases for cycling or not in SD and vice versa and with BH corrected p-value<0.1) were considered. For the common cycling features at the mRNA and transcript levels, the phase of protein was used to classify each into the light cluster (29 features) or dark cluster (27 features). For representation we selected the top 5 enriched annotations (BH corrected p-value<0.01)

**Single molecule RNA in situ hybridization**

RNAscope hybridization was performed with the RNAscope® Multiplex Fluorescent v2-kit (Advanced Cell Diagnostics, Inc.) according to manufacturer's instructions with the following modifications. Mice were perfused intracardially with artificial cerebral spinal fluid , the dissected brains post-fixed with 4% PFA for 2 h at 4°C and subsequently cryoprotected in 30% sucrose in PBS for 24 h at 4°C and frozen at -80°C for up to three months. The brains were cut coronally at 14 μm with a cryotome, mounted on a SuperFrost glass-slide (ThermoFischer) and stored at -80°C until use. Tissue sections were then dried in the ACD hybridizer at 37°C for at least 1 h, treated with hydrogen peroxide for 10 min and dried before protease-treatment at 60°C for 30 min. The boiling step in the antigen-retrieval procedure has been omitted and the sections were digested in Protease Plus (Advanced Cell Diagnostics, Inc) solution for 15 min at 40°C. Each RNA signal has been developed sequentially by specifically targeting each probe with a horseradish peroxidase (HRP), which converted fluorescently labeled tyramide (TSA Plus fluorescein, Cy3 or Cy5 kit, Perkin Elmer) into an insoluble stain around the RNA of interest. Final concentration of tyramide in TSA-buffer solution was 1:1500. Custom RNAscope target probes (all targeting mouse transcripts) were purchased from Advanced Cell Diagnostics: *Slc17a7*, *Lingo1*, *Cry1* as well as standard RNAscope positive (housekeeping genes: *PolR2a*, *PPIB* and *Ubc*) and negative (bacterial housekeeping gene: *DapB*) control probes.

For imaging we used a confocal laser-scanning microscope (LSM 710, Carl Zeiss, ZEN imaging software). The images were acquired using a 40x (NA=1.4) objective and a pinhole set at 1 airy unit, pixel dwell time 3.15 μs and laser power 1.2-2%. The images spanned the whole thickness of the brain slices (10 - 12 microns) in 1$\mu$m steps and analyzed as a maximum intensity projection across Z-stacks.

In order to reliably quantify mRNA dots in different brain regions, a custom Python-script was written using the ImageJ image-processing framework. The script can be used as a plugin and is openly available on a github repository (https://github.com/dcolam/Cluster-Analysis-Plugin). Images were binarized, segmented to separate nuclei rich region (pyramidal cell layer of the hippocampus and cell nuclei in cortex) and particle analysis was done using ImageJ. For representation purposes, mRNA dots were enlarged to improve visualization.

**Supplementary Figures**

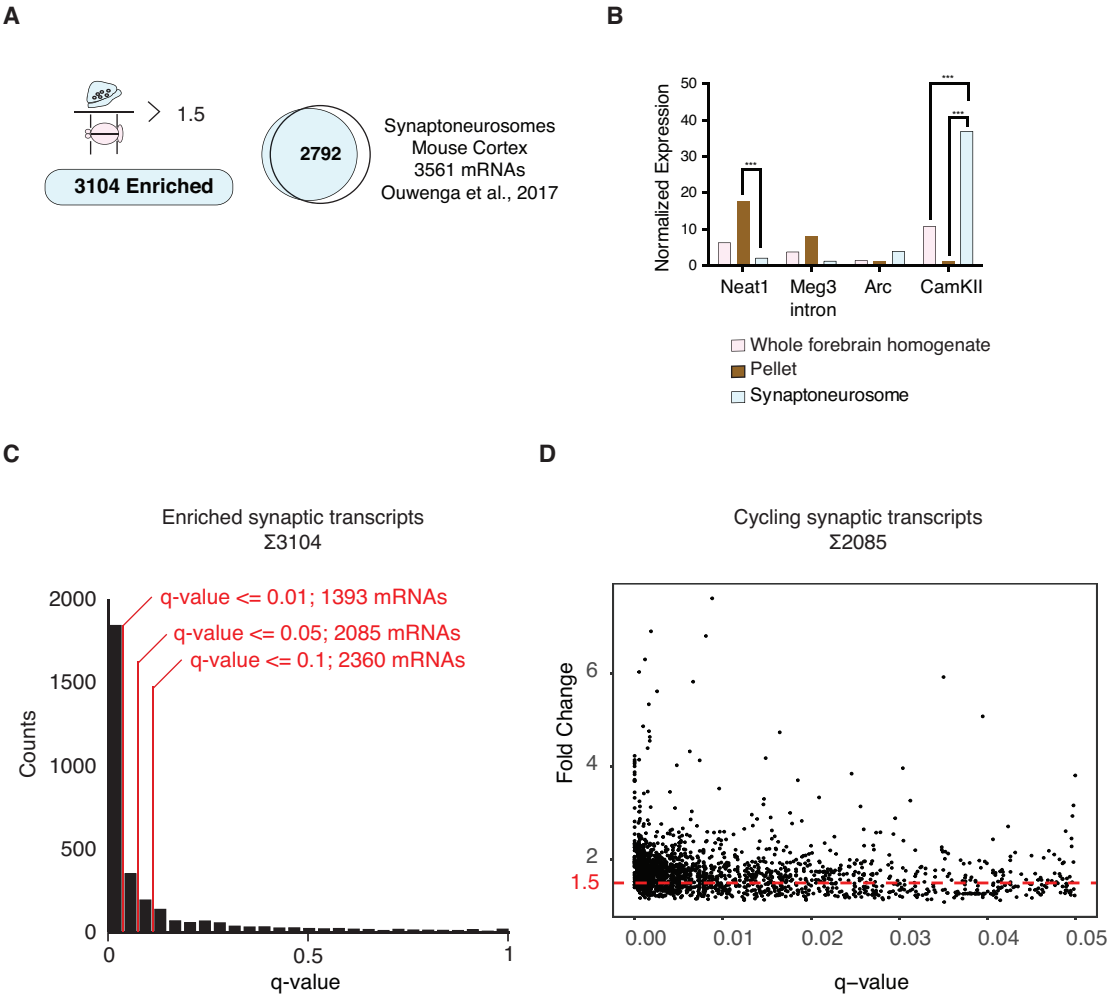


Fig. S1. (A) Overlap of the Enriched synaptic transcriptome with that from the synaptoneurosomal fraction from the mouse cortex identified in a recent study (32). (B) Quantification by real-time PCR of *Neat1*, an intronic region of *Meg3*, *Arc* and *CamKII* in whole-forebrain homogenate, pellet (containing nuclei) and gradient-purified synaptoneurosomes.

(Two-way ANOVA, ***p<0.001). (C) Distribution of q-values (Perseus Time Series Periodic analysis, period=24h). In red the number of cycling features using different q-vale cutoffs. (D) Amplitudes (represented as the Fold change (max/min)) of cycling mRNAs (Perseus Time Series Periodic analysis, period=24h, q-value<0.05) showing that our cutoff includes mainly features whose amplitude is above a log2 Fold change of 1.5 (red dashed line).

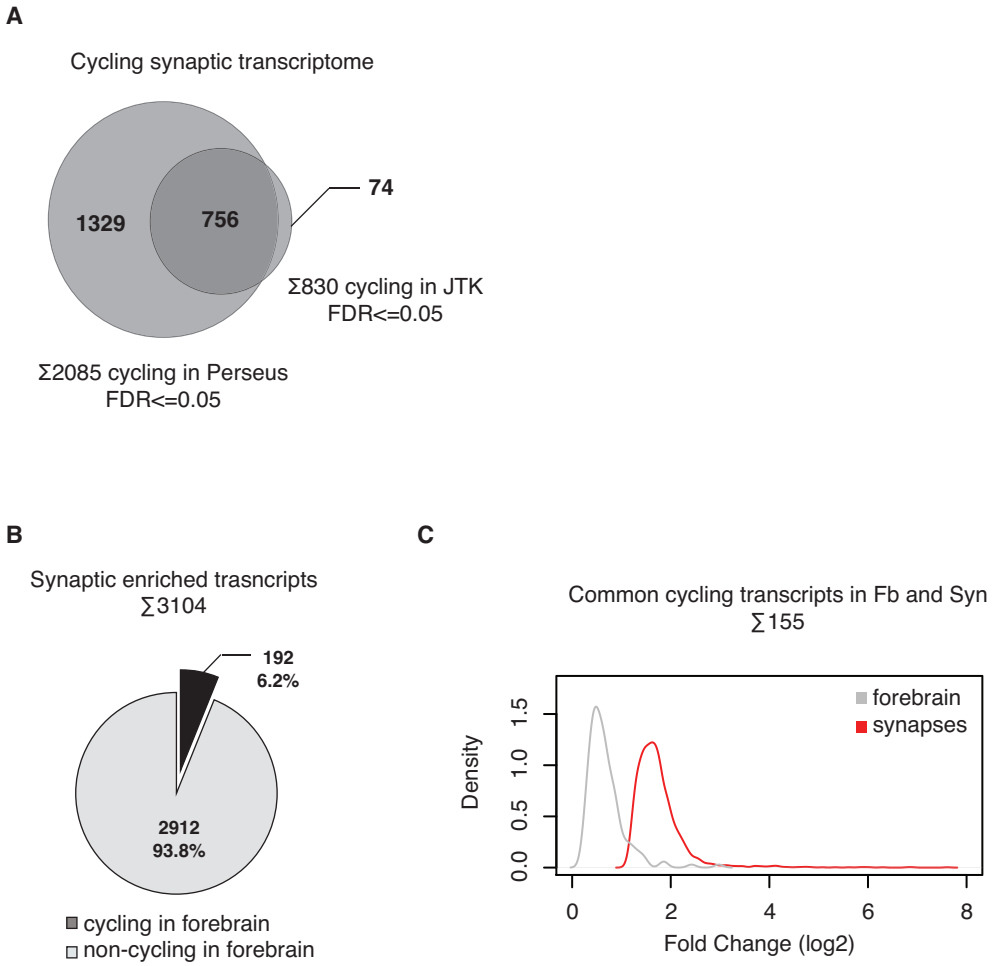


**Fig. S2. (A)** Overlap of cycling transcripts from synaptic enriched mRNAs using Perseus (Perseus Time Series Periodic analysis, period=24h, q-value<0.05) and the JTKcycle package (period=24, q-value<0.05). **(B)** Pie chart depicting the synaptic enriched mRNAs that cycle in total brain samples (Perseus Time Series Periodic analysis, period=24h, q-value<0.05). **(C)** Density distribution of circadian amplitudes (peak/trough) from common cycling transcripts in the forebrain and synapses from Fig. 1G.

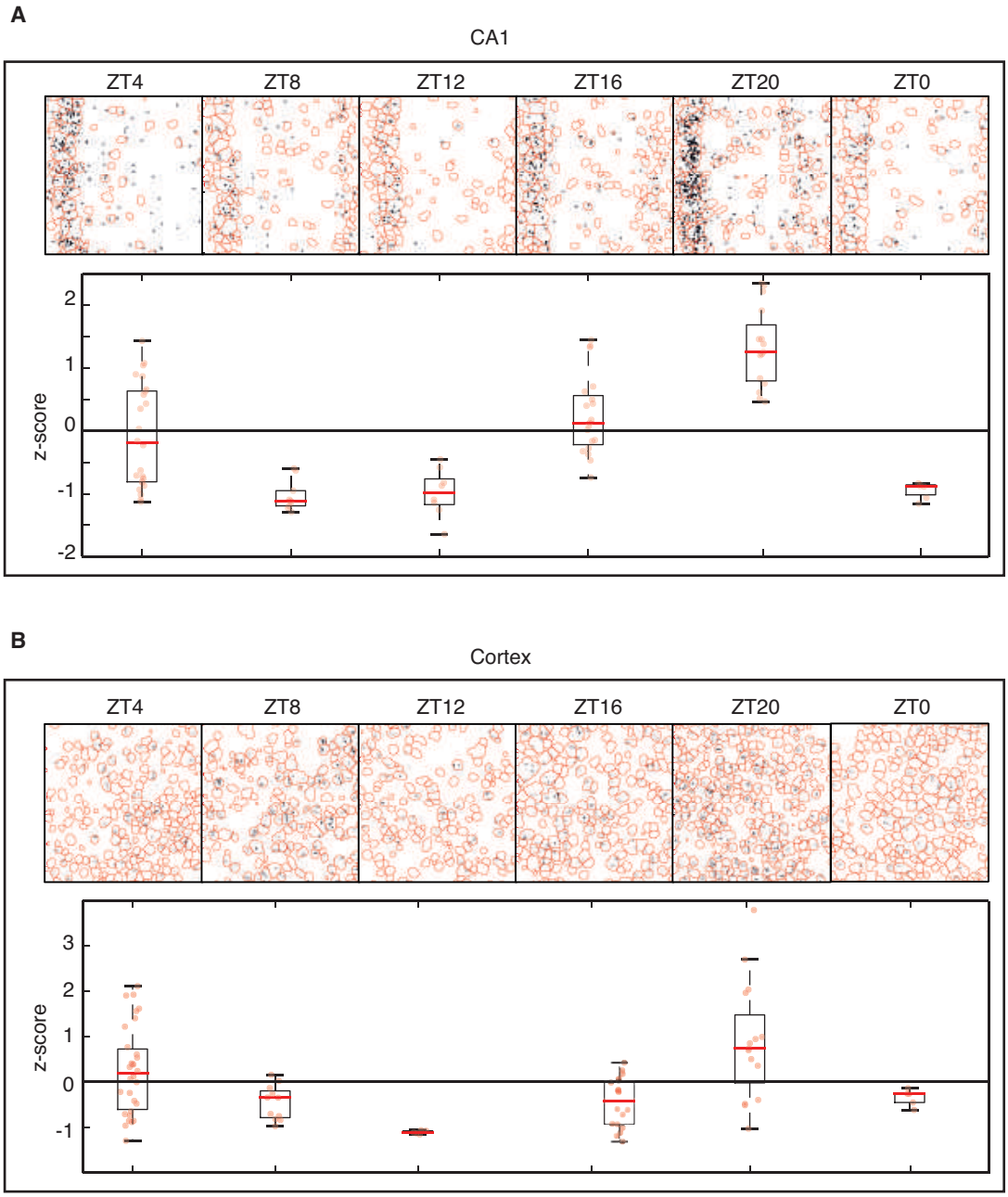


**Fig. S3. (A)** Representative images (top) of time course for single-molecule in situ hybridization of *Cry1* in the *stratum pyramidale* of the CA1 of the hippocampus. For better visualization, a red line surrounds nuclei and size of single mRNA (black dots) is increased to 0.5 μm. (Bottom) Plot showing the quantification of the in situ hybridization (n=13-18, from 3 biological replicates, Mean ± SD). **(B)** Same as in A, from the axodendritic compartment of cortex.

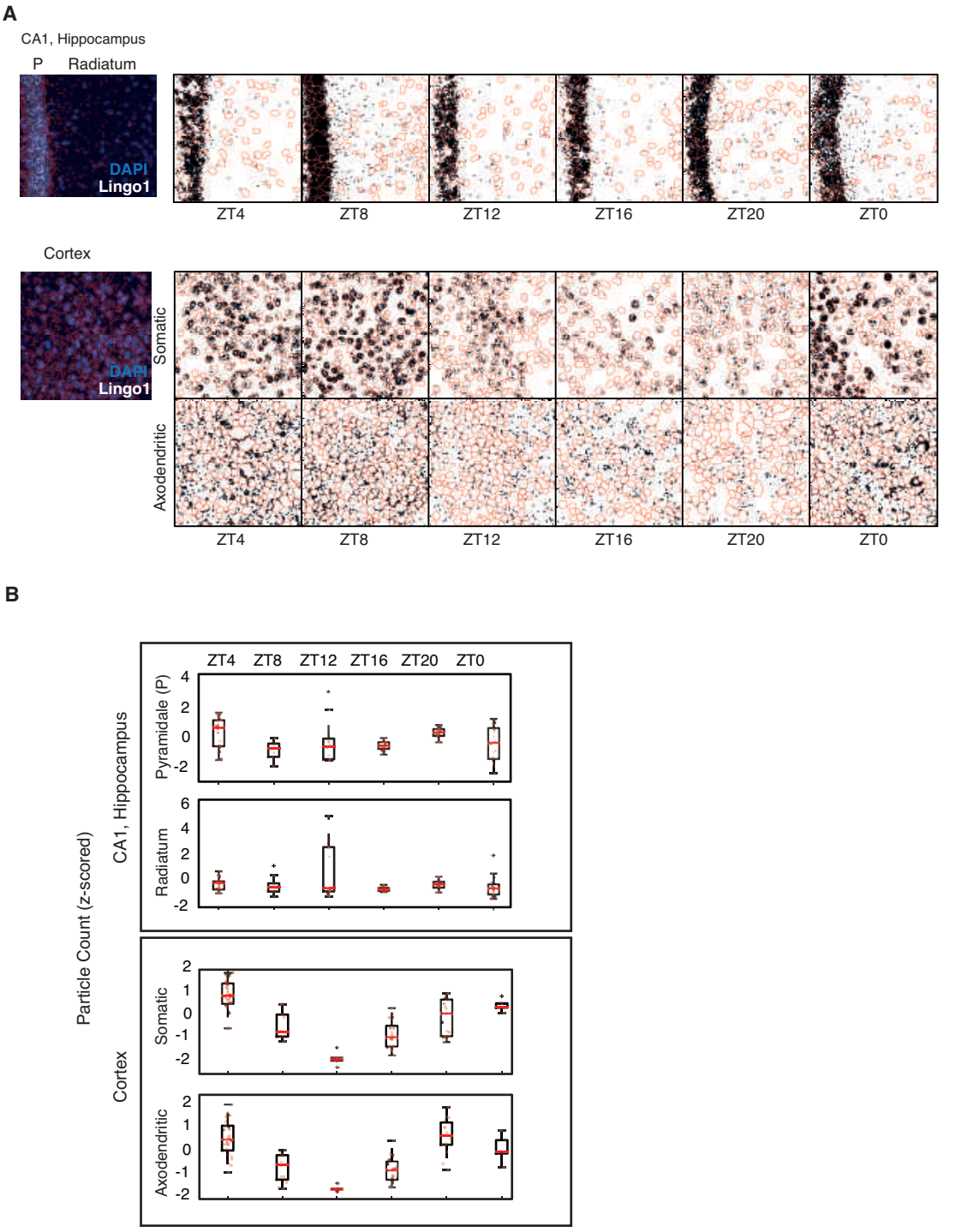


**Fig. S4. (A)** Confirmation of rhythmicity by single-molecule in situ hybridization of *Lingo1* in the *stratum radiatum* of the CA1 of the hippocampus (top panels) and in the axodendritic compartment of cortex (lower panels, top). For better visualization, a red line segments nuclei and size of single mRNA is increased to 0.5 μm. (Bottom) mRNA in the somas of the cortex. **(B)** Plot showing the quantification of the in situ hybridization of A (n=13-18, from 3 biological replicates, Mean ± SD).

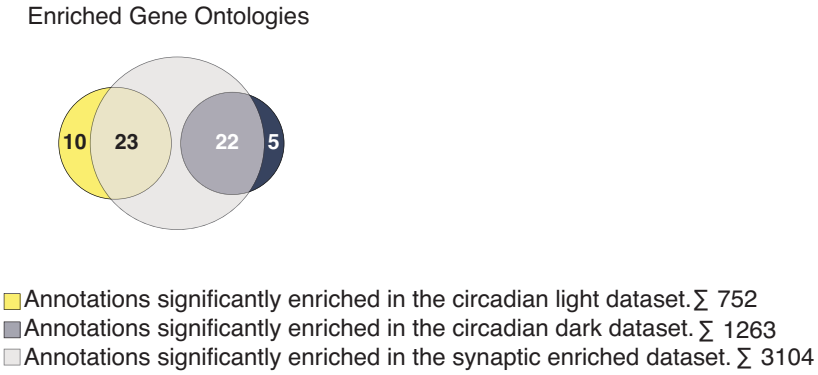


**Fig. S5.** Overlap of the GO Biological Processes enriched in the synaptic transcriptome compared to the forebrain transcriptome (grey), for transcripts peaking in the light phase, anticipating dusk (yellow), and for transcripts peaking in the dark phase, anticipating dawn (blue). Complete functional segregation is observed between light and dark phase terms (http://www.funrich.org, BH adjusted p-value <0.001).

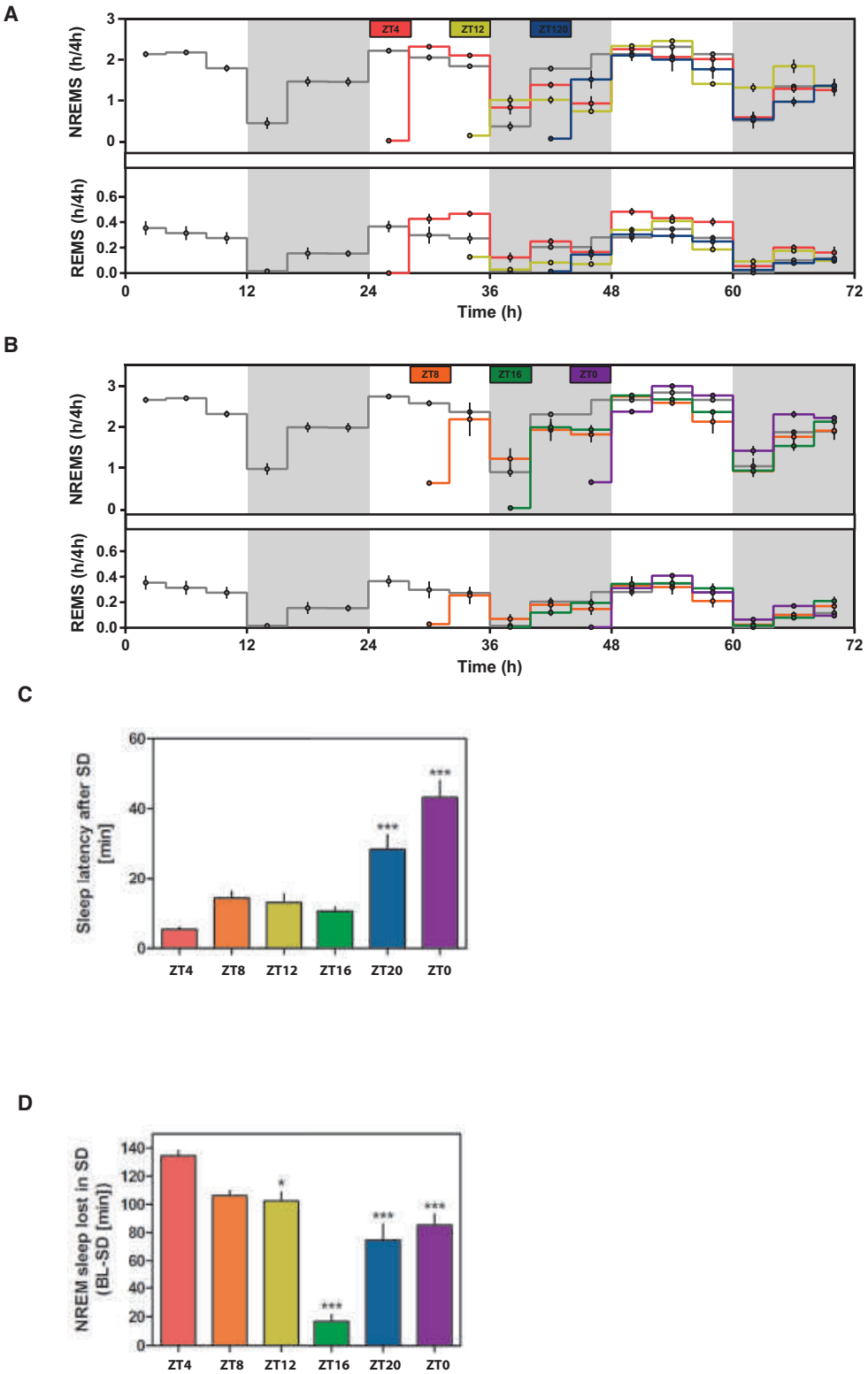


**Fig. S6. (A)** and **(B )** Time spent in NREM (up) and REM bottom during the time course. This data supplements Fig. 5A and B**. (C)** Sleep onset latency, calculated from the end of the sleep deprivation to the first consolidated NREM sleep bout (1-way ANOVA, ***P<0.001). **(D)** NREM sleep lost in SD as the mean (± SEM) difference between NREM sleep during the sleep deprivation and during the corresponding 4-h interval during baseline. Asterisks mark significant differences among sleep deprivations (1-way ANOVA, *p<0.05, ***p<0.001). Colors

indicate four 4-h sleep deprivation finishing either at ZT4 (red), at ZT8 (orange), at ZT12 (yellow), at ZT16 (green), at ZT20 (blue) or at ZT0 (purple).

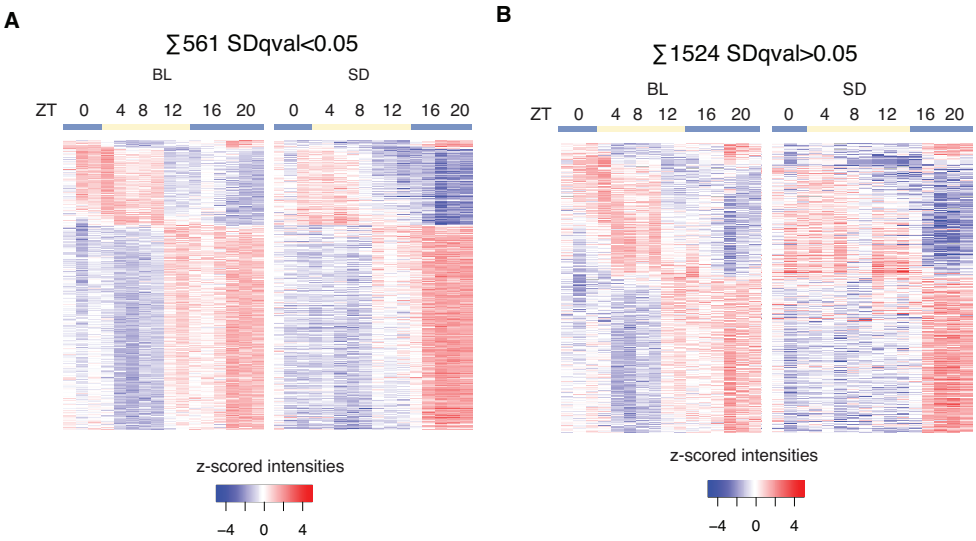


**Fig. S7. (A)** Heatmap of expression of transcripts for which cycling is not affected by SD (Perseus Time Series Periodic analysis, period=24h, q-value <0.05). Transcripts (rows) are ordered by the phase of the oscillation in BL. Values in SD for each transcript (row) and from all samples (columns) were z-scored to BL values (Blue and red represent minimal and maximal expression levels, respectively). **(B)** Same as in A but for mRNAs that are not cycling after SD (Perseus Time Series Periodic analysis, period=24h, q-value >0.05). Note that the oscillations of most transcripts are blunted after SD, but time-dependent variations remain clearly visible.

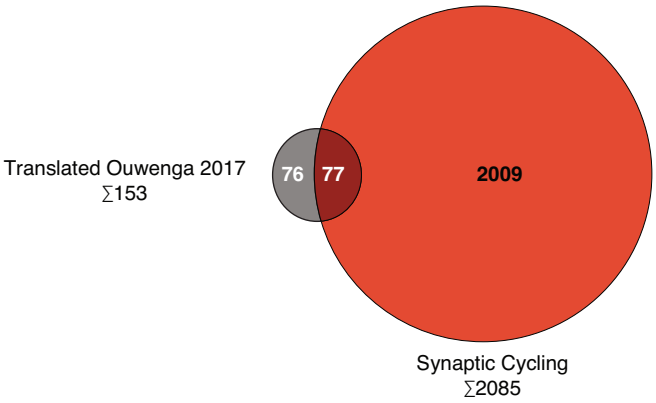


**Fig. S8. (A)** Overlap of the synaptic cycling transcriptome with synaptic locally translated RNAs identified by SynapTRAP in a recent study looking at synaptic mRNAs from the mouse cortex (*24*).

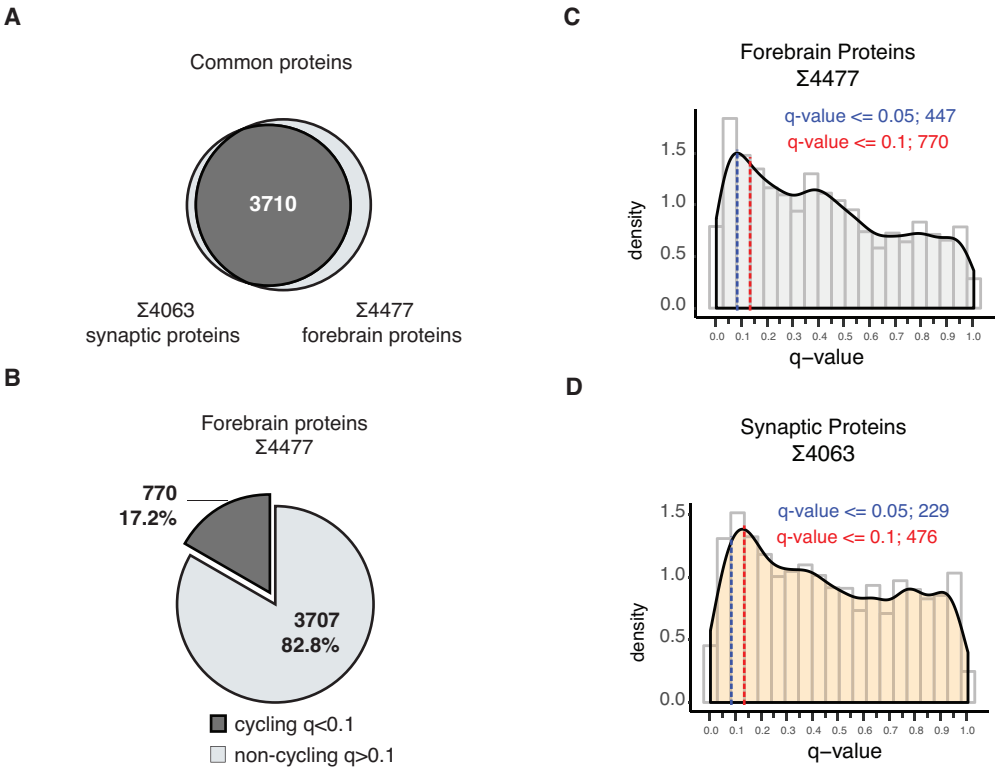


**Fig. S9. (A)** Overlap of common proteins quantified in the synaptic and corresponding forebrain proteomes. **(B)** Fraction of cycling (Perseus Time Series Periodic analysis, period=24h, q-value <0.1) proteins in the forebrain proteome. **(C)** Distribution of q-values from rhythmic analysis of the forebrain proteome obtained with Perseus software (Perseus Time Series Periodic analysis, period=24h). Red and blue dashed lines demarcate the number of cycling features using different q-value cutoffs. **(D)** Same as in (C) for the synaptic proteome.

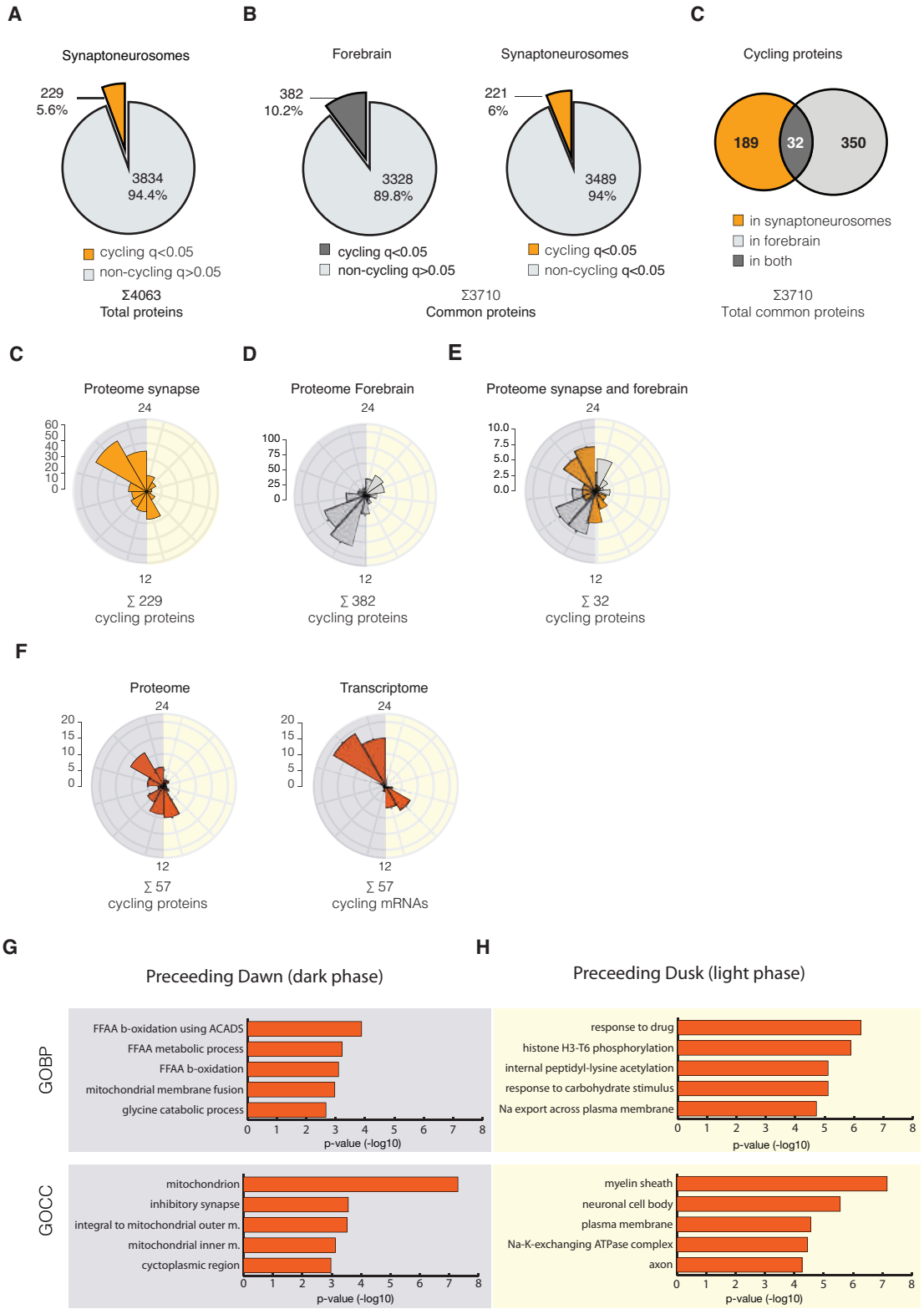


**Fig. S10. (A)** Pie chart showing the fraction of cycling proteins (Perseus Time Series Periodic analysis, period=24h, q-value <0.05) in synaptoneurosomes among the total 4063 quantified. **(B)** Overlap of the rhythmic proteome (Perseus Time Series Periodic analysis, period=24h, q-value <0.05) in synapses and in total forebrain, compared to total proteins quantified in both (3710). **(C)** Rose plots representing the frequency distribution of phases of cycling proteins in synapses, in forebrain **(D)** and the overlap of the two (in orange synaptic phases, in grey forebrain phases)

**(E)**. **(F)** Rose plots representing the frequency distribution of phases for cycling proteins and their corresponding cycling transcripts at synapses. **(G)** Enriched GO Biological Processes (GOBP) and Cellular Components (GOCC) of those synaptic cycling proteins with cycling transcripts peaking in the dark. **(H)** Same as in (G) for the light peaking proteins. (http://www.funrich.org, BH corrected p-value <0.01).

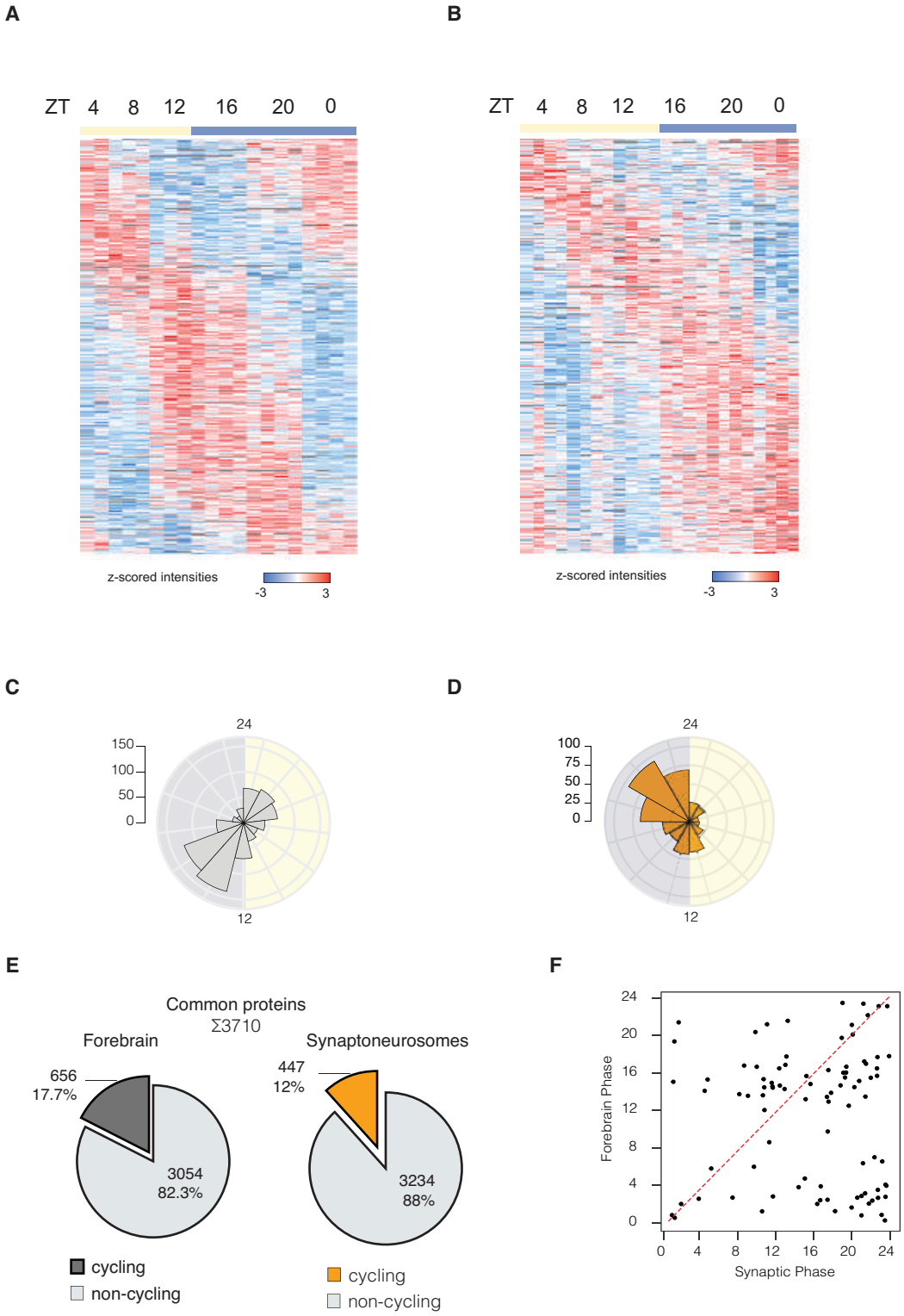


**Fig. S11. (A)** Heatmap of the intensities of cycling proteins in forebrain (Perseus Time Series Periodic analysis, period=24h, q-value <0.1). Blue and red represent minimal and maximal label

free z-scored normalized intensity values and proteins are ordered by peak of abundance. **(B)** Heatmap of the intensities of cycling proteins in synapses (Perseus Time Series Periodic analysis, period=24h, q-value <0.1). Scale color as in (A). **(C)** Rose plots representing the frequency distribution of phases from cycling proteins in total forebrain. **(D)** As in C but with cycling proteins from synaptoneurosomes. **(E)** Pie charts representing the fraction of cycling proteins in forebrain (left) and synaptoneurosomes (right) from common proteins found in both sample sets. **(F)** Scatter Plot comparing the phases in the synapses (horizontal axis) and the forebrain (vertical axis) of the 90 proteins cycling in both compartments. Note the divergence of phases for most proteins (red dashed line, phase difference=0).

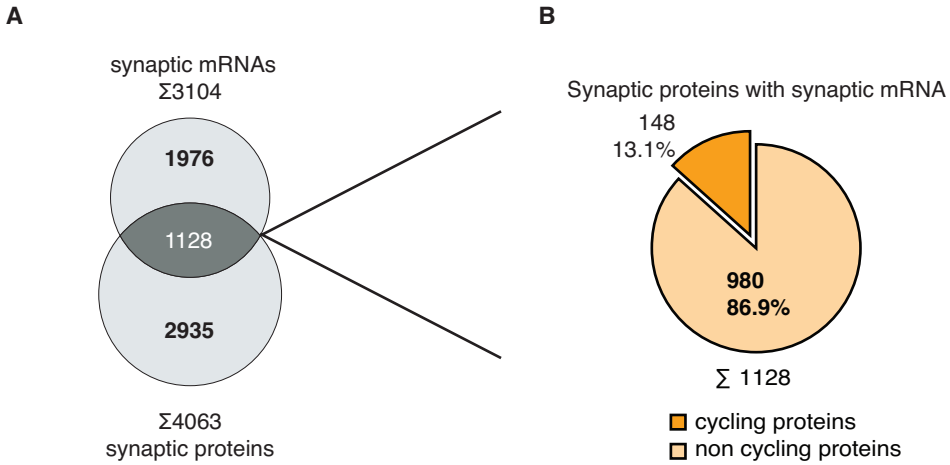


**Fig. S12. (A)** Overlap of the synaptic proteome and synaptic enriched transcriptome. **(B)** Pie chart depicting the fraction of the synaptic cycling proteome (Perseus Time Series Periodic analysis, period=24h, q-value <0.1) whose transcript is enriched in the synaptic transcriptome.

## 1.11. Additional material from manuscript 2

**This section includes:**
Materials. And Methods

Fig. S1-S13.

**Other Supplementary Materials** for this manuscript that can be accessed in the link below include the following:

Tables S1-S6.

Databases.
https://science.sciencemag.org/content/suppl/2019/10/09/366.6462.eaav361

7.DC1

**Materials and Methods**

**Animals and tissue collection**

All experiments were performed in accordance to the veterinary authorities of the Canton of Zürich. For the circadian experiments, ten -week-old male C57BL/6 mice were housed with free access to food and water and entrained to a 12 h/12 h light-dark schedule for 14 days. Mice were sacrificed at 4 h intervals over 1 day. At the time points overlapping with light transitions (ZT0 and ZT12), euthanasia was performed by cervical dislocation before the light change. For the around-the-clock sleep deprivation, mice were allowed to acclimatize to a 12-h light/12-h dark cycle for 14 days. Six groups of mice were sleep deprived for hours by gentle handling (cage exchange and introduction of novel objects) starting at different times of day (ZT0, ZT4, ZT8, ZT12, ZT16 and ZT20). Animals were sacrificed by cervical dislocation avoiding anesthetics, which are potent inhibitors of synaptic transmission. In addition, to boost preservation of phosphorylation, total preparation time was minimized, and samples were kept cooled at every step of the protocol.

**Purification of synaptoneurosomes**

Synaptoneurosomes from mouse forebrain were prepared as described previously (*34*). In brief, brain was isolated and rapidly cooled to 4°C, washed in ice-cooled sucrose buffer (320 mM Sucrose, 5 mM HEPES, pH 7.4) followed by homogenization with a Teflon-glass tissue grinder using a motor-driven pestle keeping samples cooled. Homogenate was centrifuged at 1,000 g for 10 min. 2 ml of the supernatant were loaded over discontinuous Percoll gradients (3%, 10% and 23% Percoll in sucrose buffer) and centrifuged at 31,000 g for 5 min. The fraction at the interfaces between 3-10% and 10-23% were collected and further centrifuged at 30,000 g to pellet synaptoneurosomes. All centrifugation steps were performed at 4°C. All solutions were supplemented with complete protease inhibitor cocktail (Roche®), 0.05 mM DTT, 0.1 mM PMSF and RNaseOUT 20 U (Invitrogen®).

**Sample preparation and phosphopeptides enrichment**

Synaptoneurosomes prepared from mouse forebrain were lysed (0.1 mM Tris-HCl [pH 7.6], and 4% SDS), sonicated in a bioruptor (4°C for 15 min or until homogenous suspension was formed) and boiled at 95°C for 5 min. A total of 1 mg protein lysate was treated first with 1 µl DTT (1 M) followed by 10 µl 2-Chloroacetamide (0.5 M). Each treatment was performed at room temperature (RT, 22°C) for 20 min. The lysates were precipitated with acetone and phosphopeptides were enriched using the EasyPhos method as described (*35*). In detail, pellets were resuspended in 500 µl TFE digestion buffer prior to the addition of digestion the digestion enzymes (trypsin and LysC) 1:100 (protein:enzyme). After overnight incubation at 37°C with rapid agitation (1,500 rpm) a buffer containing 150 µl 3.2 M KCl, 55 µl of 150 mM $KH_2PO_4$, 800 µl 100% acetonitrile (ACN), and 95 µl 100% trifluoroacetic acid (TFA) was added to the peptides and incubated at RT for 5 min at 1,600 rpm prior to

centrifugation. The peptide supernatant was transferred to a clean 2 ml tube, $TiO_2$ beads subsequently added at a ratio of 10:1 beads/protein, and incubated at 40°C for 5 min at 2,000 rpm. Beads with bound phosphopeptides were pelleted by centrifugation for 1 min at 3,500 g and the supernatant was discarded. Beads were then resuspended in wash buffer (60% ACN and 1% TFA) to be transferred to a clean 2 ml tube, and washed further four times with 1ml of washing buffer. After the last wash beads were resuspended in transfer buffer (80% ACN and 0.5% acetic acid) and transferred on top of C8 StageTips. After centrifugation phosphopeptides were eluted with 60 $\mu$l elution buffer (40% ACN and 15% NH4OH [25%, HPLC grade]) and collected in clean PCR tubes, concentrated in a SpeedVac for 15 min at 45°C and acidified with10 $\mu$l of 10% TFA. Peptides were then desalted using stageTips with two layers of styrenedivinylbenzene–reversed phase sulfonated (SDB-RPS; 3M Empore), washed twice with wash buffer (0.2% TFA) and one with isopropanol containing 1% TFA. Peptides were eluted by adding 60 $\mu$l SDB-RPS elution buffer (80% ACN, 1.25% $NH_4OH$ (25% HPLC grade)) and immediately concentrated in a SpeedVac for 30 min at 45°C. Concentrated peptides were then resuspended in a buffer containing 2% ACN and 0.1% TFA prior to chromatography-tandem mass spectrometry (LC-MS/MS) analysis.

**LC-MS/MS Analysis and Data Processing**

Phosphopeptides were loaded onto a 50 cm reversed-phase column (diameter 75 $\mu$M; packed in-house with 1.9 $\mu$M C18 ReproSil particles [Dr. Maisch GmbH]). The temperature of the homemade column oven was maintained at 60°C. The column was mounted to the EASY-nLC 1000 system (Thermo Fisher Scientific). The peptides were eluted with a binary buffer system consisting out of buffer A (0.1% formic acid) and buffer B (80% ACN and 0.1% formic acid). A gradient length of 140 min was chosen (5%-65% buffer B for 130 min followed

by 10 min 80% buffer B) with a flow rate of 300 nl/min. Peptides were analyzed in a Q Exactive HF mass spectrometer (MS) (Thermo Fisher Scientific) coupled to the nLC, obtaining full scans (300-1,600 m/z, R = 60,000 at 200 m/z) at a target of 3e6 ions. The 10 most abundant ions were selected and fragmented with higher-energy collisional dissociation (HCD) (target 1e5 ions, maximum injection time 120 ms, isolation window 1.6 m/z, normalized collision energy 25% underfill ratio 40%) followed by the detection in the Orbitrap (R = 15,000 at 200 m/z). Raw MS data files were processed using MaxQuant (version 1.5.5.6,(*36*)) with the Andromeda search engine with FDR < 0.01 at protein, peptide, and modification level. The default settings were used with the following modifications: (1) the variable modification methionine (M), acetylation (protein N-term), as well as phospho (STY) and the fixed modification carbamidomethyl (C) were selected, (2) only peptides with a minimal length of seven amino acids were considered, and (3) the "match between run" option was enabled with a matching time window of 0.7 min. For protein and peptide identification we used the UniProt database from mouse (September 2014) containig 51,210 entries. Each raw file was treated as one experiment and replicates were combined in the same fraction (no numerical ordering). The following samples were not considered for the final analysis due to low identification number and outlier clustering withing the replicates: replicate 4 of ZT16, 3 of ZT20 of the control group and replicate 1 of ZT0, 4 of ZT8, and 2 of ZT12 of the sleep deprived group.

**Bioinformatic and Statistical Analyses**

Processed data was uploaded in the Perseus software (*37*) with which bioinformatical analyses were performed. First, reverse sequences and potential contaminants were removed. Then the total data set was log2 transformed and filtered for at least one valid value. After expanding the site table, the data was

again filtered for one valid value. In order to statistically analyze and compare the phosphoproteome of the control group (BL) and the sleep deprived (SD) mice, a more stringent filtering was applied. For each data set (SD/BL) phosphopeptides without intensities in <12 samples were removed. Following this, the median intensity of each sample was subtracted from every phosphopeptide quantified in this sample. The Fisher's exact test enrichment analysis (FDR< 0.02) of the total BL identified phosphoproteome dataset was done calculating relative enrichment of UniProt KB -Keywords annotations compared to a total in silico mouse gene list generated by Perseus, both datasets were matched using gene names. Cycling analyses were performed as described using the computational platform Perseus (*37, 38*). Phosphopeptides with a q-value < 0.05 were classified as "cycling". Hierarchical clustering was performed in a phase preserving-manner by which the order of elements is restricted to that determined by the output of the periodicity analysis. The proteome and the phosphoproteome data were matched by Uniprot ID. Amplitudes were calculated as the difference between maximum and minimum values across all the time points using the mean of log2 intensities for the biologial replicates. To identify protein annotations with over- or underrepresented cycling phosphoproteins in the total phosphoproteome, an enrichment analysis of UniProt KB –Keywords annotation was done using the Fisher's exact test with a p-value cut-off of 0.01.

Phosphopeptides belonging to kinases (using Keyword and manual annotations) were extracted from the total list of phosphopeptides and collapsed to protein entries (kinases). Kinases with at least one cycling phosphopeptide (cycling analysis, q-value < 0.05) were defined as "cycling kinases". Gene name lists of all quantified kinases and of cycling kinases were submitted to www.kinhub.org to annotate kinases to the major families and to

generate the kinase trees. Percentages of quantify and cycling kinases in each family were calculated based on the entries for each family designated in www.kinhub.org.

For comparison of the global effect on phosphorylation of sleep deprivation we used normalized intensities of the complete phosphoproteome (7257 phosphosites in BL and 7021 in SD) and performed a non-parametric paired t-test (p-value<0.01).

**Integrated analysis and visualization of phosphoproteomic data and protein-protein interaction network**

Interactions for mouse were downloaded from STRING (v10.5) and filtered for high-confidence edges with scores of at least 0.9. Since the node identifiers in the network are Ensemble protein IDs (ENSP), the protein groups in the phosphoproteomics data were mapped ENSP IDs using the UniProt annotations in Perseus. After annotating the nodes of the network with the data, signaling functionality scores were calculated using PHOTON. In brief, for each protein in the network a moderated t-test was performed on the phosphorylation found on its neighbors in the network. Using a permutation-based FDR approach the resulting p-value was corrected for multiple testing and transformed into a final score. Intuitively, proteins with high/low scores pro-/demote the phosphorylation of their neighbors. Cycling analysis was performed on the PHOTON scores to identify kinases with an oscillatory signaling functionality score (q-value < 0.05, period 24h). For the visualization, all cycling kinases and their interactions were extracted from the network. The subnetwork was overlaid with phosphorylation data from cycling sites and plotted using the d3.js library and manual layouting.

For the protein interaction network of fig. S6 we used STRING interaction sources limited to “Textminig”, “Databases”, “Experiments” and “Co-

expression". Thickness of the connecting lines are proportional to combined STRING scores (maximum score 0.9 and minimum 0.2). Low scores from 0.2 to 0.5 were included after individual inspection of the sources and confirmation of the synaptic origin of that source.

## Supplementary Figures

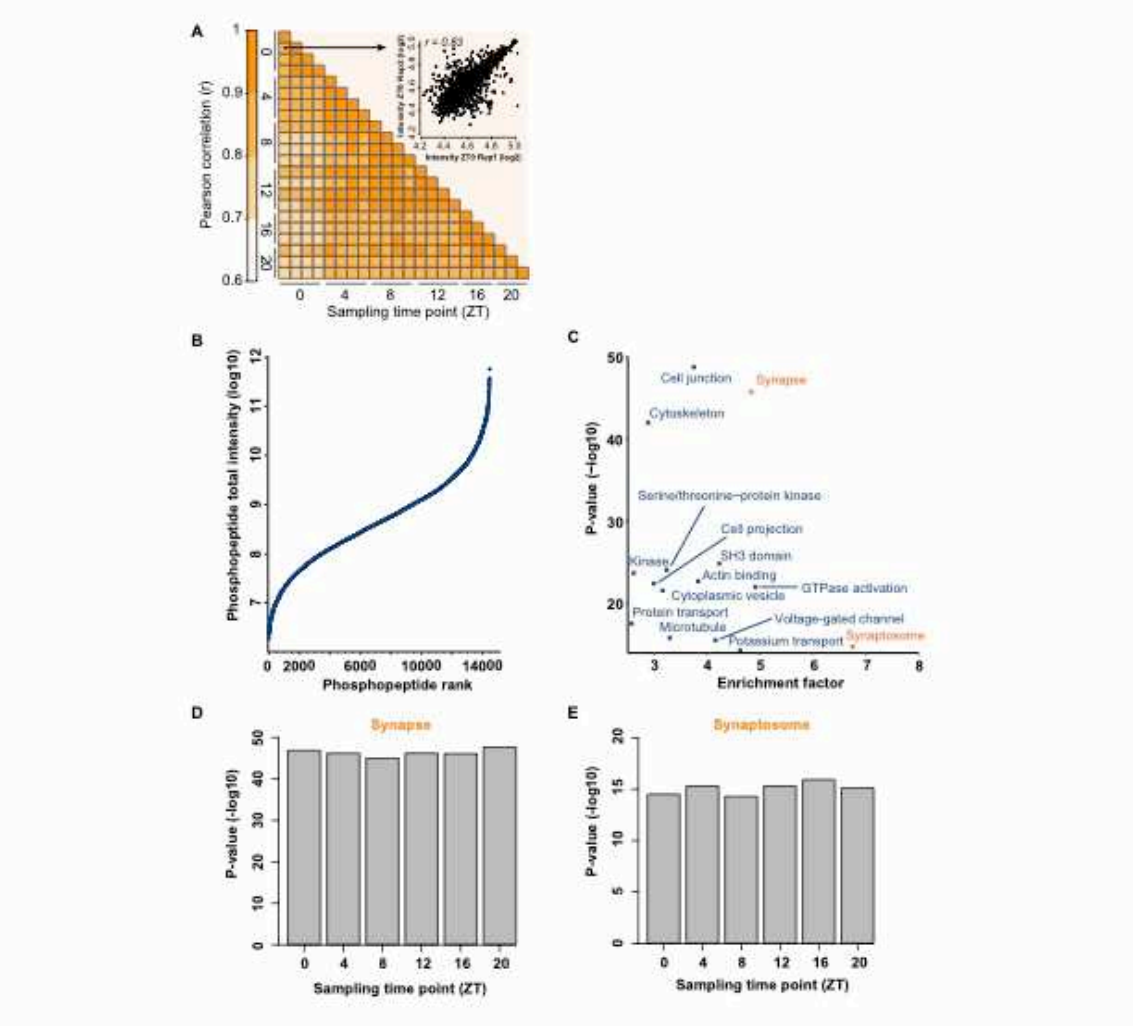


Figure S1. The phosphoproteome of isolated synaptoneurosomes collected through the day. (A) Heatmap representation of Pearson correlation coefficients calculated among phosphoproteomes. Inset: Example scatterplot of phosphopeptide intensities between two biological replicates of ZT0. (B) Total phosphopeptide intensities ranked ascending to illustrate the dynamic range of the dataset. (C) Scatterplot shows protein annotations (UniprotKB keywords) statistically enriched (Fisher's exact test FDR < 0.02) in the total synaptoneurosome phosphoproteome compared to an in-silico mouse gene list. Bar plots representing the p-value of the enrichment test (as in C) for the UniprotKB keyword annotation "Synapse" (D) and "Synaptosome" (E) in the phosphoproteomes of each time point.

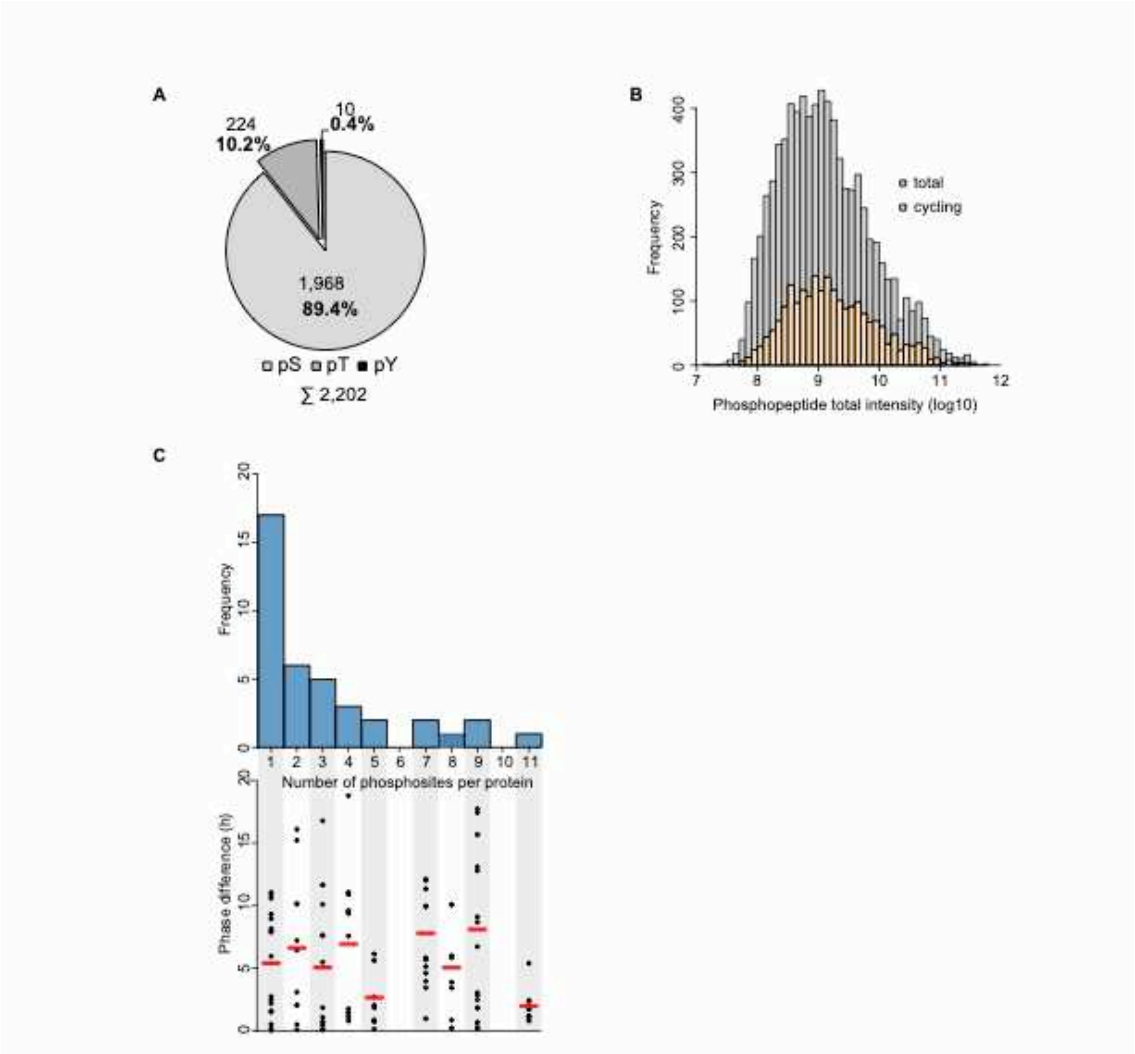


Figure S2. Characteristics of the synaptic cycling phosphoproteome. Phosphopeptides cycling in abundance in synapses are distributed among different amino acid residues (Serine (pS), Threonine (pT), and Tyrosine (pY)) from the total (A). (B) Histogram of total intensity distribution of

the total dataset (grey) and the cycling phosphopeptides (yellow). (C) Frequency distribution of cycling phosphoresidues in rhythmic proteins (top). The phase differences between cycling proteins and its phosphopeptides are represented on the bottom. The red line indicates the average phase difference.

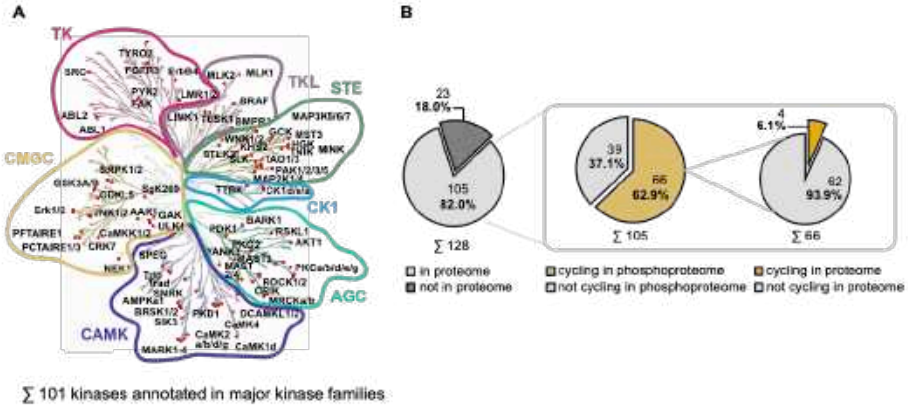


Figure S3. Synapses are kinase hubs. Out of the total 128 quantified phosphorylated kinases in synapses 101 kinases were annotated to the major kinase families (http://www.kinhub.org) (A): Tyrosine Kinases (TK), Tyrosine Kinase-Like (TKL), Homologs of the yeast STE7, STE11 and STE20 genes (STE), Casein/cell kinase 1 family (CK1), Protein Kinase A, G, C families (AGC), Calmodulin/Calcium regulated kinases and some non-calcium regulated families (CAMK), set of CDK, MAPK, GSK3 and CLK kinase families (CMGC). Atypical kinases are not shown (one annotation BCKDK in pyruvate dehydrogenase kinase) (B) Pie charts showing the percentage of phosphorylated kinases quantified in our proteome study (left), the percentage of cycling and not cycling phosphopeptides in kinases quantified at the protein level (middle) and the percentage of kinases with cycling phosphopeptides that cycle at the proteome level.

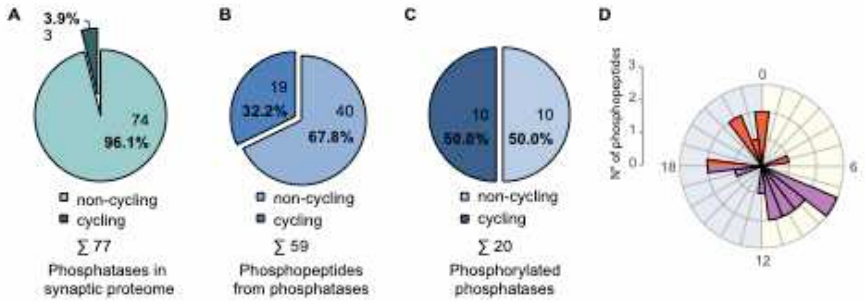


Figure S4. Synaptic phosphatases harboring phosphorylations. (A) Pie chart showing cycling and non-cycling phosphatases quantified in the synaptic proteome. Pie chart illustrating the percentage of cycling and non-cycling phosphopeptides from phosphatases (B) and the same for total phosphorylated phosphatases (C). (D) Rose plot representing the phases of cycling phosphopeptides from phosphophatases. Colors denote the clusters: wake-sleep transition (ZT18-ZT6, orange) and sleep-wake transition (ZT6-ZT18, purple) as used in our main figures.

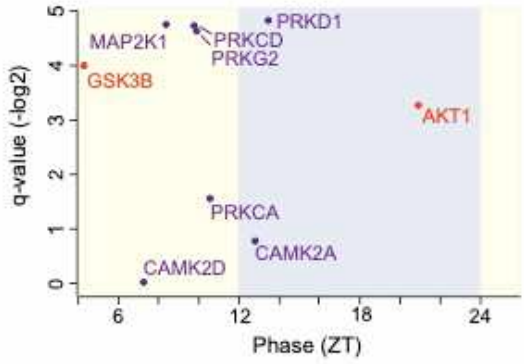


Figure S5. Kinase-substrate relationships predict temporal activated kinases in synapses. Scatter plot showing the kinase activity patterns predicted using kinase substrate enrichment analysis (KSEA) from the cycling synaptic phosphoproteome. Predicted phases are represented in the X-axis and the q-value from the cycling analysis of KSEA z-scores in the Y-axis.

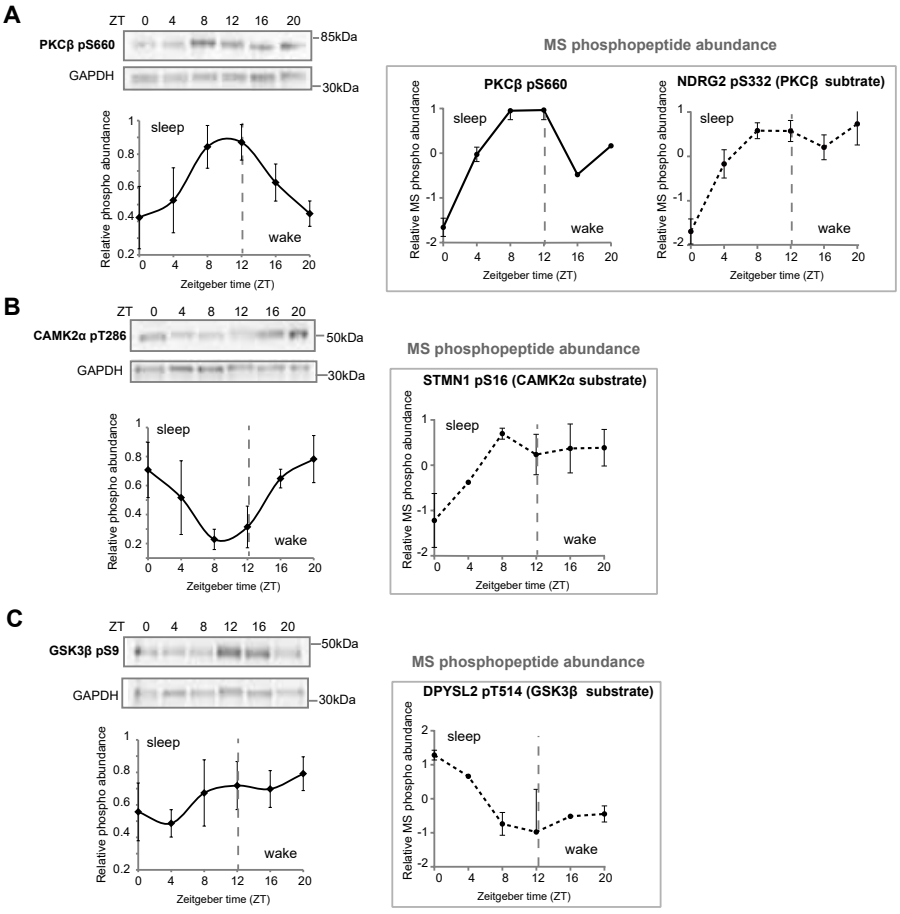


Figure S6. Western blot validation of temporally active kinases in synapses. Representative gel images for (A) PKCβ pS660, (B) CAMK2α pT286 and (C) GSK3β pS9. Panels underneath the images display the quantification (mean ± SEM) of the specific band for each antibody relative

to GAPDH for three independently experiments performed with 3 different biological replicate samples for each time point. Plots in gray boxes on the right illustrate phosphopeptide abundance profiles obtained by MS and contained in our dataset: this includes PKCβ pS660 phosphorylated peptide (solid line) and phosphopeptides with residues known to be phosphorylated by each of the temporally active kinase (dashed line). Note the correlation of the phospho-dependent activity profiles of the kinases and the MS-based phosphorylation changes of curated substrates detected in our dataset. Also note that the profile of CAMKIIα pT286 follows the data in the literature: this residue progressively and slowly autophosphorylate after the CAMKII activation by calcium- calmodulin (Lisman, Nat Rev Neurosci 2012).

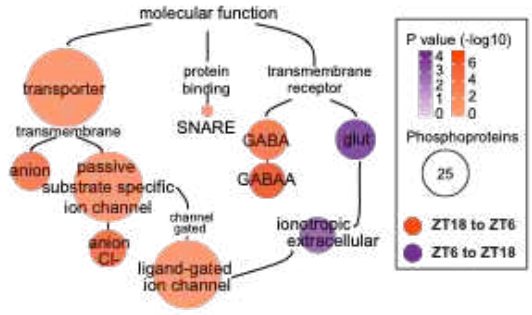


Figure S7. Predicted temporal dynamics of synaptic molecular functions. Representation of the GO Molecular Function annotations statistically enriched in a time dependent manner using the PHOTON scores (phase dependent enrichment test q-value < 0.05, see Methods). Annotations are colored based on the cluster colors of our main figures: wake-sleep transition (ZT18-ZT6, orange) and sleep-wake transition (ZT6-ZT18, purple). Size of circles is proportional to the number of cycling phosphoproteins from each annotation and color intensity to the p value of the enrichment test.

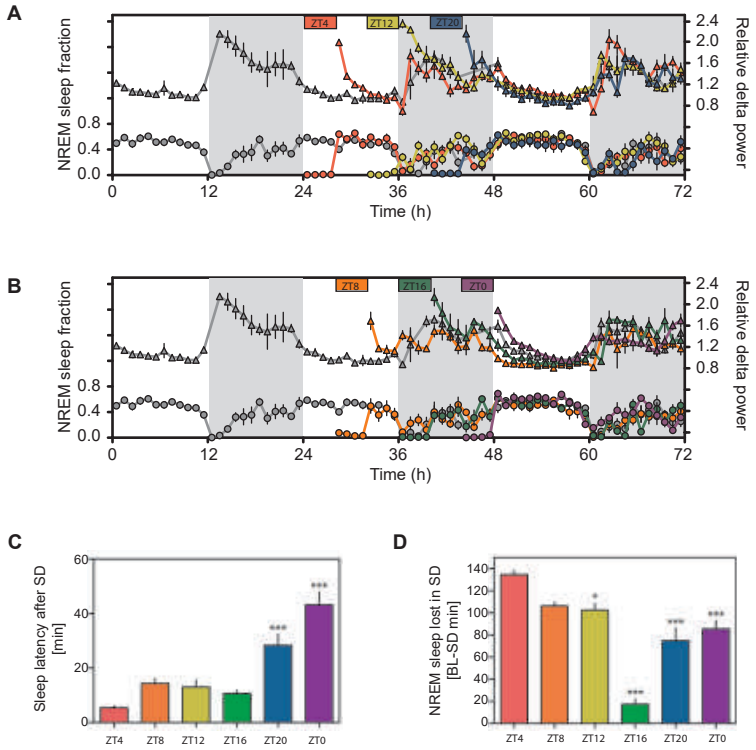


Figure S8. Sleep deprivation across the day. (A) and (B) Time course of mean (±SEM) frontal delta power during NREM sleep, relative to mean BL delta power (0.5-4Hz) at ZT8-12 (Top, triangles, right y-axis) and time spent in NREM sleep (bottom, circles; min/h; left y-axis) during 24-h baseline (grey symbols and lines), and during and after 4h sleep deprivations (SD) finished at ZT4 (red), at ZT8 (orange), at ZT12 (yellow), at ZT16 (green), at ZT20 (blue) or at ZT0 (purple). The data was divided into two panels for better visualization, with baseline reproduced in both. Grey areas delineate dark periods during 12:12 light:dark cycle. (C) Sleep onset latency, calculated from the end of the sleep deprivation to the first consolidated NREM sleep bout (1-way ANOVA, ***P<0.001). (D) Mean (± SEM) difference between NREM sleep during the sleep deprivation and during the corresponding 4h interval during baseline. Asterisks mark significant differences among sleep deprivations (1-way ANOVA, *p-value<0.05, ***p-value<0.001). Color code for sleep deprivation timing as in panels (A) and (B). ZT times refer to the end of the sleep deprivations. Figure copied from Noya et al. 2019 (11).

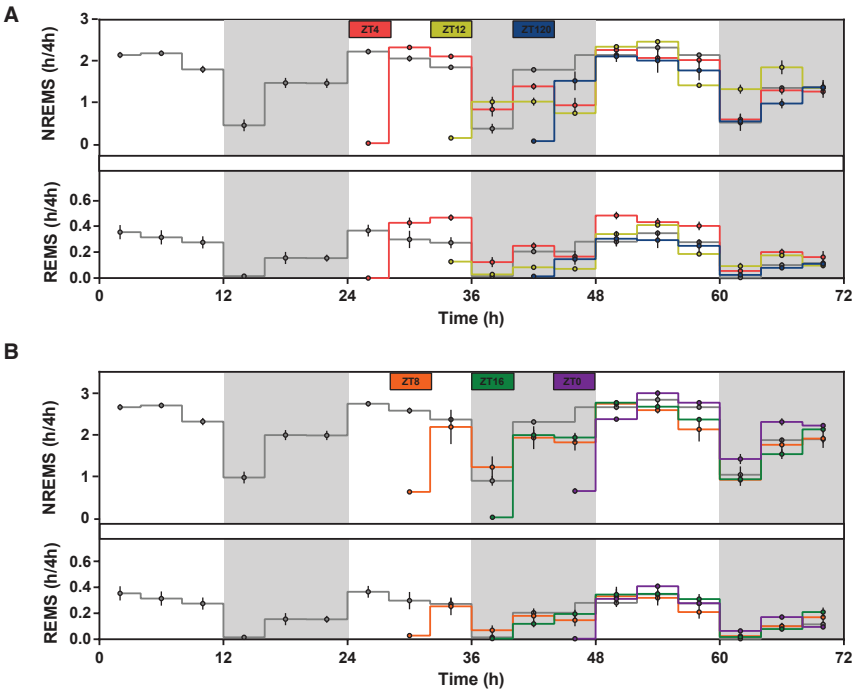


Figure S9. Sleep deprivation across the day. (A) and (B)Time spent in NREM (up) and REM bottom during the time course. This data supplements Fig. S8A and B. Figure copied from Noya et al. 2019 (11).

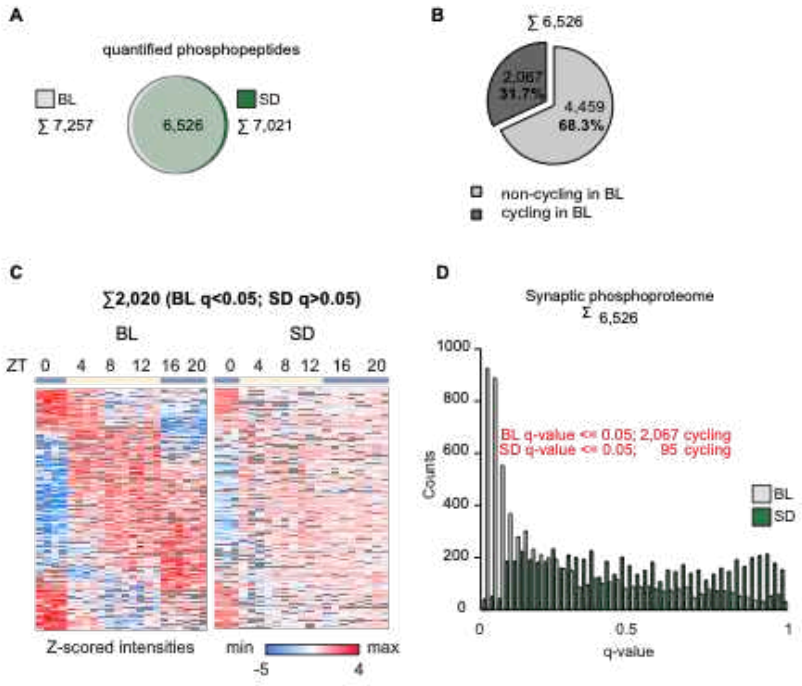

Figure S10. Phosphorylation cycles are perturbed by sleep deprivation. (A) Overlap between the quantified phosphopeptides in BL and SD time series. (B) Pie chart showing fraction of cycling (period=24h, q-value <0.05) phosphopeptides in BL conditions among those quantified in both BL and SD conditions. (C) Heat map of the intensities (z-scored log2) in BL (left) and SD (right) of phosphopeptides rhythmic (period=24h, q-value <0.05) in BL but arrhythmic in SD (period=24h, q-value >0.05). (D) Distribution of the q-values resulted from the cycling analysis in BL and SD conditions of common quantified phosphopeptides (6,526). Grey bars represent the q-values obtained with the BL dataset and the green those q-values from the SD dataset. Note the reduction of statistically significant entries in SD versus BL (period 24h, q-value < 0.05).

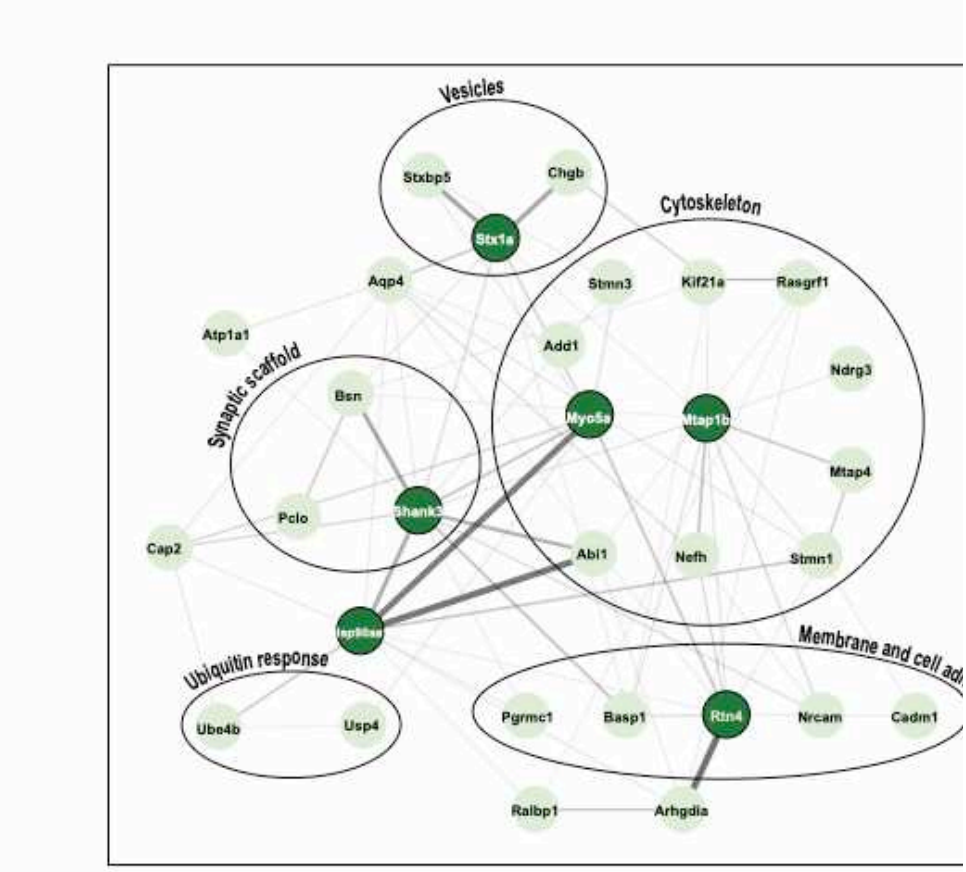


Figure S11. Proteins with cycling phosphorylations persisting under sleep deprivation. Protein interaction network of synaptic proteins with rhythmic phosphorylations in both, BL and SD conditions. Core components are colored in green. Thickness of connecting lines is based on STRING interaction scores, visualization was done with Cytoscape.

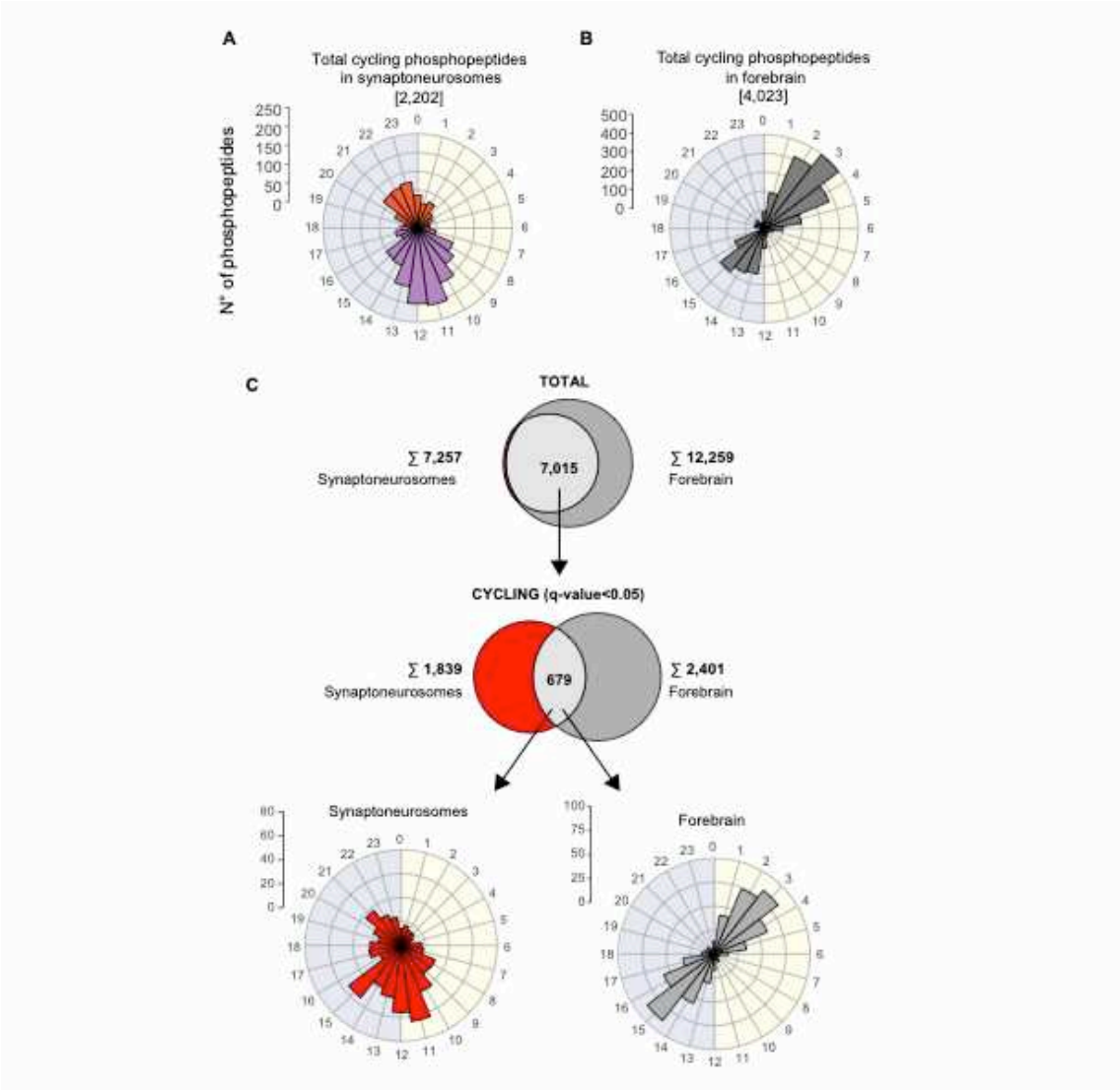


Figure S12. Divergence between total forebrain and synaptic phosphoproteome. Rose plot showing the phases of the cycling phosphopeptides in isolated synaptoneurosomes (A) and in total input forebrains (B). (C) Venn diagrams illustrating the overlap between quantified phosphopeptides in synaptoneurosomes and in forebrain samples (top) and the overlap of cycling phosphopeptides between both fractions (bottom). Lower rose plots show the phase distribution of the common 679 cycling phosphopeptides in synaptoneurosome (left) and in total forebrain (right).

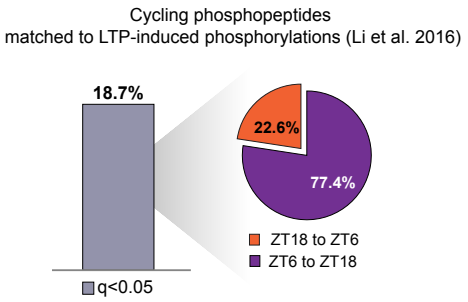


Figure S13. LTP-induced phosphorylations largely peak at the sleep-wake transition. Bar shows the percentage of CA1 hippocampal LTP-induced phosphoresidues (according to Lie et al. (2016)) found cycling in our synaptoneurosome phosphoproteome. Pie chart indicates the percentage of those phosphoresidues with peaks at the wake-sleep transition (ZT18-ZT6, orange) and at the sleep-wake transition (ZT6-ZT18, purple.)